Redundant, exclusive, and cooperative functions of alternative exons in *Drosophila* Ca_v2 channels

Dissertation

Zur Erlangung des Grades

Doktor der Naturwissenschaften (Dr. rer. nat.)

Am Fachbereich Biologie

Der Johannes Gutenberg-Universität Mainz

Lukas Kilo

geb. am 28.08.1990, in Wiesbaden

Mainz, 2021

Dekan:

1. Berichterstatter:

2. Berichterstatter:

Tag der mündlichen Prüfung:

Abstract

The diversity of voltage gated calcium channel (VGCC) functions greatly outnumbers the count of voltage gated calcium channel genes. One of the ways to increase VGCC functional diversity is alternative splicing. In this thesis I could show for the *Drosophila* VGCC *cacophony*, a homolog to the vertebrate Ca_v2 calcium channel family, that functional diversity is indeed linked to alternative splicing. By using CRISPR/Cas for exon excision as well as electrophysiological methods, confocal microscopy, and behavioral assays, both isoform-specific properties and degenerate functions of exon dependent isoform subsets could be identified. Two alternative exon pairs encoding part of the voltage sensor or accessory subunit binding sites, respectively, were investigated. Differences in isoform localization as well as channel kinetics suggest a division of labor in some parts of the nervous system. Indeed, some of the isoforms fulfill essential functions with behavioral relevance, while others function in a degenerate manner. Although, whether these degenerate ones also exert unique functions under specific conditions remains to be determined. In addition to this, a novel collaborative interaction between two isoforms of the same gene could be discovered. Specifically, lethality resulting from the deletion of one essential isoform and behavioral impairments resulting from the deletion from the other alternative isoform are both fully rescued in trans heterozygous flies carrying both deletions. Both alternative exons have rather similar channel properties but different global and subcellular localizations. They are both required in concert throughout the nervous system for survival and normal motor behavior.

Index

Abstract I

Abbreviations: VI

1 Introduction 1

1.1 Voltage Gated Calcium channels 1

1.2 Voltage gated calcium channels in *Drosophila* 3

1.3 Cacophony 4

1.4 Alternative splicing 4

1.5 Mutually exclusive alternative splice sites in *cacophony* 5

1.6 Channelopathies associated with VGCC splicing 6

1.7 Aims of this study 6

2 Material and Methods 9

2.1 Fly keeping 9

2.1.1 General fly rearing 9

2.1.2 Common fly stocks used and crossing schemes 9

2.2 Molecular biology 11

2.2.1 Standard molecular techniques employed in this thesis 11

2.2.2 Transgenic fly lines carrying specific isoforms of *cacophony* 16

2.2.3 Crispr design 17

2.3 Behavioral paradigms 20

2.3.1 Larval Crawling 20

2.3.2 Courtship success 20

2.3.3 Courtship Song 20

2.3.4 Flight initiation & inflight muscle recordings 21

2.3.5 Climbing assay 21

2.4 Imaging 22

2.4.1 Immunohistochemistry 22

2.4.2 CLSM 24
2.4.3 Digital data processing 24
2.5 Electrophysiology 24
2.5.1 whole cell patch clamp adult/pupae 24
2.5.2 Current clamp recordings pupae 26
2.5.3 Calcium imaging 26
2.5.4 Electroretinogram adult 27
2.6 Data analysis and Statistics 27
3 Results 29
3.1 Generation, verification, and initial assessment of the CRISPR/Cas9 mediated exon excision variants 29
3.1.1 Cacophony voltage gated calcium channel isoform variability can be reduced by deletion of alternative exons with CRISPR/Cas9 29
3.1.2 Excision verification 29
3.1.2 Both alternative exons for the voltage sensor are necessary for healthy flies 35
3.2 Both alternative IS4 exons but not both alternative I-II exons are required for larval and adult motor behaviors 38
3.2.1 Animals lacking IS4A show severely reduced flight initiation 39
3.2.2 Larval crawling distance is significantly reduced in animals lacking IS4 A 44
3.2.3 Exon IS4 A is necessary for successful courtship 46
3.3 Excision of specific alternative exons affects the localization of cacophony in the nervous system 52
3.3.1 Loss of IS4B results in loss of cacophony in the larval VNC, but excision of other alternative exons does not cause differences of cacophony localization in the larval VNC 52
3.3.2 The larval VNC expression patterns are recapitulated in adult VNC 55
3.3.3 Cacophony expression pattens in the *Drosophila* brain are isoform specific 57

3.3.4 Alternative exons for the IS4A locus induce complementary expression pattern in parts of the optic lobes 60
3.3.5 Reduced light responsiveness can be found in animals lacking cacophony in the lamina 63
3.4 Subcellular localization of cacophony in controls and in exon excision mutants 65
3.4.1 Exons I-IIA and IS4A are not required for somatic cacophony expression 66
3.4.2 Larval motor axons carry cacophony in animals lacking IS4A or I-IIA 68
3.4.3 Loss of exon IS4 B abolishes synaptic cacophony in larval NMJ 70
3.4.4 Active zone density per bouton is unaffected by loss of specific cacophony exons 72
3.4.5 Loss of exon IS4A is reflected in altered of colocalization coefficients at the AZ ... 76
3.4.6 Lack of either exon IS4A or I-IIA does not affect somatodendritic cacophony expression in DLM motoneurons 78
3.4.7 Distribution of cacophony along the axon remains unchanged in ΔI-II A and ΔIS4 A, but loss of IS4B also results in loss of axonal cacophony 79
3.5 Exon excisions affect cacophony mediated channel properties 82
3.5.1 Loss of the exons IS4 A and I-IIA has opposite effects on calcium signals in the pupal *Drosophila* motoneuron 5 82
3.5.2 Both, loss of I-II A and IS4A induces APs with double peaks upon somatic stimulation in pupal MN5 85
3.5.3 IS4A and I-IIA do not affect cacophony mediated calcium current amplitude in pupae 88
3.5.4 Loss of IS4A produces lowers HVA threshold in adult *Drosophila* MN5 90
3.5.5 Epilepsy like phenotype in variant with decreased activation threshold in adults . 91
3.5.6 Locomotive defects of loss of IS4A can be alleviated by trans-heterozygous expression of ΔIS4B 93
4 Discussion 98
4.1 I-II locus 99
4.1.1 I-II mediates predominantly redundant functions 99

4.1.2 I-IIA mediates exclusive functions in the visual system on a level of interaction with accessory subunits 100
4.2 IS4 locus 101
4.2.1 IS4B is essential and mediates calcium currents with lowered activation threshold in the adult VNC 101
4.2.2 IS4A operates in sensory processing and is necessary for regular life expectancy 103
4.2.3 IS4 splice isoforms cooperate to generate physiological function 105
4.4 Outlook 106
5. Appendix 116
Salines, buffers and gels 116
Other chemicals and reagents used 118
Ratios of antibody combinations for the different imaging experiments 119
Programs used, version and application 119
Plasmid maps and sequences 121

Abbreviations:

AMMC: antennal mechanosensory and motor center

ANOVA: analysis of variance

AP: action potential

AZ: active zone

bp: base pairs

Brp: bruchpilot

Bss: $para^{bss}$

Cac: cacophony

Cas9: CRISPR associated protein 9

CLSM: confocal laser scanning microscopy

CNS: central nervous system

CPG: central pattern generator

CRISPR: clustered regularly interspaced short palindromic repeat

CS: Canton Special

DLM: dorsolongitudinal muscle

DNA: deoxyribonucleic acid

EPSP: excitatory postsynaptic potential

ER: endoplasmic reticulum

ERG: electroretinogram

sfGFP: super folder green fluorescent protein

gRNA: guide RNA

HVA: high voltage activated

I-II: loop connecting the first and second homologous domain

IS4: fourth transmembrane segment of the first homologous domain

kDa: kilo Dalton

L3: larval stage 3

LVA: low voltage activated

MN: motoneuron

NMJ: neuro muscular junction

P8/9: pupal stage 8/9

PBS: phosphate buffered saline

PBT: phosphate buffered saline with Triton-X

PAM: protospacer adjacent motif

PCR: polymerase chain reaction

RFP: red fluorescent protein

RNA: ribonucleic acid

TBE: tris borate EDTA

TBS: tris buffered saline

TBST: tris buffered saline with Tween20

TTX: tetrodotoxin

UAS: upstream activation sequence

VGCC: voltage gated calcium channel

VNC: ventral nerve cord

1 Introduction

One of the driving factors for neuroscience research is the broad range of neurological diseases without appropriate treatment. The physiological origins of these pathologies are progressively being identified. Many of them could be traced back to pathological changes in ion channel function. Particularly voltage gated calcium channels (VGCCs) and their corresponding channelopathies underlie many different neurological disorders such as epilepsy, autism spectrum disorders, different forms of ataxia, and others (Cain and Snutch, 2011). In the last years evidence has accumulated that some of these channelopathies are due to defects of specific splice isoforms of the relevant VGCCs or the splice regulation of them. Recent studies are still discovering new splice sites and subsequently new variants of those channels (Clark *et al.*, 2020). These defects in splicing and the resulting imbalances in isoform specific expression levels have been studied in many different *in vitro* and analogous expression systems (Lipscombe and Lopez Soto, 2019), usually focusing on one specific disease homologue or defect. Therefore, a more comprehensive study of different isoforms and their functional consequences could provide a better understanding of the physiological interplay between different splice isoforms. Such inter isoform interactions are still largely unknown. *In vivo* studies on specific VGCC gene splice isoforms with functional readouts across different developmental stages, brain parts, and subcellular compartments are sparse.

1.1 Voltage Gated Calcium channels

Neurons receive, compute, and transmit information. Ion channels are a principal regulator of neural activity. Their vast diversity serves adequate fulfillment of an overwhelming richness of different functions. One of the major groups of ion channels are voltage gated channels i.e., membrane pores, which can exist in different opening states. Some of those conformational changes, from one state to another, are dependent on cell membrane voltage. Depending on the specificity of the respective channel, different ions can move across these channels, following the concentration gradient. Among these ions, calcium takes on a special role since it can fulfill many other functions aside from its core function as a charge carrier. Calcium influx into a neuron, can for example trigger exocytosis of synaptic transmitters via the SNARE protein complex (Dolphin and Lee, 2020), function as a second messenger in signaling cascades promoting gene transcription, or instruct neuronal growth via local sub-cellular mechanisms (Lohmann, Myhr and Wong, 2002) to mention but a few. Voltage gated calcium

channels have, therefore, been a focus of many previous studies. In recent years the ultrastructure of primary vertebrate muscle VGCC, $Ca_v1.1$, could be determined (Wu *et al.*, 2016), confirming the assumptions on VGCC configuration which generally is as follows. Voltage gated calcium channels classically consist of different subunits: The central, pore-forming unit is the α1 subunit, whereas the accessory α2δ-subunit may affect channel properties and influences trafficking, localization, and surfacing of the channel (Dolphin, 2013). Another accessory subunit, the β-subunit, is involved in altering the channel properties and acting as a gatekeeper for other interaction partners of the channel, such as calmodulins or G-protein subunits, which in turn are involved in many signaling cascades (Buraei and Yang, 2010, 2013). The accessory γ-subunit is mainly associated with channel trafficking and localization (Klugbauer *et al.*, 2000). These basic rules for voltage gated calcium channels are well conserved across the animal kingdom (Dolphin, 2016).

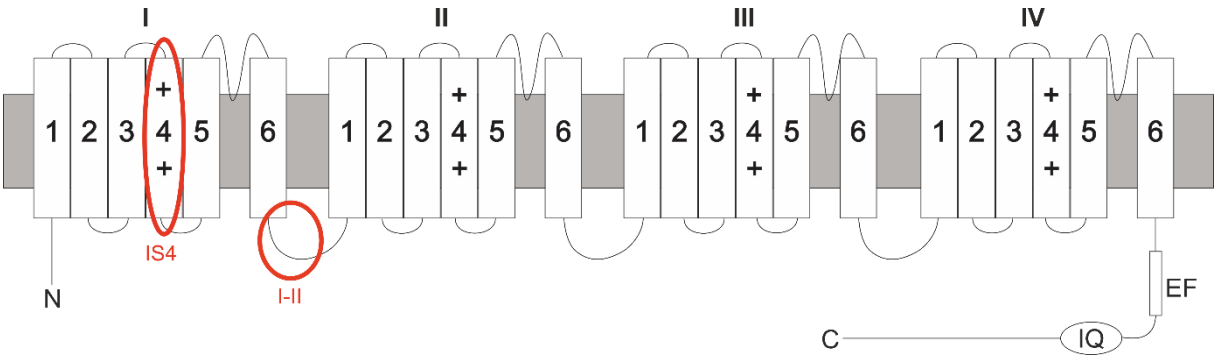

*Figure 1: **Schematic of a VGCC α1 Subunit**, marked in red are the areas of interest for the cacophony VGCC examined further in this thesis.*

In general, α1 subunits of voltage gated calcium channels are a monomer made up of four homologous repeats also called domains as shown in Figure 1. Each of those domains consists of six transmembrane segments (S). The N-terminal, as well as the C-terminal end of these channels, is located intracellularly. Each of the homologous repeats is interconnected with a loop to the next. Transmembrane segments of specific interest in this study are the fourth transmembrane segment in each homologous repeat, which play important roles in voltage sensing, as well as the fifth and sixth segments which together constitute the pore forming part of each homologous repeat. Furthermore, the loop between the homologous repeats I and II is a prominent binding site for accessory subunits such as the β and G-protein βγ subunits. The intracellular C-terminus of the channel, furthermore, contains two other sites of note. Namely the IQ-motif and the EF-hand, both of which are necessary for the interaction

with calmodulin and, therefore, involved in calcium binding (Cens *et al.*, 2006; Christel and Lee, 2012) and calcium dependent inactivation of the channel.

This general configuration of the α_1 subunit is an arrangement found across all three VGCC subfamilies. In vertebrates these families are called Ca_v 1-3. This subdivision is based on phylogenetic similarities and reflected in properties unique to the channel families. The activation voltage, current kinetics and the susceptibility to specific toxins are all factors which can differ in between VGCC subfamilies.

1.2 Voltage gated calcium channels in *Drosophila*

Each of those three vertebrate gene families has a single homologous gene in the *Drosophila* model system. These three genes encoding the *Drosophila* VGCC variants are termed Dmca1A, Dmca1D and Dmca1G. The Dmca1A gene also has more classical *Drosophila*-specific names, originating in mutant phenotypes. This nomenclature is shown in Table 1.

Table 1: Different VGCC genes/families in vertebrates and Drosophila*, high voltage activated (HVA), low voltage activated (LVA)*

Vertebrate Nomenclature	Current Type	*Drosophila* Homolog	Activation Voltage
$Ca_v1.1$	L-Type	Dmca1D	HVA
$Ca_v1.2$			
$Ca_v1.3$			
$Ca_v1.4$			
$Ca_v2.1$	P/Q -Type	Dmca1A; cacophony (cac); nightblind-A (nb-A)	HVA / LVA (cac)*
$Ca_v2.2$	N-Type		
$Ca_v2.3$	R-Type		
$Ca_v3.1$	T-Type	Dmca1G / Dmα1T	LVA
$Ca_v3.2$			
$Ca_v3.3$			

* Ryglewski et al. 2012

1.3 Cacophony

This thesis will focus on investigating the *Drosophila* homologue to the Ca_V2 family, which will be referred to interchangeably with its *Drosophila* name *cacophony*. The name for this gene harkens back to some of the most common impairments for the fruit fly in case of a perturbed cacophony expression. i.e., the courtship song of the fly is affected in a way which impairs its mating success (Von Schilcher, 1976; 1977). Similarly, another less commonly used name for *cacophony* is *nightblind-A*, also rooted in the description of a mutant for this gene, which shows reduced response of the flies to optical stimuli (Smith *et al.*, 1996, 1998). It was later determined that *cacophony* and *nightblind-A* were alleles of the same gene.

Previous studies have shown that the *cacophony* voltage gated calcium channel can mediate a high voltage activated and, contrary to sequence homology based predictions, a low voltage activated current, each with distinctly different kinetics (Ryglewski *et al.*, 2012). These findings could not be clearly linked to any known properties of the protein. Instead, several different possible explanations presented themselves. Mainly it was assumed that either pairing of the α1 subunit with different variants of the accessory subunits, or alternative splicing of the *cacophony* gene could be responsible for such severe effects onto currents. Prior studies have examined the effect and impact of pairing with accessory subunits (Heinrich and Ryglewski, 2020). In contrast, this thesis focuses on the impact alternative splicing could have on the currents mediated by the *cacophony* gene products. Other post-transcriptional modifications such as A-to-I pre-mRNA editing were already tested in this context and did not produce alterations in current properties strong enough to explain the observed effects (Stefanie Ryglewski personal communication).

1.4 Alternative splicing

Splicing is a common mechanism to edit pre-mRNA after its transcription and before converting it into fully prepared mRNA with a poly-A tail and caps needed for mRNA stability and targeting of the mRNA. One of the main classical benefits of splicing is the increase in functional gene products without the need to encode each of them individually. Splicing generally occurs in several ways, primarily, to remove the noncoding introns in between the coding exons to produce an uninterrupted template for transcription. This simple excision of the introns can be more complex, for example in cases in which not all exons are present in all gene products of one gene. This is called alternative splicing, where on top of the removal

of introns some exons are also removed from the pre-mRNA, broadening the possible gene products from one gene. Lastly, there is a specific sub-variant of this, in which two exons can occupy the same spot in the mRNA but are never expressed at the same time. This mutually exclusive form of alternative splicing can also be seen in the *cacophony* gene. Fundamental studies into the general makeup of the *cacophony* gene, its exons, introns and splice sites have revealed at least two sites for mutually exclusive alternative splicing (Peixoto, Smith and Hall, 1997; Kawasaki, Collins and Ordway, 2002).

1.5 Mutually exclusive alternative splice sites in *cacophony*

As shown in Figure 1, two splice sites in the *cacophony* gene are of specific interest for this thesis. Namely the alternative exons spanning the voltage sensor of the first homologous repeat, located in the fourth transmembrane segment (IS4). The other site of relevance for this thesis is the intracellular loop linking the first and second homologous repeats (I-II), which provides a site for VGCC β-subunit or G-protein βγ-subunit binding. Due to their properties regarding voltage sensing(IS4) or subunit binding(I-II) ,these alternative exons are likely to have a substantial impact on channel kinetics and could thus explain the sustained HVA and transient LVA currents mediated by *cacophony* as shown in Ryglewski et al 2012. For both splice sites relevant to this thesis there are two exons present in the genome which can be alternatively incorporated into the mRNA. Furthermore, both exons in both locations can be found in the official annotation of the fly genome. For the remainder of this thesis, I will refer to the 6th exon of *cacophony* as IS4A, while IS4B refers to the 7th exon of *cacophony*, similarly I-IIA refers to exon 11, while I-IIB refers to exon 12. The *cacophony* gene currently (flybase version 6.40) has 40 annotated exons Considering all the variations for the UTRs and combinations of coding exons, a total of roughly 23000 putative cac mRNAs are possible. So far, in flies only 18 of these variants could be found. These variants, as well as their respective exon combinations are presented in Table 2.

***Table 2: cacophony transcripts currently annotated on flybase**, identifying the exon inclusion for the splice sites of interest to this thesis. IS4A (exon 6, X: 11979055 – 11979155); IS4B exon nr 7, X: 11977462 – 11977562); I-IIA (exon nr11, X: 11975746 – 11975861); I-IIB (exon nr 12, X: 11974224 – 11974339).*

Transcript Title	Flybase Identifier	IS4 Variant	I-II Variant
cac-ra	FBtr0307318	B	A
cac-rb	FBtr0307321	A	A
cac-rc	FBtr0307317	B	B

cac-rd	FBtr0307319	A	B
cac-re	FBtr0307322	B	A
cac-rf	FBtr0307320	A	B
cac-rg	FBtr0307313	A	B
cac-rh	FBtr0307314	B	A
cac-ri	FBtr0307315	B	A
cac-rj	FBtr0307316	A	B
cac-rl	FBtr0307323	B	A
cac-rm	FBtr0307324	B	A
cac-rn	FBtr0307325	B	A
cac-ro	FBtr0308609	B	A
cac-rp	FBtr0332391	B	A
cac-rs	FBtr0474239	B	B
cac-rt	FBtr0474240	B	B
cac-ru	FBtr0474241	B	B

1.6 Channelopathies associated with VGCC splicing

As briefly stated above, in humans, many channelopathies, diseases or pathological effects are associated with defects in voltage gated calcium channels (Ashcroft, 2006; Zamponi *et al.*, 2015; Striessnig, 2016). There are several subsets of channelopathies which are specifically the result of one alternative splice variant harboring an aberrant exon or some other kind of genetic defect such as a premature stop or other missense mutations. This is the case for spinocerebellar ataxia type 6 in which exon 47 carries a polyglutamine expansion ((CAG)n) and is expressed disproportionally more frequent in patients as compared to healthy controls (Liao, Zhang and Soong, 2009; Du *et al.*, 2013). This limitation of the aberrant phenotype to only a few of the gene products of the affected gene can lead to the varying onsets and degrees of severity (Adams *et al.*, 2009).

1.7 Aims of this study

This study aims to elucidate the distinct roles and interactions of different VGCC splice isoforms in an organism wide context at the example of the *Drosophila* VGCC *cacophony*.

The first hypothesis of this study is that cacophony splice variants indeed mediate different

channel properties. Secondly, some but not all these splice isoforms of cacophony are necessary for the animal's survival. Thirdly, some of the splice isoforms could fully or at least in part compensate for one another, in case of loss, thereby serving a degenerate (Edelman and Gally, 2001) function. In addition to these possible degenerate functions splice variants might mediate very specific properties, not essential for survival. Lastly, it could be possible that some of the individual splice isoforms cooperate, be it through different localization or varying gating properties, to mediate survival and full behavioral range of the animals.

Specific predictions:

Different splice variants mediate different channel properties and localizations

> Previous data could show different currents mediated by cacophony across different developmental stages and moreover with different properties in the same cell (Ryglewski *et al.*, 2012; Ryglewski, Kilo and Duch, 2014). Therefore, I would expect that some of the cacophony isoforms show different properties to mediate these currents. For example, the location of a splice site resulting in one of the voltage-sensing domains (IS4) could mediate the different activation voltages observed. Variation in the splice site resulting in the loop connecting the first and second domain (I-II) could affect the coupling with accessory subunit and thereby influence other gating properties. Additionally, possibly different properties could be necessary at different subcellular locations or even in different tissues altogether, thereby suggesting varying expression patterns for different isoforms.

Only a subset of cacophony isoforms is sufficient for survival of the animals.

> A lethal null mutation of cacophony can be rescued via expression of a single isoform (cac^1 (Kawasaki, Collins and Ordway, 2002)). Therefore, I would expect any subset of cacophony isoforms, including the exon combination in cac^1, to be sufficient for general survival of animals. Whether other exon combinations are capable of the same will be addressed in this thesis. Due to the localization of cac^1 at the presynaptic active zone in the *Drosophila* neuromuscular junction I would expect any other isoform variations capable of rescuing lethality to also be found in this location as well.

Some cacophony isoforms can compensate for one another

Due to the number of different isoforms known for cacophony and the high similarity among them, it is likely that some can, in part, compensate for the loss of one another. This compensation could be taking place via classical forms of degeneracy among the different isoforms (Edelman and Gally, 2001).

To test for these putative isoform functions, I employed two main experimental approaches to generate these different isoforms. Firstly, the generation of transgenic animals expressing only one of the various isoforms and examining their function in a *cacophony* null background, in short, a knock-in strategy. Secondly, an exclusion approach by removing the capabilities to produce specific isoforms was conducted. These newly generated isoform-reduced variants/single-isoform variants would then be characterized in different behavior assays; additional functional assessment was done via electrophysiology. Lastly, the localization on cellular and subcellular level was assessed by immunohistochemistry to pinpoint their specific differences and commonalities.

2 Material and Methods

2.1 Fly keeping

2.1.1 General fly rearing

Flies were raised in plastic vials (diameter: 2cm) on a cornmeal yeast agar, on a 12-hour light/dark regimen at room temperature (25°C). Stocks for long term storage were kept at 18°C and but shifted to RT for a generation before conducting experiments.

2.1.2 Common fly stocks used and crossing schemes

2.1.2.1 Stocks

Table 3: persistent fly stocks used in the thesis

Shorthand	Genotype	Supplier/origin	Additional notes
CS	Canton Spezial		Common laboratory strain
Cac^{sfGFP}	$\frac{cac^{sfGFP}}{cac^{sfGFP}};+;+;+$	this study	Loss of w^- by crossing over from $cac^{sfGFP\text{-}N}$ (Gratz *et al.*, 2019)
Cac^{sfGFP} ΔIS4 A	$\frac{cac^{sfGFP\ \Delta IS4\ A}}{cac^{sfGFP\ \Delta IS4\ A}};+;+;+$	this study	CRISPR mediated genomic excision of the IS4 A exon
Cac^{sfGFP} ΔI-II A	$\frac{cac^{sfGFP\ \Delta I-II\ A}}{cac^{sfGFP\ \Delta I-II\ A}};+;+;+$	this study	CRISPR mediated genomic excision of the I-II A exon
Cac^{sfGFP} ΔI-II B	$\frac{cac^{sfGFP\ \Delta I-II\ B}}{cac^{sfGFP\ \Delta I-II\ B}};+;+;+$	this study	CRISPR mediated genomic excision of the I-II B exon
Cac^{sfGFP} ΔIS4 B	$\frac{cac^{sfGFP\ \Delta IS4\ B}}{FM6\ B};+;+;+$	this study	CRISPR mediated genomic excision of the IS4 B exon
Cac ΔIS4 A	$\frac{cac^{\Delta IS4\ A}}{cac^{\Delta IS4\ A}};+;+;+$	this study	CRISPR mediated genomic excision of the IS4 A exon
Cac ΔI-II A	$\frac{cac^{\Delta I-II\ A}}{cac^{\Delta I-II\ A}};+;+;+$	this study	CRISPR mediated genomic excision of the I-II A exon
Cac ΔIS4 B	$\frac{cac^{\Delta IS4\ B}}{FM6\ B};+;+;+$	this study	CRISPR mediated genomic excision of the IS4 B exon

Cac^{tagRFP}	$\frac{cac^{tagRFP}}{cac^{tagRFP}}; +; +; +$	this study	Loss of w^- by crossing over from $cac^{sfGFP\text{-}N}$ (Gratz *et al.*, 2019)
Cac^{tagRFP}ΔIS4 A	$\frac{cac^{tagRFP\ \Delta IS4\ A}}{cac^{tagRFP\ \Delta IS4\ A}}; +; +; +$	this study	CRISPR mediated genomic excision of the IS4 A exon
Cac^{tagRFP}ΔI-II A	$\frac{cac^{tagRFP\ \Delta I-II\ A}}{cac^{tagRFP\ \Delta I-II\ A}}; +; +; +$	this study	CRISPR mediated genomic excision of the I-II A exon
Cac^{tagRFP} ΔIS4 B	$\frac{cac^{tagRFP\ \Delta IS4\ B}}{FM6\ B}; +; +; +$	this study	CRISPR mediated genomic excision of the IS4 B exon
bss^1	$\frac{para^{bss\ 1}}{para^{bss\ 1}}; +; +; +$	Ganetzky and Wu, 1982	
bss^2	$\frac{para^{bss\ 2}}{para^{bss\ 2}}; +; +; +$	Ganetzky and Wu, 1982	
cac^{H18}	cac[H18]	Bloomington stock center #: 42245	
Cac^1	+;+;P{w[+mC]=UAS-cac^1-EGFP}786C	Derived from Bloomington stock center #: 8581	
TBX-0002	y1 v1 P{nos-phiC31\int.NLS}X; attP40 (II)	NIG-FLY #: TBX-0002	Landing site for gRNA plasmids
Cas9	$+; \frac{attP40\{nos-Cas9\}}{CyO}$	This study	Based of NIG-FLY #: CAS-0001
Cac^{tagRFP} Cas9	$Cac^{tagRFP}; \frac{attP40\{nos-Cas9\}}{CyO}$	This study	Based of NIG-FLY #: CAS-0001
Cac^{sfGFP} Cas9	$Cac^{sfGFP}; \frac{attP40\{nos-Cas9\}}{CyO}$	This study	Based of NIG-FLY #: CAS-0001
	$\frac{vnd^{mutant}}{FM6B}; \frac{sna\ Sco}{CyO}$	Made in the lab	Double balancer stock vnd is homozygous lethal

	$y^2cho^2v^1; \frac{sna^{Sco}}{CyO}$	Made in the lab	Derived from NIG-FLY#: CAS-0001

2.1.2.2 Common crosses

2.1.2.2.1 Putative integrase success isolation

y1 v1 P{nos-phiC31\int.NLS}X; attP40{gRNA?} X $y^2cho^2v^1; \frac{sna^{Sco}}{CyO}$

Offspring is screened for rescue of vermillion eyes, if unsure, further back cross with y^2 cho^2 v^1; $\frac{sna^{Sco}}{CyO}$ leads to easily identifiable dark eye color due to cho^2 but rescued v^1 in stark contrast to regular vermillion eyes in animals without plasmid integration.

2.1.2.2.2 Exemplary CRISPR crossing scheme

1. $+; \frac{attP40\{nos-Cas9\}}{CyO}$ X $\frac{y^2cho^2v^1}{Y}$; attP40{gRNA}
2. $\frac{vnd^{mutant}}{FM6B}; \frac{sna\ Sco}{CyO}$ X $\frac{+}{Y}; \frac{attP40\{nos-Cas9\}}{attP40\{gRNA\}}$
3. $\frac{+\ cac^{excision}}{FM6B}; \frac{attP40\{nos-Cas9\} or\ attP40\{gRNA\}}{Cyo}$ X $\frac{FM6B}{Y}; \frac{sna\ Sco}{CyO}$

Virgin female offspring of the 2nd cross are individually paired with the males to have the same kind of deletion in all further offspring. After the females of the third cross have laid eggs, they can already be used for sequencing possible exon deletions.

4. $\frac{+\ cac^{excision}}{FM6B}; \frac{sna\ Sco}{CyO}$ X $\frac{+\ cac^{excision}}{Y}; \frac{sna\ Sco}{CyO}$

The offspring of the 3rd cross can be used to establish as stock such as shown in the 4th cross. If the deletion is lethal the only male offspring found is carrying the x-chromosomal balancer.

2.2 Molecular biology

2.2.1 Standard molecular techniques employed in this thesis

2.2.1.1 Restriction digests

For classical molecular biology restriction digests were performed to generate the plasmids/constructs carrying specific isoforms of cacophony corresponding to a single cDNA. Furthermore, they were employed in the generation of the gRNA carrying plasmids. Usually one or more restriction enzymes were chosen, corresponding to the desired cleavage sites

flanking the parts of the DNA needed. Here the restriction enzymes can affect the needed buffers and temperature for the digest.

A standard restriction digest is as follows: A total rection volume of 50µl consists of 5µl 10x reaction buffer (e.g.: CutSmart (NEB, # B7204S)), 1ng of target plasmid (volume varies depending on concentration), ddH_2O and lastly the restriction enzyme(s) (volume varies depending on the efficiency of the enzyme, although often 1µl is sufficient). The ddH_2O, the buffer, the plasmid and lastly the enzyme are added into a tube while on ice. The tube is then put into a water bath or a thermoblock. Temperature and duration vary depending on the specific enzymes used. After the incubation the mixture is run on a regular electrophoresis gel to separate the different fragments by size.

2.2.1.2 Gel-electrophoresis

To isolate the results of restriction digests or PCRs standard gel electrophoresis is employed. Here, an agarose gel, usually 0.7-0.8% in TBE (see appendix) is cast in a standard gel casting chamber, with a comb inserted to produce the wells which are loaded later. The agarose TBE mixture can easily be melted in a microwave. After the gel has cooled down a little and shortly before casting GelRed (VWR, #: 41003) is added to the gel, to visualize the DNA afterwards. After the cast gel is hardened it is transferred into an electrophoresis chamber filled with TBE. The samples are loaded into the wells after they have been mixed with a loading dye (e.g.: NEB, #: B7025S). A DNA ladder (e.g.: NEB. #: N3232S) is also loaded into at least one of the wells to accurately judge the size of the DNA fragments afterwards. The power source is connected, and the electrophoresis started. The runtime of the gel varies depending on the expected size of the DNA bands. The gel is now analyzed in a gel documentation device (e.g.: EBOX VX5, Peqlab), the gel can be imaged for documentation purposes and if the fragments are needed for further experiments, they can be excised from the gel.

2.2.1.3 DNA extraction from gel slices

DNA is extracted from gel slices by using a commercially available gel extraction kit (QUIAGEN, #: 28704). Here, the gel is melted, the DNA then bound to membrane, washed, and again extracted from the membrane by elution.

2.2.1.4 Primer design

Primers for this study were designed in silico. Depending on the need for the primer different parameters were considered. For primers needed to extract and amplify specific gene regions

of the fly genome for example primer pairs were chosen to have similar melting temperatures. General requirements for the primers were a CG rich beginning and end to improve primer binding to the template, most primers were chosen with a total length of 18 - 22 nucleotides, additionally a GC-content of roughly 60% was chosen. If possible, the primers were also selected to have little to none self-dimerization or in case of primer pairs if anything only little hetero-dimerization. These general guidelines were respected as rigorously as possible. Although often the need for specific sequences, particularly when amplifying fragments of DNA for further use, limits the primer section noticeably. Any primers used in this study were then ordered from integrated DNA Technologies or Sigma (MERK).

2.2.1.5 PCR

Regular Polymerase Chain Reaction (PCR) was employed to isolate and amplify specific gene fragments from genomic or plasmid DNA. All PCRs were performed using a standard Thermocycler (T-Gradient, Biometra). Depending on the desired quality of the PCR product different polymerases were chosen. If the PCR product was intended for further cloning or sequencing a polymerase with lesser likelihood of errors was employed (Phusion, NEB #:M0530S). If the PCR product only needed to verify the presence of a construct via gel electrophoresis a cheaper not as rigorous polymerase (Taq – Polymerase/ NEB, #M0267S) was sufficient.

Table 4: standard PCR protocol for either Taq or Phusion polymerase

Temperature [°C]	Duration	# of Cycles	notes
95	30 secs	/	Initial denaturation
95	15 sec	25-35 cycles	Denaturation per step
* (varies for different primers)	~30 sec		Annealing temperature
68 (Taq) 72 (Phusion)	1 min per kb 30 sec per kb		Extension time
68 (Taq) 72 (Phusion)	5 min	/	Final extension
4-10	∞ Until manually ended	/	Holding temperature

2.2.1.6 Ligation of plasmids

To determine the amount of vector and insert needed for ligations the following formula was used: (kb of insert/kb of vector) ×ng of vector=ng of insert

If possible, the ratio of 3:1 in favor of the insert was used to maximize ligation efficiency. To ligate vector and insert, a standard total reaction volume would be 20µl. This consists 2µl of the 10x ligation buffer (e.g.: T4 Ligase Reaction Buffer NEB, #: B0202S), the vector and insert and 1µl ligase (e.g.: T4 Ligase, NEB, #: M0202S), the remaining volume is filled up with ddH_2O. The rection mix is assembled on ice. The ligation itself is then carried out overnight at 16°C or at room temperature for 2 hours, before transformation the ligase needs to be inactivated by heating the mixture to 65 °C for 10 minutes.

2.2.1.7 Transformation of bacteria

Plasmid amplification was done via transformation of Bacteria with the plasmid of choice and letting the bacteria grow overnight on plates. Individual bacteria colonies were then used to inoculate a bigger volume of media to produce bacteria quantities necessary for substantial plasmid yield. Here mostly, chemically competent Dh5α bacteria were used.

The fully ligated plasmid is added to the Dh5α bacteria, which have been thawed on ice. The suspension is incubated for 30 minutes on ice. Afterwards the bacteria suspension is heat-shocked at 42°C for 35-45 seconds and put back on ice for 2 minutes. ~500ml of SOC media are added to the bacteria suspension which is then incubated at 37°C for additional 1-2 hours. ~100ml of the resulting bacteria suspension is plated on an agar-LB-media plate containing an antibiotic against which the transformed plasmid confers resistance. The plate is incubated at 37°C overnight. If a low yield of transformed bacteria is expected the remaining suspension can be briefly and gently spun down in a tabletop centrifuge (10000 rpm for 4 min) afterwards the resulting pellet can be resuspended in only 100µl of the suspension and then also streaked on a LB-media plate. On the following day individual colonies of bacteria containing the plasmid should have grown. These colonies can then be picked with a sterile pipette tip to further inoculate 4ml of LB media, again treated with the antibiotic corresponding to the plasmid's resistance. After 16-18 hours at 37°C on an orbital shaker (220 rpm) these bacteria can then be used to make a glycerol stock for further preservation of the bacteria stock or used to inoculate a bigger volume of media for a bigger yield, or lastly for extraction of the plasmid from the bacteria in a small scale. If used for a bigger volume, a 1 l conical flask was

filled with 250 ml LB media with the corresponding antibiotic and incubated on an orbital shaker (220 rpm @37°C) for 18h before plasmid isolation.

2.2.1.8 Plasmid isolation

To extract the now amplified plasmid DNA form bacteria plasmid isolation was done using commercially available kits. Depending on the volume a miniprep (4ml) (Quiagen. #: 27104) or a maxi prep (250ml) (Quiagen, #: 12143) was done.

Pellets produced by the kits were resuspended in nuclease free ddH_2O, with ~50µl for the minipreps and 150-500µl for the midi prep. Here, as little water as possible was used to keep the plasmid concentration high. The quality of the extracted plasmid was verified using a UV-Vis Spectrophotometer (e.g., NanoDrop 1000).

2.2.1.9 Genome preparation

To extract genomic DNA from individual flies a short extraction protocol was used. Here, individual flies were put into a 0.5ml tube. Proteinase K (Invitrogen, #: 25530049) was added to squishing buffer (see appendix) for a final concentration of 200µg/ml proteinase K. Flies are squashed with a pipet tip containing 50 µl of the squishing buffer proteinase mix. After the fly is homogenized, the remaining buffer is expelled into the tube and the mixture is incubated for 30 minutes at 37°C. afterwards the proteinase is inactivated by a heat shock in a 95°C water bath for 2-3 minutes. The extracted DNA can now be used for PCR, sequencing, or other downstream applications. This mixture keeps for several months if stored properly at 4°C.

2.2.1.10 Sequencing

For genomic or plasmid DNA sequencing an external sequencing service (StarSEQ® GmbH) was used.

2.2.1.11 Western blotting

To verify the protein expression of the cacophony variants generated in the following western blotting was performed. Here, brains of the different genotypes were used as the tissue samples used. Brains of the animals were extracted, similar to the preparation for the imaging (see below 2.4.1.1.), in PBS and collected into 6xSDS (see appendix) buffer. The brains were homogenized and afterwards boiled for 10 minutes at 96 °C. They could now be stored at -20°C before application of all samples to the gel. The western gel was poured in two steps with the running gel (see appendix) and the stacking gel (see appendix) on top afterwards. The

samples were loaded into the wells with 20µl homogenized sample and 10µl protein marker per lane. The gel was run with a voltage of 100V. After running the gel was transferred onto a nitrocellulose membrane overnight (at 4°C & 30V) using a standard blotting chamber, submerged in transfer buffer (see appendix). Following blotting the membrane was cut into two around the 80kDa. Both parts of the membrane were then washed 3x20min with TBST (see appendix). Afterwards the membranes were blocked with 10% skim milk -TBST for 2 hours. After washing with TBST like before, again for three times á 20 minutes, the membranes were incubated individually with primary antibody (the part with the heaver molecular weights: rabbit anti-GFP 1: 1000; the lower molecular weights: mouse anti-actin: 1:1000) eluted in 2.5%dried milk-TBST overnight. The next day the unbound antibody was washed off by washing with TBST three times for 20 minutes. The secondary antibody (heavy molecular weights: goat anti-rabbit IgG HRP 1:10000; lighter molecular weights: goat anti-mouse IgG HRP: 1: 5000 each diluted in TBST) was applied for 2 hours at 25°C before washing again three times for 20 minutes each in TBST and once for additional 20 minutes in TBS. Lastly, before analysis the membranes were incubated in Immobiolon Western Chemiluminescent HRP substrate (Milipore, #: WBKLS0500) for 2-3 minutes. The membranes were now imaged using a Software Odyssey Fc Imaging System with an exposure time of 4 minutes.

2.2.2 Transgenic fly lines carrying specific isoforms of *cacophony*

2.2.2.1 Approach

Initially I planned to express individual Isoforms using the classical GAL4/UAS conditional expression system well established in *Drosophila* and perform my assessment of the specific isoforms in a null background or in specific cell types. The isoforms needed for this approach were unfortunately not readily available and therefore needed to be constructed. The only transgene expressing a single isoform was UAS-cac^{1} (Kawasaki, Collins and Ordway, 2002). This isoform carries the B variant for both exon sites of interest to this thesis. The strategy to clone the constructs containing the other isoforms was based on modifying the existing plasmid of cac^{1} to instead contain one of the other three combinations for this locus.

2.2.2.2 Tried methods

To generate these UAS Gal4 plasmids I used the original UAS- cac^{1}-GFP vector initially produced by the Ordway lab as a template. Initial cloning steps were aimed at subcloning the UAS- cac^{1} into a new vector, with a new GFP tag at the N-terminus of cac^{1} instead of the

already existing C-terminal tag. This was done to reduce the putative effects the GFP tag could have on cacophony function, since as explained above, the C-terminus of VGCCs can influence the gating properties. After some adjustments in PCR fragment size, such as splitting the cacophony cDNA into several pieces and reassembling them after removal of the C-terminal GFP and subsequent addition of the N-terminal cacophony the first cloning steps worked as expected. Every time the final assembly of n-terminally tagged cacophony was done, no positive colonies could be detected. This persisted through many different cloning approaches, such as different cloning patterns, e.g., adding only the terminal parts last or joining the construct in the middle, different bacterial strains, such as standard Dh5α, JM108 or other more robust bacterial strains as well as different cloning techniques, from restriction digests to assembly-based systems from different suppliers. Assuming this failure to transform the final cacophony was due to some unforeseen secondary structures, I also tried single base exchanges of nucleotides in parts of the N-terminally tagged cacophony to reduce the likelihood of this occurring while keeping the resulting amino acid sequence intact. Simultaneously developed cacophony expression plasmids (B. Altenhein, JGU Mainz/ University of Cologne) containing some introns to circumvent the lethality to the bacteria did also seldomly yield bacterial colonies and no functional fly lines after injection. Ultimately none of these attempts was able to reliably produce a novel transgenic cacophony fly line. Therefore the different intermediate steps of plasmids, oligos and bacterial colonies, albeit possibly useful in future cloning applications were not of use for this thesis.

2.2.3 Crispr design

The originally intended primary approach for this project, to generate individual transgenic animals expressing only one isoform in a null background, did not work as intended. All the different cloning steps undertaken did not yield a strong enough bacterial culture to amplify potential transgenic constructs, as described above. Therefore, the secondary approach, the exclusion approach mentioned in the introduction became the primary approach. Here the CRISPR/Cas9 system (Doudna and Charpentier, 2014; Sternberg and Doudna, 2015) was used to edit the genomic DNA of the animals, as described in the following. Here, a short RNA fragment, the guide RNA (gRNA) complement to a part of the target DNA is designed and deployed into the animal while simultaneously also providing the Cas9 enzyme. This enzyme performs the cleavage itself after being directed to the cleavage site by the aforementioned gRNA. This process has been streamlined for easy manipulation of genomic DNA. The system

works in autosomal as well as in gonosomal cells. Here CRISPR /Cas9 is employed to excise specific exons from the fly genome. Effectively reducing the total amount of possible splicing results. CRISPR /Cas in *Drosophila* can be done in several different ways for the actual application, many of which have been discussed previously (Gratz *et al.*, 2013; Bier *et al.*, 2018). The CRISPR delivery method used in this thesis generates permanent transgenic fly lines expressing the gRNAs needed for the excision of one specific exon in the germline. These fly lines are then crossed to a fly line expressing the Cas9, also in the germline. CRISPR events then occur in the gametes of these animals. The offspring of this acute cross is then balanced on the first chromosome, to account for potentially lethal exon excisions. These putative exon excision animals are then screened via PCR for loss of the desired exon. The main advantage of this method is the ease of use as soon as the gRNA lines are established. For the crosses and the scoring of offspring only basic *Drosophila* handling skills and standard molecular methods are needed.

2.2.3.1 Determining possible cleavage sites and gRNA design

Possible cleavage sites for the CRISPR driven double strand breaks were chosen using by examining the intronic region surrounding the exon destined to be removed. Here several factors were key in deciding on the specific site. First and foremost, the eligibility for Cas9 cleavage was assessed, core needed properties are the protospacer adjacent motif (PAM) NGG flanking the 20bp gRNA to facilitate the site recognition, and a 5' G as the vector used for gRNA expression later used the U6 promotor. Conveniently this is easily possible via online tools such as the CRISPR optimal target finder (Gratz *et al.*, 2014, http://targetfinder.flycrispr.neuro.brown.edu/index.php) and the Cas9 target finder (https://shigen.nig.ac.jp/fly/nigfly/cas9/cas9TargetFinder.jsp). These requirements already limit the eligible sites, among those specific care was applied to not disrupt the recognition sites for the splice machinery. Therefore, sites for double strand breaks were picked at a distance from the intron exon borders to not affect the splice acceptor sites. Furthermore, they were also removed from sites known to impact splice efficiency (Blanchette, 2005; Brooks *et al.*, 2011). After following these principles, I also selected the sites to for minimal loss of total genomic region and picked the gRNA sequences with as little as possible predicted off-target cleavage sites. Lastly, the double strand break and the subsequent non homologous end joining are expected to often delete more than only one nucleotide. This needs to be taken into account when planning the break site particularly close to relevant parts of the

genome. Whether the final site is oriented in + or – direction is irrelevant for the generation of simple double strand breaks. For each of the four target exons a pair of gRNAs was needed, which was picked following the guidelines stated above.

2.2.3.3 construction of gRNA vectors for injection

The construction of the gRNA vectors was done accordingly to the protocols provided on NIG-FLY (https://shigen.nig.ac.jp/fly/nigfly/cas9/protocols.jsp). For each gRNA two oligomers were designed, one for the top and one for the bottom strand. A 4 base pair long CTTC sequence needs to be added in front of the 5' end of the 20 nucleotides starting with a G which are also flanked with a 3' NGG. On the complimentary strand a AAAC sequence is added 5' of the sequence. These two oligos are then annealed by heating 4µl of each oligo with a concentration of 100µM together with 2µL of polymerase buffer (e.g., Phusion HF Buffer (NEB)) to 95°C in a heat block and then letting it cool down back to room temperature. The overhangs adjacent to the gRNA sequence are corresponding to the overhangs generated by the BbsI restriction enzyme (NEB, #: R0539S). This enzyme is used to open the pBFv-U6.2 and pBFv-U6.2B vectors (Kondo and Ueda, 2013, see appendix), which contain the remaining scaffolding for a gRNA as well as the U6.2 promotor which is active in the *Drosophila* germline. The gRNA template for one of the double strand breaks is then ligated into the open pBFv-U6.2 vector while the other double strand break needed for the exon excision is ligated into the B variant of the same vector. To reduce the amount of individual transgenic loci in the flies the gRNA was shuttled with promotor and scaffold via *NotI* and *EcoRI* from pBFv-U6.2 into pBFv-U6.2B, resulting in one vector carrying both gRNAs. The resulting vector is then injected into flies (either BestGene or in the lab) via ϕC31-integrase e.g., at the attP40 locus. Additionally, these vectors carry a fragment of the vermillion gene, which rescues the *Drosophila* eye color variation associated with a mutant vermillion locus, thereby functioning as an easily scoreable marker for successful integration of the inserts.

These flies carrying the gRNAs are crossed to a fly line containing germline driven Cas9 (*nos*-Cas9). Their offspring, now housing both the gRNA and Cas9, are crossed into a balancer line, immediately separating Cas9 and the gRNAs to prevent continuous CRISPR events. These flies are screened for possible CRISPR mediated double strand breaks. This method, albeit initially more time consuming then directly injecting the Cas9 flies with the gRNA plasmid, is more reliable and easier to repeat if needed.

2.3 Behavioral paradigms

2.3.1 Larval Crawling

Foraging L3 larvae were collected and put into a 1.5ml Eppendorf tube to starve for 5 minutes. After the starvation period they were put into a crawling arena, consisting of a 1% agar/aqua dest. crawling pad with a diameter of 10cm. This crawling pad is freshly poured each recording session. The larvae are then put into the middle of the arena, filmed with a camera (Basler 2000) for 3 minutes with a framerate of 4 frames per second and recorded with pylon viewer (Version 5/6). After crawling the larvae can then be kept for further experiments or discarded. The movies produced in this manner are analyzed via the open-source program Tracker (https://physlets.org/tracker,version 5.1.5).

2.3.2 Courtship success

Initial courtship success studies were performed in a standard courtship array consisting of a main chamber and separating plastic sliders. Here, virgin females and virgin males were put into the courtship chambers separately and brought together only after a refractory period of 10 minutes to allow for acclimatization of the flies with the new environment the plastic panel separating the pairs was removed and the time was stopped till successful courtship was observed. If no courtship success could be observed after 10 minutes the experiment was aborted and the time to court was set at greater than 600 seconds.

2.3.3 Courtship Song

Similar to the courtship success recordings, virgin flies of both genders were put into a courtship chamber. This time the chambers allow only for a single fly pair and have a hole in the courtship arena, which is covered with a fine nylon net. This design allows the courtship song produced by the male flies to be recorded by the microphone paced below the courtship chamber. Again, a time of 10 minutes is used to acclimatize the flies to this new environment. The recording setup is placed in a soundproof box (Bachelor thesis Tom Vierus 2013) to reduce noise from outside the recording setup. Furthermore, a second microphone is put up in the soundproof chamber to record remaining noise for later subtraction from the courtship track. A camera is placed on top of the mating chamber to enable video feedback while recording. The flies are then brought together over the microphone and the soundproof chamber is closed. Simultaneously the recording is started. After 10 minutes the recording is stopped. The recording itself ids done via a self-built microphone (Bachelor Thesis Vierus 2013), hooked

up to a digitizer (AD Instruments, Powerlab/4SP) which feeds into a PC running Lab Chart (AD Instruments, Version 7). The sampling rate chosen for the recordings is 40000Hz. A video is in parallel recorded using a simple USB camera (Digital Microscope camera 9MP, Conrad Components).

Analysis of the recorded traces is done via the program Spike 2 (Version 7.20), although the data is filtered once before analysis, this is done in ClampFit (Version 10.7) with a Bandpass filter (Bessel 8-pole, low pass 90Hz, high pass 300Hz).

2.3.4 Flight initiation & inflight muscle recordings

After cold induced immobilization flies were glued to a tungsten hook with an UV-glue (Super Glue Corporation). This hook is placed between thorax and head to allow the fly unhindered stationary flight. The glue is hardened by illumination with UV light for 50 seconds. The tethered flies are now given an air puff as a stimulus to initiate flight. The fly is now mounted in a way that the wing passes through a light barrier with every beat, allowing the recording of the wing beat frequency. To also get a measure of the motoneuron firing responsible simultaneously also a sharpened tungsten electrode is introduced dorsally into the thorax to record the excitatory post synaptic potential of the DLMs 4-6. Since DLM 4 is innervated by MN4 and DLM 5&6 together by MN5 the changes in membrane potential indirectly allow an assessment of the motoneuron firing frequency (Ikeda, Koenig and Tsuruhara, 1980). The whole setup us grounded with an electrode in the abdomen of the fly. The signal detected by the recording electrode is fed into a differential amplifier (A-M Systems, Model 1700), where the signal is amplified a hundred-fold and filtered with a high pass filter (500Hz) and a lowpass filter (100Hz). The signal is then converted fed through a digitizer (Micro1401-3) and recorded with Axoscope and analyzed with spike 2 (version 7.20).

2.3.5 Climbing assay

Two to four days old adult flies were put in a fly vial. The fly was banged to the bottom of the vial and their climbing speed along the wall of the vial, following their inverse geotaxis was measured. This was done by recording their climbing with the same camera setup already described for the crawling assay (see above). To quantify the distance climbed a ruler was glued next to the vial. Recording frame rate was 33 frames per second. To estimate climbing speed the frames per distance were counted and transformed into cm per second. These data were analyzed in Microsoft Excel and GraphPad Prism.

2.4 Imaging

2.4.1 Immunohistochemistry

2.4.1.1 Adult brain preparation

Whole mount preparations were performed as explained in Williamson and Hiesinger, 2010. The fly is cooled or anesthetized via CO2, then the head is removed from the rest of the body. Fine forceps are used to tear the cuticle along the middle of the head, allowing for removal of the retina. This reduces potential auto fluorescent background from remaining rhodopsin in the retina. Special care was taken to preserve the lamina layer when removing the retina. Lastly any clearly visible trachea is also removed to prevent the brains from floating up in the subsequent immunocytochemical washes. The preparation is performed in the extracellular saline used for adult patch clamp experiments to reduce damage potential to the tissue. The brains are collected into a 1.5 low protein bind Eppendorf tubes containing saline. The preparation is done for around 30 minutes, which should be enough time to collect 4-8 brains.

After collection, the brains are given the chance to settle to the ground of the tube, after which the saline is removed and replaced with 100% Bouins Fixative (Sigma, #: HT10132). The fixation step is performed for one hour, on ice. After the fixation step the Bouins fixative is discarded, and the brains are gently rinsed a couple times with 0.3% Triton-X diluted in PBS. This is repeated until the solution itself is no longer yellow. Then the samples are permeabilized three times with 2%PBT (PBS with Triton-X) for 15 minutes. Afterwards the preparation is blocked for 1 hour with a solution of 10% normal donkey serum (Sigma, #: D9663) in 2% PBT. Now the primary antibody is applied, eluted in 10% normal donkey serum in 0.2% PBT. This incubation is carried out for approximately 72 hours at 4°C. After removal of the primary antibody solution the brains are washed with the same solutions (2%PBT) as before. Again 3 times for 15 minutes each. Afterwards the secondary antibody is applied, eluted in 0.2%PBT with 10 % normal donkey serum. This incubation is also conducted for roughly 72 hours at 4°C in a light protected environment. After thorough removal of the secondary antibody the samples are again washed 3 times for 15 minutes each with 2% PBT. To further reduce the background another washing step in pure PBS is added before mounting, here the wash lasts about two days at 4°C in darkness. Before embedding the samples in vectashield (Vector Laboratories, #H-1000) 3 more washes in PBS are conducted. Embedding is done in vectashield as a clearing agent. The samples are mounted in a 188µm thick metal

cover slip, which has a circular hole. This hole is glued shut with a coverslip of a refractive index of 1.5. The brains are then arranged as desired on this coverslip in the vectashield. The samples are enclosed in vectashield with another coverslip with the same refractive index.

2.4.1.2 Larval open book preparation

The larval preparation was conducted as described previously (e.g. Brent, Werner and McCabe, 2009). Wandering L3 *Drosophila* larvae are collected and fixated with small metal needles in a Sylgard covered falcon dish. After submersion in PBS/Saline the larva is then opened with a cut along the ventral side. Additional pins are used to fixate the body wall to the dish, stretching the larva a little bit. The whole gut as well as the trachea lining the body wall are carefully removed, keeping only the ventral nerve cord, the lobes, as well as the body wall muscles intact.

After the preparation, the saline is removed, and the larvae are fixed with ice-cold 100% EtOH for 5 minutes. Afterwards the larvae are rinsed with PBS before they are washed twice with PBS for 15 minutes each to remove remaining EtOH. Now the samples are permeabilized with 0.3% PBT for 20 minutes (6 times) then the samples are blocked overnight with 0.4% BlockAce (BioRad, #BUF029) in 0.3%PBT. After removal of the BlockAce, the samples are washed once more with 0.3PBT and afterwards the primary antibody is applied, in a 0.3% PBT solution, the primary antibody is once again incubated overnight. To remove excessive unbound primary antibody from the larvae several washing steps in 0.3%PBS are performed. The secondary antibody is washed in overnight in PBS at 4 degrees Celsius, while in darkness. Lastly before mounting several more wash steps to remove the secondary antibody are needed, this wash time can be extended over two days to get a better reduction of background fluorescence. In contrast to the brains, the larvae are mounted on thinner metal slides with a circular hole, here the thickness of the slide is only 100µm. The mounting media is again vectashield.

For the active zone/bouton counting experiments the following protocol was used. After preparation (as above) the animals were fixed by application pf 4% paraformaldehyde (PFA) in PBS for 30 minutes at ~25°C. The PFA is rinsed off using PBS, after which the samples are washed for four times 15 minutes at room temperature on an orbital shaker. The samples are permeabilized by application of 0.5% PBT (6X for 15 minutes). The primary antibodies are eluted in 0.3% PBT and incubated overnight at 4°C on a shaker. The following day the samples are washed eight times with PBS for 15 minutes each. The secondary antibodies are eluted in

PBS and applied for at least 2 hours on a shaker with a light protective cover, to prevent bleaching of the fluorophores. After additional 8 iterations of 15 minutes PBS washes the samples are dehydrated in an ascending EtOH series (50, 70, 90, and 100% for 10 minutes each). Embedding is done in the 100 µm thick metal slides, as above, although here methyl salicylate (Sigma, #: 240826) is used as an embedding agent.

2.4.2 CLSM

The various embedded samples are recorded using a Leica SP 8 confocal laser scanning microscope. For quantitative measurements such as the colocalization studies the settings were kept constant across all recordings.

2.4.3 Digital data processing

For the counting of the active zones and the boutons the data was first renamed and rearranged via FIJI, before automated count of boutons and active zones with a FIJI script named Macro-Drosophila_NMJ_Morphometrics_20161129.ijm (Castells-Nobau *et al.*, 2017).

2.5 Electrophysiology

2.5.1 whole cell patch clamp adult/pupae

To facilitate in situ whole cell patch clamp of MN5 a uniquely identifiable neuron innervating the DLM flight power muscles the animals were prepared as follows (Ryglewski and Duch, 2012).

2.5.1.1 Prep for pupal/ adult patch clamp

The preparation for both pupal and adult MN5 patch clamp recordings is done fundamentally the same. In case of the pupae animals in pupal stages P8 (as defined by Bainbridge and Bownes, 1981) were used for the experiments as they still exhibit a strong calcium current which disappears in latter pupal stages (Ryglewski, Kilo and Duch, 2014). To prepare the pupae, first the puparium is removed. Here, the pupa is gripped with forceps at the posterior end and the operculum is cut, afterwards the remaining puparium is removed. To preserve the pupa, a forceps is used to incrementally open the puparium and slowly unwrap the pupa. After the puparium is removed. A very sharp pin is used to fixate the abdomen of the pupa to the sylgard covered dish. The pupa is now covered with saline and the rest of the preparation carried out in saline. To prevent the pupa from bursting careful incisions are performed surrounding the neck of the fly to open the sheath encapsulating the pupa. Now the head of the animal is fixed

with another pin to the dish. Now the preparation is the same as the adult preparation. The adult animals are anesthetized by placing them in a vial on ice before the preparation. The anesthetized animal is now taken to a sylgard covered dish where the wings as well as the legs of the animal are removed, as close to their base as possible. The animal is now fixated using pins in the lower abdomen and the head and covered in saline. From here on the preparation is the same for the pupa and the adult fly. The thorax of the fly is opened using fine scissors. Here, a flat incision is made through the flight muscles, from the posterior end of the thorax all the way through the thorax to the neck of the fly. The cut is done right in the middle of the thorax, while the flat angle of the cut is done to preserve the underlying ventral nerve cord from inadvertent damage. The parts of the thorax are now spread open and fixed with additional pins to the dish, providing access to the ventral nerve cord. The open thorax is gently washed with saline to remove fat bodies and other loose debris. The gut, passing over the VNC is now cut of and removed. For these preparations the head is also removed, as well as the pin fixing it. Now the preparation is cleaned by gentle suction and reapplication of the saline, additionally any trachea directly on top of the VNC are gently removed, as well as salivary glands flanking the VNC. The animals are now ready to be moved to the patch clamp setups for removal of the ganglionic sheath surrounding the soma of MN5 and subsequent experiments.

To provide access to cell membrane of MN5 a sheath surrounding the soma has to be removed before hand. This is accomplished by using a recording electrode with a broken tip, filled with *Streptomyces griseus* protease type XIV (2% in saline). The electrode is used to expel the protease on top of the soma of mn5 to soften the sheath, afterwards using gentle pulling and pushing with the broken electrode tip to remove the sheath from the soma under visual control. After a short wash step to fully remove the protease the broken cleaning electrode can be removed and replaced with a recording electrode for the path clamp experiments.

2.5.1.2 Patch clamp recordings

The dishes with the animals prepared as described above are amounted in an upright microscope (Zeiss Axio Examiner A1) on a fixed stage. For the whole cell patch clamp recordings glass pipettes are pulled using borosilicate glass pipettes (no filament, inner diameter: 1 mm, outer diameter 1.5 mm; World Precision Instruments) with a target resistance of 4-5MΩ. The soma of MN5 is approached by the electrode and a light pressure is exerted on the pipette before contacting the cell membrane. After relieving the pressure, a

seal is formed, and the membrane is ruptured in a controlled manner to break open the cell. Before starting the recordings, the cell is allowed to recover and stabilize for about two minutes. For the voltage clamp experiments the voltage clamp saline (saline, see appendix) is used as an external solution supplied via perfusion, with the matching intracellular solution (Intracell voltage clamp, see appendix) in the recording electrode. Prior to the voltage clamp experiments the perfusion was turned off and tetrodotoxin (TTX) for a final concentration of 100nM was applied to the bath and incubated for 2 minutes to abolish voltage gated sodium channel activity, in addition to the block of voltage gated potassium channels by tetraethylammonium (TEA) and 4-amminopyridine (4-AP) which are already part of the saline. Cells with resistances of ~10 MΩ as shown by the amplifier after compensation were used. The cells were clamped to a holding potential of -90 mV, for current recordings a protocol of 10 mV voltage steps between -90mV and 20mV run, each voltage step was 200 ms long. Leak subtraction was done via an average of the first three sweeps of a recording.

All patch clamp recordings were done with an Axopatch 200B amplifier (Molecular Devices) and fed into a digitizer (Digidata 1440a, Molecular Devices) with a rate of 20 kHz, before being filtered with a 5-kHz Bessel filter. The data were then acquired and analyzed using pClamp 10.7 (Molecular Devices)

Normalized data was fitted either in Graph Pad Prism (version 9.1.) or Clampfit (version 10.7). The pupal calcium currents were fitted with a sigmoidal Boltzmann equation. Y=Bottom+(Top-Bottom)/(1+exp((V50-X)/Slope))

The adult HVA recordings were fitted with a custom equation: $I = \frac{g(V-VR)}{1+e^{(-0.03937*z*(V-V1/2))}}$

LVA adult currents were fitted with a charge-voltage Boltzmann equation: f(V)= (Imax/1 + $e^{(Vmid-V)/Vc}$) + C.

2.5.2 Current clamp recordings pupae

The current clamp recordings were done like the voltage clamp recordings, utilizing other salines (current clamp saline intra and extracell, see appendix) and appropriate recording modes on the amplifier. The APs were elicited by a square current injection.

2.5.3 Calcium imaging

For calcium imaging experiments in the pupae, preparation and patch were done as above, with the main difference being the use of other salines (ca-imaging saline, see appendix). For

the recording of the fluorescence changes in the animals a camera (Hamamatsu Orca flash) was mounted on the microscope. The stimulation of the neurons was done via patch clamp as described above. Current was injected into the soma as either a 400ms 1nA ramp or in such a way that two action potentials are elicited.

2.5.4 Electroretinogram adult

For the electroretinogram of the adult flies the animals were anesthetized and their wings and legs were removed to reduce the movement of the flies. They were then mounted approximately 1 cm in front of a LED lamp, and a grounding electrode was inserted into their abdomen, while an extracellular recording electrode filled with 3M KCl was put in contact with the fly eye. This setup was then put in darkness and the fly could acclimate to the experimental setup for 5 minutes before the light stimulus protocol was run. The light stimulus was applied via a pulse stimulator at 4.2V, at which the maximum light intensity of the LED was reached. 10 stimuli of 1 sec each were given with an inter pulse interval of 1 second. The recordings of the ERG were done via Axoscope and analyzed in Clampfit.

2.6 Data analysis and Statistics

All Data analysis was done using Excel version 2106 (Microsoft) and Prism (GraphPad Software) version 9.1. All quantitative data was examined for normal distribution using a Shapiro-Wilk test. Normally distributed data were compared using a t-test if two groups were compared using an ANOVA for more than two groups. Significance was assumed with a p-value smaller than 0.05. In case of significant differences after using an ANOVA, post hoc tests were conducted to perform specific comparisons, depending on the type of data analyzed. The specific test chosen is denoted in the experiments, but Bonferroni and Tukey post hoc tests/multiple comparisons were used. In case of not normally distributed data a Mann-Whitney test was used for comparison of two groups and a Kruskal-Wallis ANOVA for more than two groups. If the Kruskal-Wallis ANOVA was significant a Dunn's Post-hoc test was performed for multiple comparisons among the tested groups. The longevity/survival data was analyzed using a Kaplan-Meier-Curve. The individual comparisons were done by manual Bonferroni adjustment to the significant p-value for multiple comparisons and using the mantel-cox logrank test to compare the two groups.

3 Results

3.1 Generation, verification, and initial assessment of the CRISPR/Cas9 mediated exon excision variants

3.1.1 Cacophony voltage gated calcium channel isoform variability can be reduced by deletion of alternative exons with CRISPR/Cas9

Utilizing the approach outlined in the methods section of the thesis, the CRISPR gRNAs were designed, the flies injected, and the crossings to remove Cas9 were conducted. Due to the time and effort needed to newly establish this strategy in the lab, the focus of this thesis was to create single exon excisions for alternative exons coding for part of the fourth transmembrane domains of the first homologous repeat (IS4) and the intracellular linker connecting the first and second homologous repeats which contain the binding sites for Ca-β and (or G-protein βγ subunits (I-II). I also established the tools needed to create double exon excisions and characterized the effects of single exon excisions for IS4A, IS4B, and I-IIA. During my work all four single exon excisions (IS4A, IS4B, I-II A, and I-IIB) were completed (Table 5). However, characterization was only done for IS4A, IS4B, and I-IIB. The combinations of deletions in the IS4 and the I-II locus have been further pursued in the lab using the findings, tools and fly stocks created by myself over the course of this thesis. Due to the permanent expression of the respective gRNAs as recognition target for Cas9 (see Methods), single and double exon excisions of IS4 and I-II can be achieved by simple fly husbandry.

3.1.2 Excision verification

Verification of a successful excision was done in a two-step process: First, PCRs were performed with the candidate flies, after several rounds of egg laying. Second, the flies showing a deletion in the PCRs were then sequenced.

Table 5: *nt sizes, AA sequences, gRNAs, deletions, primers and expected PCR product sizes for the deletions generated: nt: nucleotide, AA: amino acid, Ca_{β}: VGCC β-subunit, $G_{\beta\gamma}$: G-protein βγ-subunit, SU: subunit, veri: verification, FWD: forward, REV: reverse*

Exon excised	IS4 A (Exon 6)	IS4 B (Exon 7)	I-II A (Exon 11)	I-II B (Exon 12)
exon size	99 bp	99 bp	115 bp	115 bp

AA seq	AMTIFAEANIDVDLRMLRSFRVLRPLKLVSRIP	FMTQYPQIGPEVDLRTLRAIRVLRPLKLVSGIP	GEFSNERNRVERRMEFQKCRFRAMFQTAMVSYLDWITQA	GEFAKEREKVENRQEFLKLRRQQQLERELNGYVEWICKA
of note	6 positively charged residues	5 positively charged residues	binding site for Ca_{β} SU	binding site for Ca_{β} and $G_{\beta\gamma}$ SU
gRNA pre-exon	ccaatatcacctatg|tttaagtc	ccgaaactatagagt|gactgacc	gctacgtg|catgtgcatacacgg	ccagtaaatgatttc|gactttct
gRNA post-exon	gttgctac|taccaaaaacctagg	gtggcaca|tgattgtcgtggagg	ccaagtaaactgcca|taatcaac	ccccatatgttcat|ccacatcc
assumed excision	476 bp	926 bp	388 bp	508 bp
actual excision	506 bp	965 bp	380(+7) bp	528 (+10) bp
Untagged	✔	✔	✔	-
sfGFP tagged	✔	✔	✔	✔
tagRFP tagged	✔	✔	✔	-
Viability if lost	Decreased motor control & lifespan	Homozygous lethal	No obvious defects	No obvious defects
Veri primer FWD	cacgccgtgcaagcattatc	ctgtgtgtgattctcgcgac	gccacttctacaccagttcac	ctcattgaaggttcccgtc
Veri primer REV	cctaaattcgtggctaccac	ccgttccgattcgatccag	gaactctttgtagccgggg	ggagagggatgctaagaatg

band + exon	~988	~1305	~951	~954
band Δ exon	~482	~340	~571	~446

Table 5 summarizes the molecular information on the deletion generated as well as the expected results of the PCRs. Canonical exon number is shown in brackets (based on flybase JBrowse, *Drosophila melanogaster* genome version 6.40) after the more functional exon names such as IS4A. The exon sizes of each of the alternative exons are the same (Table 5, row 1), meaning that inclusion of one or the other alternative exon has no direct influence on the following exons, for example via a frame shift. The amino acid sequences resulting from these exons show differences, the most noteworthy for the IS4 locus is the difference in the positive charges (Table 5, row 2, red letters), where IS4A has a positively charged arginine more than the IS4B variant. This could affect the activation voltage of *cac* isoforms. For the I-II locus the main difference is in the binding sites for accessory subunits, with I-IIA binding only the Ca-β subunit, while I-IIB can also bind βγ subunits of G-Proteins. The gRNA sequences used for the CRISPR is depicted in Table 5 rows 4&5, with red lines denoting the predicted breakpoint for the CRISPR mediated double strand break. The blue nucleotides in the same rows highlight the PAM-sequences needed for the Cas9 enzyme. Excision size based on the predicted breakpoints, assuming a clean break with no fraying of adjacent DNA, can be seen in Table 5 row 6. The actual excision sizes as confirmed by sequencing (Figure 3) as shown in row 7 are slightly different from the predicted sizes. This fraying effect was expected since repair of the double strand breaks in this application of the CRISPR/Cas9 system is known to lose base pairs adjacent to the cleavage site. This variation from the expected breakpoints should not introduce additional complication since the cleavage sites are chosen at locations beyond well-known splice starts, stops, or regulators (Brooks *et al.*, 2011). As mentioned in the method section, several different fly lines were used as a point of origin for the CRISPR based modifications. *Cacophony* tagged in its genomic locus (cac^{sfGFP}/cac^{tagRFP} from Gratz *et al.*, 2019) was used as a template, to easily address experimental questions concerning localization of isoform reduced variants. Rows 8-10 show which of the variants are available with or without tag. Striking phenotypes concerning general viability of the flies are shown in row 11. No differences were observed in animals expressing tagged or untagged cacophony channels with

the same deletion. Lastly, the primers used for verification via PCR and sequencing are listed as well as the expected PCR product sizes (rows 12-15). These PCRs followed a simple approach, producing a product in any case, the size of which then indicates the presence or absence of the exon of interest. Figure 2 shows exemplary gels with the PCR products loaded. Candidates for successful excision of IS4A, IS4B, I-IIA, and I-IIB are denoted by the asterisks with nucleotide lengths of about the expected size (Table 5).

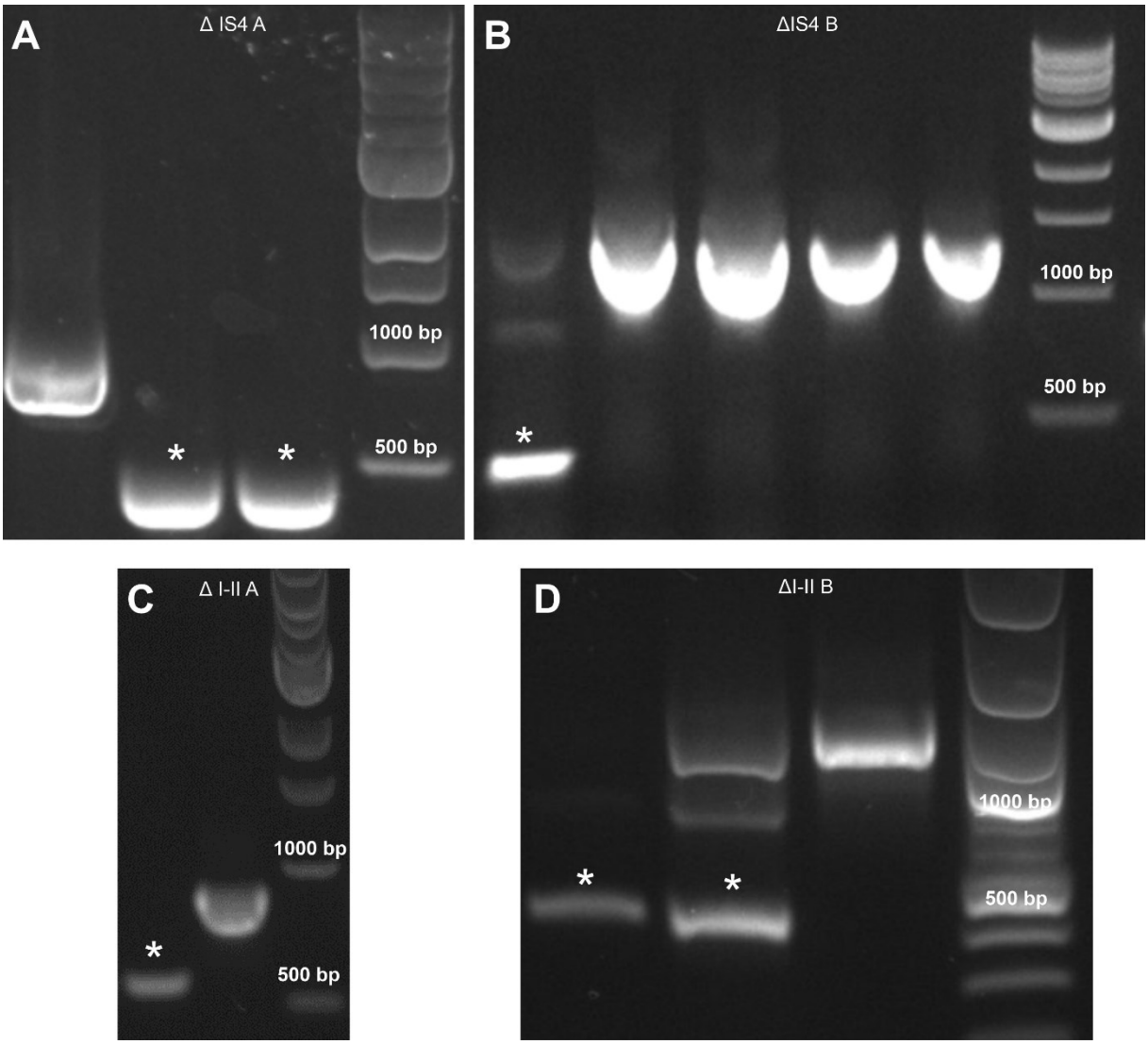

***Figure 2**: PCR verification of CRISPR based excision of target exons, asterisks denote the PCR product missing the respective exon, **A**: excision of the IS4 A exon, **B:** excision of exon IS4 B, the animals tested in this case were heterozygous thus explaining the bands in the lane with the asterisk around the size of the whole genome fragment, **C:** excision of the I-II A exon **D**: excision of the I-IIB exon*

Of the lines screened that way, positive hits were picked and subjected to genomic sequencing of the target locus to verify exactly at which point in the *cacophony* genomic locus the CRISPR/Cas9 mediated deletion occurred. The exact genomic deletions can be seen in Figure 3. Figure 3 shows the sequences or lack thereof for successful deletion of each of the four

exons in question, meaning that here only the remaining genomic DNA can be seen. A dashed line indicates the site of deletion. In all cases additional base pairs were lost during the double strand break, resulting in discrepancies between expected loss of base pairs and actual loss of base pairs as shown in Table 5 rows 6 & 7. As mentioned above, this loss of bases is within the expected variance for this application of CRISPR/Cas9 and should not interfere any further with the animals than the actual deletion itself. In addition to this loss of 380bp the sequenced ΔI-II A animals showed a repeat of the first seven base pairs right after the excised genomic region (Figure 3). These surplus bases were not deemed to have any additive impact on the resulting fly lines, since they would only be found in the intronic region formed from the remainder of introns surrounding the excision joined together for a new artificial intron. The same is true for the 528 bp lost in the I-IIB excision and the addition of the 10 bp in between breakpoints as shown in Figure 3.

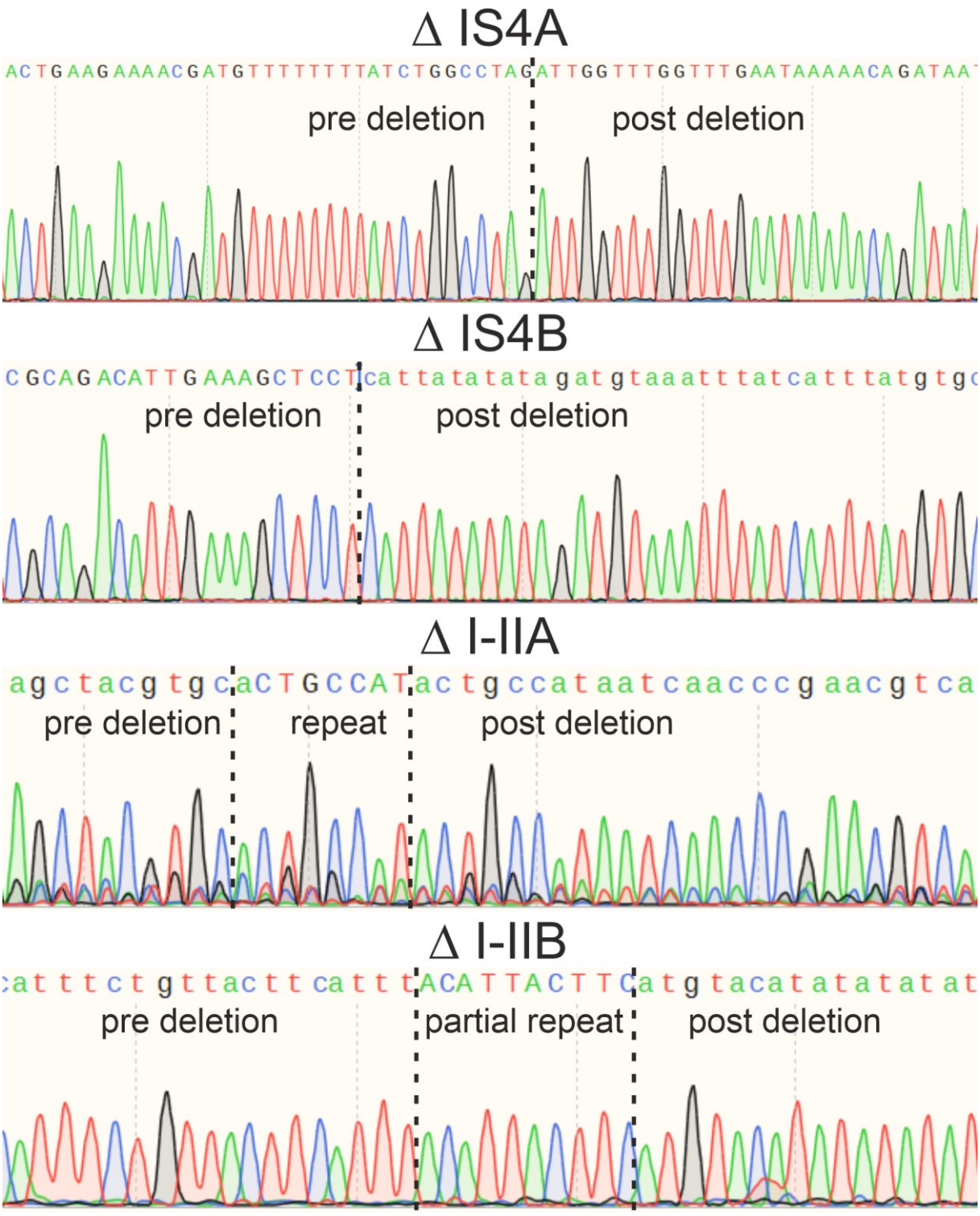

Figure 3: *sequencing data of the fly strains missing one of the deleted exons each: dashed lines indicate missing sequence, in ΔI-II A during the deletion a repetition of 7bp of the genomic DNA directly past the deletion occurred, similarly a part of the ΔI-IIB sequence can be found in the midst of the excision sites for I-IIB excision.*

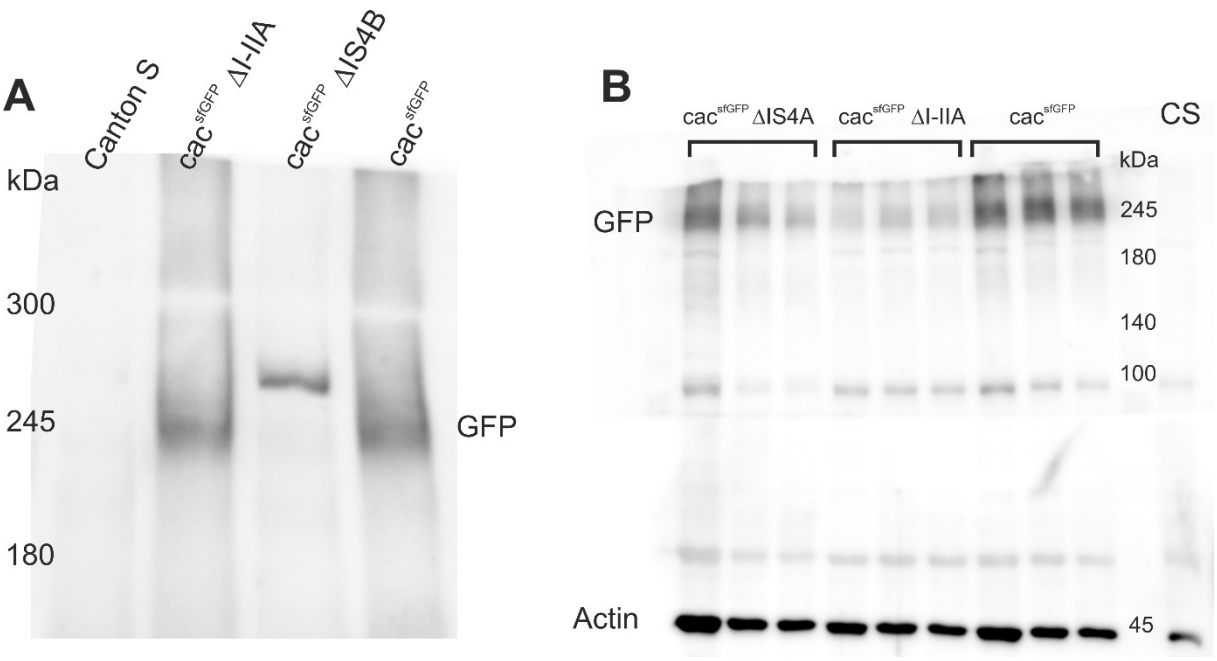

Figure 4: *Western blot confirms presence of sfGFP-tagged cacophony protein after exon excision. A: Western blot of adult* Drosophila *brains. 15 brains per lane, except 30 brains for* cac^{sfGFP} *ΔIS4B since the animals were heterozygous, cacophony associated GFP can be found at around 245 kDa (cac ~215 kDa + sfGFP ~30 kDa). Higher molecular weight of cac missing IS4B possibly due to remaining cac being predominantly of a longer isoform. B: Western blot of adult* Drosophila *brains 15 per genotype of the following genotypes:* cac^{sfGFP} *ΔIS4A,* cac^{sfGFP} *ΔI-IIA,* cac^{sfGFP}*, and Canton S. Cacophony associated GFP can be found at around 245 kDa.*

To confirm the presence of the proteins derived from exon excision from the genomic locus of *cacophony*, western blotting was conducted (Figure 4). Figure 4 B demonstrates that IS4A and I-IIA excision from cacophony-GFP yields expression of cacophony protein as evidenced by the bands visualized with anti GFP antibody at around 245 kDa. The average cacophony molecular weight is around 215 kDa while sfGFP is around 30 kDa. Similarly, the protein labeled in Figure 4 A also confirms the presence of cacophony in animals lacking the IS4B exon albeit at a higher molecular weight. A likely explanation for the increased molecular weight in these proteins is a possible skewering of the likelihood of expressed isoforms towards some which have a higher molecular weight. An alternative explanation could be altered charge in the protein resulting in affected transfer of the cacophony protein through the gel.

3.1.2 Both alternative exons for the voltage sensor are necessary for healthy flies

3.1.2.1 Loss of exon IS4B is homozygous lethal

At the point in the CRISPR crossing scheme (see methods) at which the first hemi/homozygous animals carrying the ΔIS4B variant should start to appear the first major finding of this thesis became apparent. Animals lacking the IS4B exon are homozygous lethal.

This proved that the B variant of the IS4 exons is required for fly survival, as had been suspected, due to previous findings showing the rescue of otherwise lethal *cacophony* null mutants by expressing UAS- cac^{1} pan-neuronally under the control of elav-GAL4 (Kawasaki, Collins and Ordway, 2002). Cac^{1} is currently the only transgenic *cacophony* construct, it is based on cDNA containing the B variant at both, the IS4 as well as the I-II locus.

None of the other exon-out variants generated for this thesis show a lethal phenotype. More precisely, animals lacking I-IIA or I-IIB show no immediate impairments. In contrast, flies missing the IS4A locus, meaning the flies only express IS4B, show greatly reduced mobility and rarely initiate flight on their own in a tethered flight experiment. Based on these initial observations that exon IS4B is required for survival of the animals and IS4 A for normal motor performance, further tests on the effect of IS4A excision on life expectancy and motor performance were conducted.

3.1.2.2 Loss of IS4 A severely reduces life expectancy

Cacophony is essential for survival. Therefore, a longitudinal study was performed with the non-lethal exon excision fly strains, to assess life expectancy. The results of this study are visualized as a Kaplan-Meier-Curve in Figure 5. This graph shows the lifespan in percent surviving flies over the course of 120 days. To address potential dominant effects in ΔIS4B flies, heterozygous animals (females, as cacophony is localized on the X-chromosome) are included in this study. Furthermore, Canton S (CS) controls were taken from both genders since it has been reported that female *Drosophila* can have a lower life expectancy (Gaitanidis et al., 2019) and controls for heterozygous Δ IS4B flies needed to be female. Quite glaringly, the ΔIS4 A animals show a vastly reduced survival as compared to all the other genotypes. The median survival for ΔIS4 A males is around 16.5 days, 192 animals of this genotype were tested. Male CS flies showed a median survival of 81.5 days with 94 tested animals. Their female counter part had a slightly reduced median survival of 75.5 days across 100 animals tested. For cac^{sfGFP} ΔI-II A 126 males were tested which showed a median survival of 90 days. The 120 heterozygous females for the cac^{sfGFP} ΔIS4 B animals presented with a median survival of 76 days.

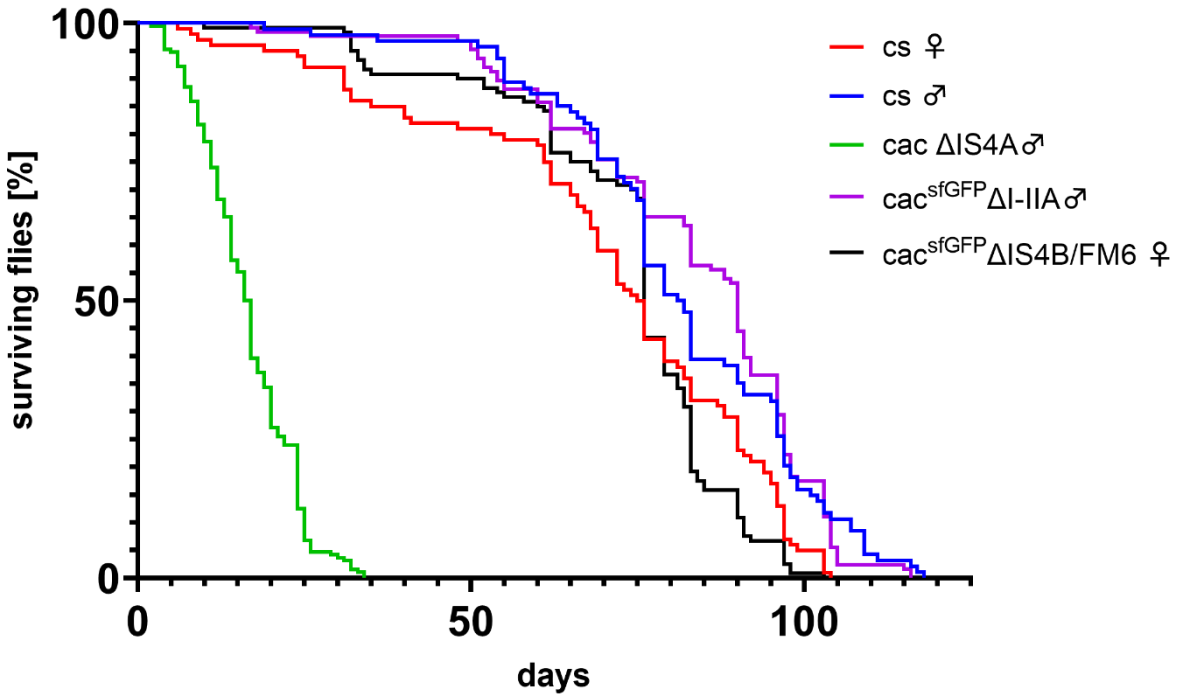

Figure 5: ΔIS4 A animals have ~80 %reduced survival when compared to controls: *Survival proportions of different isoform reduced fly lines and respective controls. Animals per genotype: CS♂: 94; CS♀: 100; cac ΔIS4A♂: 192; cac^{GFP}ΔI-II^{A}♂: 126; cac$^{GFP\Delta IS4B}$/FM6 ♀: 120*

A mantel-cox test across all tested groups reveals a highly significant difference in overall survival ($p<0.0001$). For the following comparisons, the significance threshold of 0.05 was Bonferroni adjusted to $p<0.005$ by dividing the p-value of 0.05 by the amount of possible individual comparisons K (here 10). The reduced lifespan for females ($p=0.0007$) as compared to males was expected as mentioned above (Gaitanidis *et al.*, 2019). The heterozygous expression of the homozygous lethal cac ΔIS4B leads to no significant differences in survival chance when compared to control females (mantel-cox: $p=0.2822$). Similarly, hemizygous male flies of the ΔI-II A variant also exhibit no significant difference to the control males (mantel-cox: $p=0.8901$). This strongly suggests that loss of IS4A albeit not immediately lethal, has such a severely detrimental effect on the animals' health that their lifespan is reduced by about 80% when compared to controls. Since IS4 is part of the voltage sensor, loss of IS4A may affect excitability (see Figure 32) which in turn could cause reduced life expectancy.

Taken together with the initial findings concerning the lethal phenotype of the ΔIS4 B animals one can reliably assume that both alternative exons in the IS4 locus take on critical functions for the general performance and wellbeing of the flies. Thus, both exons are unambiguously

necessary for healthy animals, with command over their full range of motor functions, as will be further elaborated on in the following. By contrast, excision of I-IIA does neither cause lethality nor does it reduce life-expectancy. Therefore, exons I-IIA and I-IIB likely serve redundant functions, at least in terms of general health. This does however not exclude the possibility that I-IIA and I-IIB serve non-redundant functions regarding other sensory, motor, cognitive, or other aspects of nervous system function.

As to why both IS4 exons are required for normal health several explanations seem possible. First, both exons could be required for the same essential function, only in different parts of the nervous system. One such function could be release of synaptic vesicles during synaptic transmission at chemical synapses. Second, they could both be required for different but nonetheless essential functions in all neurons. And third, both could be required for different functions in different parts of the nervous system. The finding that animals missing I-IIA show no effect on lifespan and are viable could be explained by fully redundant functions of both exons, or by non-redundant functions which only become apparent when testing specific behaviors, or only during specific challenges.

To distinguish these possibilities, I next tested the excision variants in different behavioral paradigms. Then I analyzed the localization of different cacophony variants with exon excisions in the brain and in the ventral nerve cord as well as their sub-cellular localization in identified motoneurons. And finally, I tested them on the level of single neuron electro- and optophysiology.

3.2 Both alternative IS4 exons but not both alternative I-II exons are required for larval and adult motor behaviors

In light of the previous findings showing severe phenotypes for alterations of the IS4 locus but not the I-II locus, further behavioral experiments were conducted. These experiments were chosen to investigate whether ΔI-IIA would show a phenotype in more rigorous testing for specific motor behaviors and also to quantify the locomotor defects of ΔIS4A which could already be observed qualitatively during fly rearing. Given that it is already known that the VGCCs can mediate different functions in larval versus adult *Drosophila* motoneurons (Ryglewski *et al.*, 2012; Kadas *et al.*, 2017), different motor behaviors are examined at the larval and adult stage.

3.2.1 Animals lacking IS4A show severely reduced flight initiation

First, the namesake behavior of the fly was analyzed, namely different aspects of insect flight. For these experiments the flies are tethered to a metal hook and a mechanosensory stimulus via a puff of air is applied to initiate flight. To show this behavior, the fly needs to register the stimulus, assess it correctly, pass it further along its nervous system and activate the flight muscles. The first parameter assessed is flight initiation (Figure 6). Either the flies did initiate flight upon one of three consecutive air puffs (Brembs *et al.*, 2007) or they did not.

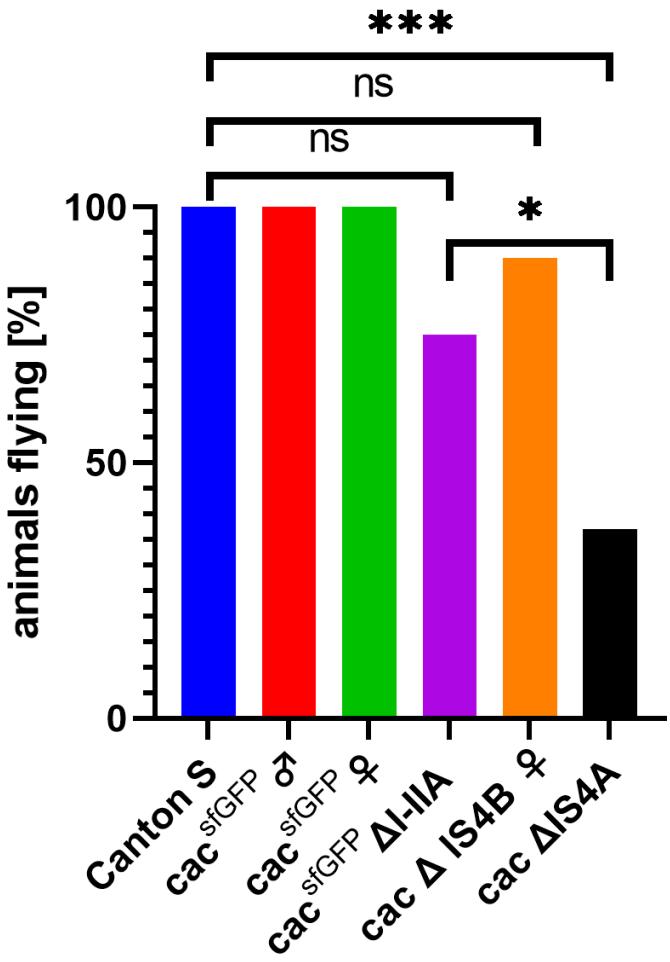

Figure 6: Flight initiation is severely reduced by loss of IS4 A: *percent of animals initiating flight after mechanosensory stimulus (air puff): percentage (animals initiating flight/animals tested): CS=100% (14/14), ΔIS4 A=37% (10/27), female cac^{sfGFP}=100% (8/8), heterozygous ΔIS4 B females=90% (9/10), male cac^{sfGFP}=100% (9/9), cac^{sfGFP} ΔI-II A= 75% (9/12); Fisher's exact test: CS vs ΔIS4 A: p=0.0001; cac^{sfGFP} vs cac^{sfGFP} ΔI-II A: p=0.2421; cac^{sfGFP} ΔI-II A vs ΔIS4 A: p=0.0407 (p < 0.05*; p < 0.01**; p < 0.001***; p<0.0001****)*

All tested flies of the following genotypes did initiate flight as expected: Canton S (14 out of 14), female cac^{sfGFP} (eight out of eight), male cac^{sfGFP} (nine out of nine) animals. This already shows that at least for this behavior the GFP tag did not influence flight response, neither did

the gender of the tested animals. All other genotypes tested had at least some tested flies which did not initiate flight upon stimulus. Heterozygous ΔIS4B animals, again to test for any dominant negative effects (see also above), did also not show any significant differences to the controls (CS vs cac ΔIS4B Fisher's exact test: p= 0.4167) even though one of the ten animals did not initiate flight, further proving no apparent dominant negative effects of loss of IS4B. For the ΔI-IIA animals, a quarter of the tested animals did not initiate flight upon stimulus, meaning only 9 out of 12 tested animals flew. But still, when compared to matched cac^{sfGFP} controls no significant difference could be found (Fisher's exact test: p=0.2421), again reinforcing the nonessential function of I-IIA, at least for this kind of assessment. Most notably, the ΔIS4 A animals showed a significantly (Fisher's exact test p= 0.0001) reduced percentage of flight initiation in comparison to the Canton S controls with only 10 of the tested 27 animals initiating flight, which corresponds to only 37% of animals tested. The ΔIS4 A animals are furthermore also significantly different from the ΔI-IIA animals (Fisher's exact test: p=0.0407), reinforcing the strong effect of only the loss of IS4A.

In principle, the observed reduction in flight initiation of the animals lacking IS4A could be caused by defective sensory encoding of the stimulus, defective decision-making processes, impaired central pattern generator function, impaired neuro muscular transmission or by impaired muscle function. Some of these possibilities (CPG function, neuromuscular transmission, and muscle function) can already be excluded by testing whether the animals initiating flight can maintain this flight normally or not. Impaired neuromuscular transmission would for example not only affect flight initiation but also maintenance. Therefore, after assessing the response of the flies to the air puff stimulus, their ability to sustain flight was tested. The time spent flying per animal was recorded, when an animal stopped flight, it was again given air puff stimuli until it did not respond to three consecutive air puffs (Brembs *et al.*, 2007). In addition, motoneuron activity during flight was measured extracellularly with tungsten electrodes from the respective target flight muscle fibers to test whether CPG output was normal or not (Ryglewski *et al.*, 2014).

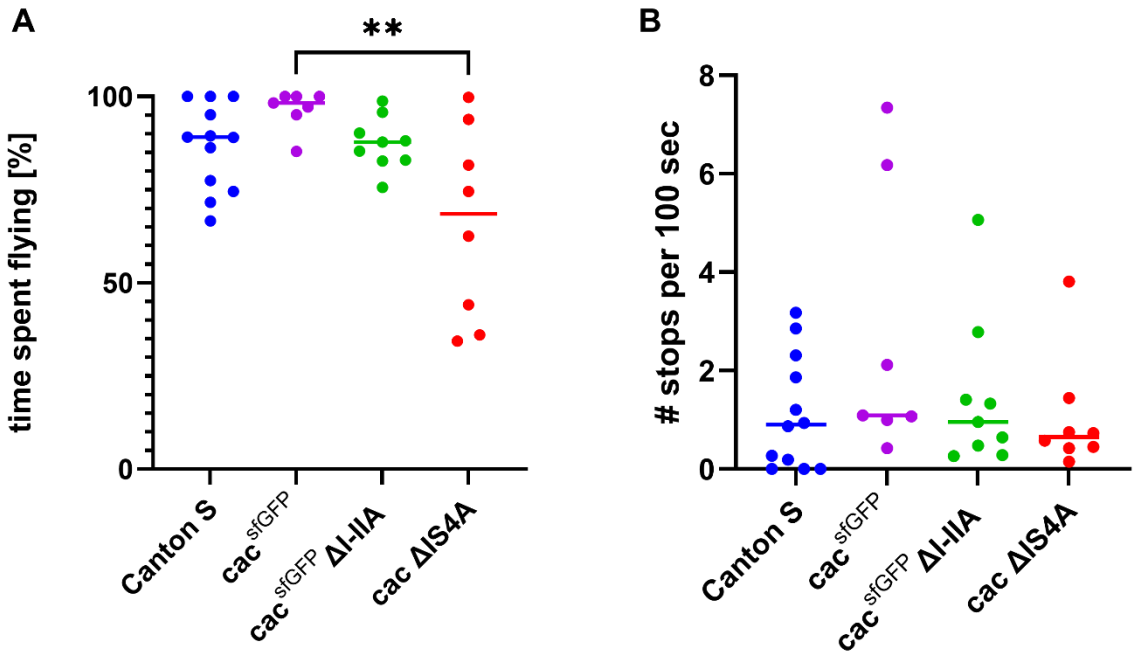

Figure 7**: **loss of IS4A leads to reduced flight time due to reduced flight initiation**: **A**: flight duration relative to recording length, ΔIS4A significantly reduced in comparison to cac^{sfGFP} (overall Kruskal-Wallis ANOVA: p=0.014 cac^{sfGFP} vs cac ΔIS4 A Dunn's multiple comparison: p=0.007) all other comparisons were not significant **B**: number of stops per flight recording relative to 100 seconds recording time, Kruskal-Wallis ANOVA: p=0.3339; A and B: Canton S: n=12, cac^{sfGFP}: n=7: cac^{sfGFP} ΔI-II A: n=9, cac ΔIS4 A: n=8; bars show median (p < 0.05*; p < 0.01**; p < 0.001; p<0.0001****)*

Due to a variation in recording duration, the time spent flying was normalized to the total recording time. The stops while flying were also recorded and can be seen in Figure 7 B, again due to the varying recording lengths, the number of stops is normalized to stops per 100 seconds. The Canton S animals (Figure 7 A blue dots) spent about 89.09% of the recording time flying, with a median of 0.9015 stops per 100 seconds (Figure 7 blue dots). The cac^{sfGFP} animals showed tighter distribution of their time spent flying with a median of 98.25% of the recording time, and a slightly higher median of 1,092 stops per 100 sec. The ΔI-II A animals look quite similar to the controls with a median of 87.74% time spent flying and a median of 0.9551 stops per 100 seconds. Lastly, the data of ΔIS4A animals show a broader distribution than the other examined genotypes with a median of only 68.52% of the recording time spent flying, meanwhile the median number of stops did not show any significant differences to the other recorded animals with 0.6531 stops per 100 s. When comparing time spent flying across all tested groups a significant difference can be found (Kruskal-Wallis ANOVA: p=0.014) with only cac^{sfGFP} compared to cac ΔIS4A showing a significant difference after post hoc testing (Dunn's multiple comparison: p=0.007). For the number of stops no such difference can be found (Kruskal-Wallis ANOVA: p=0.3339). When examining these findings together they

strongly suggest that the animals missing IS4 A do not have a problem maintaining flight but rather cannot initiate flight as easily after stopping. This recapitulates the findings from the initial flight initiation experiment (Figure 6) and indicates that IS4A is required in the sensory systems decoding the air puff stimuli, or in the decision-making process to activate the flight CPG. By contrast, once flight is initiated IS4A does not seem to be required for flight maintenance, indicating that IS4A may not be required for CPG function, neuromuscular transmission, or muscle function. Animals lacking I-IIA show no differences to the controls and thereby reinforce the findings that locomotor behavior, may not require the presence of I-II A.

To further exclude any influence of IS4A excision on CPG, motoneuron, neuromuscular, or muscle function, electrodes were introduced into the dorsolongitudinal flight power muscles (DLM) of *Drosophila*, and the spikes of the motoneurons innervating the DLM fibers were recorded during flight. In this case this was done with a single recording electrode inserted into muscle fibers 4-6, thus recording the EPSPs caused by firing of the motoneurons MN4 and MN5 (Ikeda and Koenig, 1988; Ryglewski, Kilo and Duch, 2014).

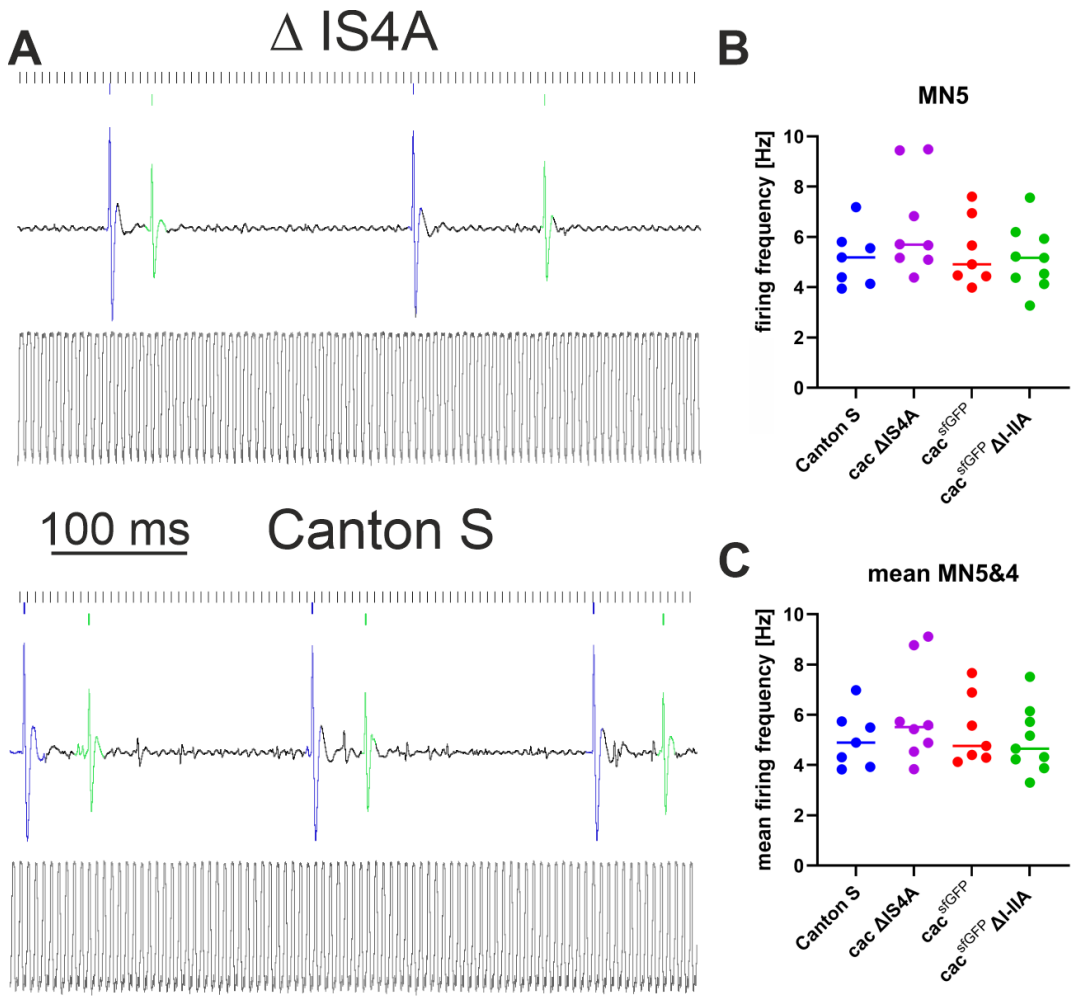

Figure 8 *Motoneuron firing frequency is unaffected by loss of either exon I-IIA or IS4A: A: representative recordings of motoneuron firing during flight, MN5 (blue spikes) and MN4 (green spikes) were recorded with sharpened tungsten electrodes during stationary flight, a laser recorded the wingbeat (high frequency black spikes in the lower part of the panel) B: MN5 firing is not affected by either the tag or loss of IS4A or I-IIA (ANOVA: p=0.26) C: mean firing frequency of MN4&5 also do not show significant differences (ANOVA p=0.5114) number of animals tested for B&C: Canton S: n=7, cac ΔIS4A: n=8, cac^{sfGFP}: n=7, cac^{sfGFP} ΔI-IIA: n=9*

The firing of MN 4 (Figure 8A, green spikes) and MN 5 (Figure 8A, blue spikes) can be seen in Figure 8A. Here, representative recordings of two of the assessed genotypes are shown, specifically ΔIS4A since previous experiments have already shown several locomotor defects for this mutant. The firing frequency of motoneuron 5 is quantified in Figure 8B. When comparing the firing frequencies of MN 5 across all analyzed variants no significant differences could be found (ANOVA: p=0.26). The same holds true when examining the mean of the firing frequencies of MN4 and 5 ((ANOVA p=0.5114), Figure 8C). Taken together with the other flight data, this further underscores that indeed the initiation of flight is the main hurdle for the ΔIS4A animals when attempting to fly. The lack of effect on the firing frequency confirms that the synaptic transmission from the motoneuron to the flight muscle is still intact and functioning. A possible explanation for this could be that the sensory information cannot be

detected that well in the IS4A deficient animals, for example, by lacking cacophony expression in specific cells or subcellular compartments involved in sensory systems (see chapter 3.3.3-3.3.5). An alternative explanation could be that IS4A mediates a channel property specifically needed for sensory neurons. Lastly, aside from sensory defects, motivation and/or decision-making defects could be a consequence of loss of IS4A causing impaired flight initiation.

3.2.2 Larval crawling distance is significantly reduced in animals lacking IS4 A

The behaviors investigated so far were all adult locomotion behaviors. Splicing regulation or gene expression can vary over the course of development. Moreover, it is already known that larval and adult *Drosophila* motoneurons utilize different HVA calcium channels in their somatodendritic domain (Ryglewski *et al.*, 2012; Kadas *et al.*, 2017). Therefore, locomotor behavior was also examined in the larval stage. Investigating larval crawling has another advantage: the *Drosophila* larval NMJ is often used as a model for glutamatergic synaptic function (Atwood and Karunanithi, 2002), so that locomotor defects can be related to possible impairments in neuromuscular transmission.

The key parameter measured here was the crawling distance (defined as path length) per given crawling time. Larvae were collected from developmental stage L3 (foraging) and set onto an agarose gel to record them with a camera while crawling. These movies were then used to track the larva, allowing a measure of the distance travelled per unit time.

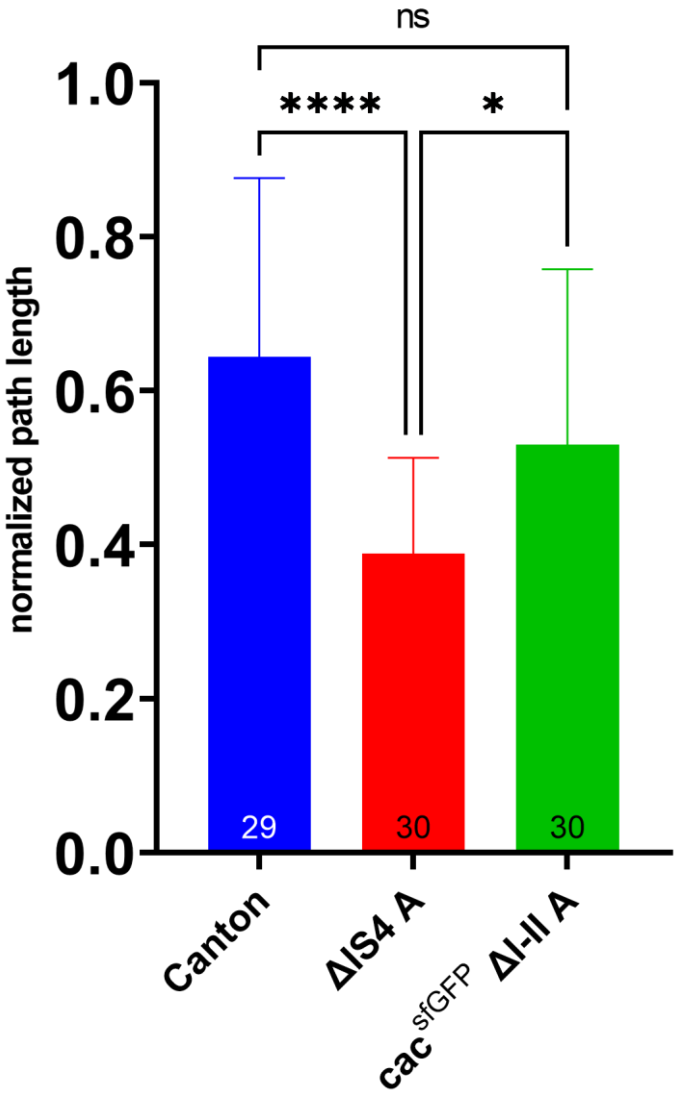

Figure 8: loss of IS4 A severely hampers larval crawling performance: *Crawling path length over a course of three minutes normalized to the furthest CS distance across several recording sessions: CS n= 29, ΔIS4 A n= 30, cac^{sfGFP} ΔI-II A n =30. Statistical Tests: all groups are normally distributed. One-way ANOVA p<0.0001 Bonferroni post-hoc tests: CS vs. ΔIS4 A: p< 0.001; CS vs cac^{sfGFP} ΔI-II A p=0.0939; cac^{sfGFP} ΔI-II A vs ΔIS4 A: p=0.022; (p < 0.05*; p<0.0001****)*

As can be seen in Figure 8, the path length varies significantly between genotypes (ANOVA p < 0.001). The ΔIS4 A animals show a highly significant decrease (Bonferroni post hoc: p<0.001) in path length as compared to controls (CS). No such difference was observed when comparing the cac^{sfGFP} ΔI-II A animals to the Canton S control animals (Bonferroni post hoc: p=0.0939). A significant difference was observed by comparing the two exon excision variants (cac^{sfGFP} ΔI-II A vs ΔIS4 A: p=0.022). This clearly shows that the locomotor defects of the animals missing IS4A are persistent across developmental stages. However, the ΔI-IIA animals show a slight

but not significant decrease in locomotion speed, an effect also consistent across behaviors and developmental stages.

In addition, the locomotor behavior of the larvae while crawling was examined qualitatively. Therefore, the paths the larvae took were traced to visualize the crawling pattern. Figure 9 shows representative crawling traces for the genotypes tested. Notably, the CS control animals prefer long strides with little deviances or turns, while the ΔIS4 A animals show a preference for turning on the spot and going around in circles (see end of ΔIS4 A track, Figure 9 orange). This is in accordance with the reduced mobility of these animals in the adult stage.

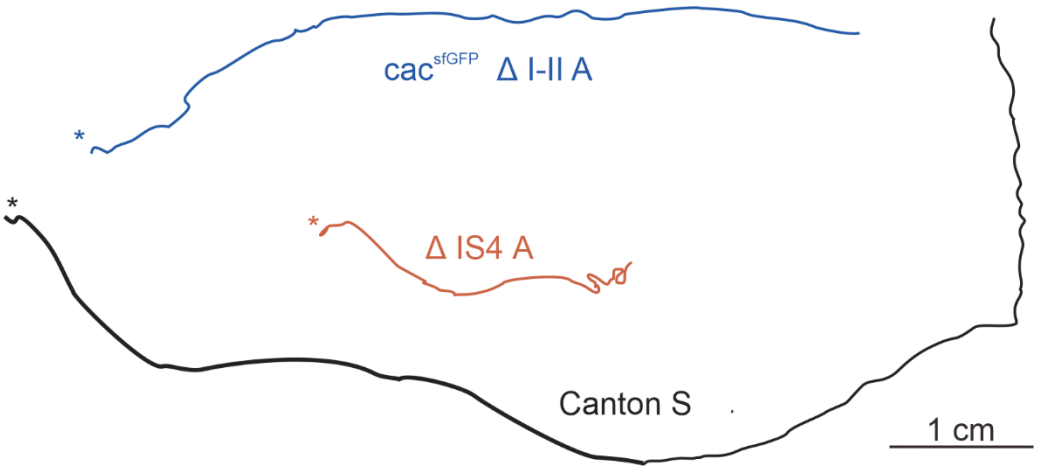

***Figure 9**: representative crawling traces of L3 foraging larvae over an observed time of 3 minutes. Canton S (black), cac ΔIS4A (orange), and cac^{sfGFP} ΔI-IIA (blue) are shown, asterisks indicating the start of the crawling track, scalebar: 1cm*

These larval locomotor deficits can be due to a number of reasons, as is the case for the findings on adult flight. In the larval stage these include a lack of motivation of the animals to crawl, impaired sensory function, or impaired motoneuron, neuromuscular, or muscle function. Furthermore, as evidenced by the erratic crawling behavior with many turns, an increase in excitability in the thoracic segments, as they are responsible for the turning motion (Clark *et al.*, 2016). As for the manipulations concerning the I-IIA locus, again, the change in developmental stage and behavior assayed did not show a phenotype indicating a necessary function for I-IIA.

3.2.3 Exon IS4 A is necessary for successful courtship

One if not the most essential task of any organism is procreation and ensuring the continuation of their genetic lineage, and thus to entice a partner to mate. *Drosophila* does this by utilizing a rather complex courtship ritual. Among other motifs, this ritual involves a

clearly defined courtship song (Von Schilcher, 1976). Early screens have identified critical functions of the cacophony VGCC in song production (Kulkarni and Hall, 1987). In the present thesis, it was tested whether excision of IS4A influenced courtship song and mating success. Among numerous parameters during the courtship ritual orderly courtship song production is thought to enhance mating success (Greenspan and Ferveur, 2000). A first measure taken was the mating success of the animals and next the song patterns were recorded with sensitive mini microphones.

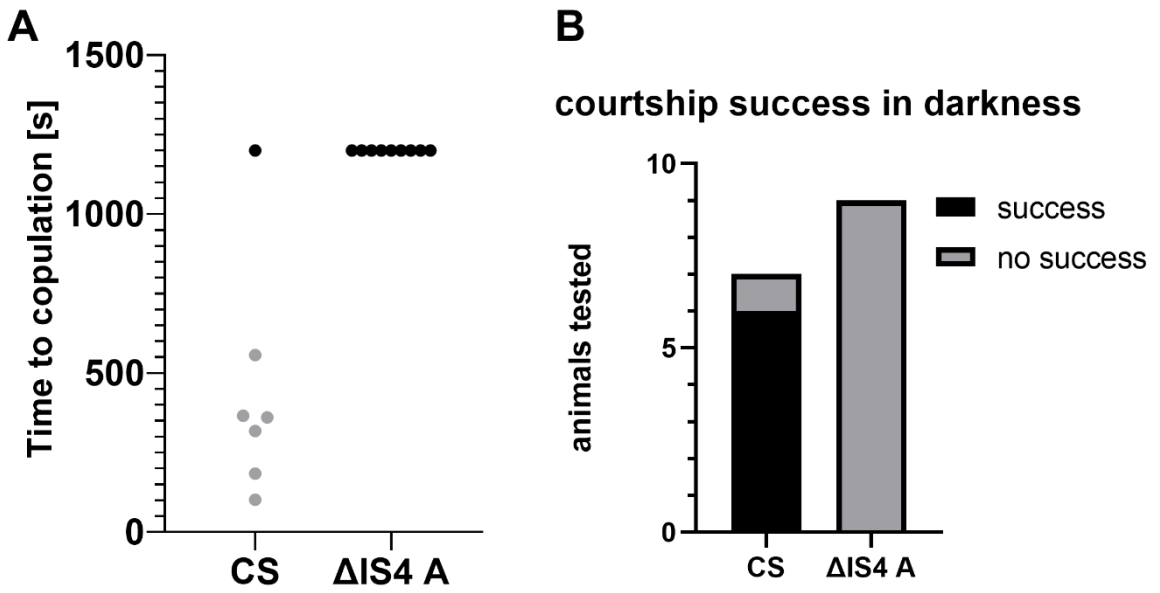

***Figure 10*:loss of IS4 A prohibits successful courtship over a course of 20 minutes:** *A: Time needed in seconds for a naive male to successfully initiate copulation with a virgin female of the same genotype in darkness, median CS=360,6 sec[n=7] for ΔIS4 A =1200[n=9] black datapoints.1200s means the animal did not copulate in the time set for the experiment B: overall courtship success over a course of 20 minutes in darkness (CS: 8/9, ΔIS4A: 0/9) is highly significantly different (Fisher's exact test p=0.0009)*

Figure 10 A shows that ΔIS4 A animals did not engage in mating behavior within 20 minutes, a duration in which nearly all CS control animals engaged into copulation. Moreover, ΔIS4 A animals did not copulate successfully within the allotted time. By contrast, all but one of the Canton flies succeeded to copulate even within 10 minutes (Figure 10 B). This difference in courtship success is highly significant (Fisher's exact test p=0.0009). One possible cause for the reduced engagement of ΔIS4A animals into flight (see above) or courtship behavior is reduced vision, as some *cacophony* mutants have been reported blind (Smith *et al.*, 1998). Therefore, I compared courtship success between ΔIS4A and control animals in the dark (Figure 10 B) and confirmed significantly reduced mating success in ΔIS4A animals.

The significant lack of mating success in ΔIS4A animals could be caused by a reduced motivation to initiate courtship behavior or by an inability to perform specific aspects of the courtship ritual, such as chasing the female or song production. It is not caused by an inability to mate, because homozygous ΔIS4A animals can be reared under normal laboratory conditions.

To test whether song production was impaired, I recorded and analyzed courtship song patterns in some ΔIS4A flies that initiated song. Recordings were conducted with a custom built highly sensitive microphone (see methods 2.3.3.), digitized, and analyzed. Normal courtship song consists of two components, first so-called sine song that is characterized by low amplitude up and down movements of one wing at a frequency of roughly 160 Hz, and second, pulses song that is characterized by high amplitude downstrokes of one wing at an inter pulse interval of 34ms (Kulkarni and Hall, 1987). Both song components can be readily identified in recordings of singing male control flies (Figure 11, upper trace) and in recordings of ΔIS4A males (Figure 11, lower trace). No qualitative differences were observed between control and ΔIS4A animals with regard to the interval between subsequent pulses or sine song frequency (Figure 11). Given the low occurrence of song in ΔIS4A animals, these data were not further quantified. However, the microphone recordings clearly demonstrate that ΔIS4A animals show both song components at normal frequencies once courtship song is initiated. Therefore, the virtually nonexistent courtship success of ΔIS4A in this paradigm cannot be explained by an inability to produce song or by false song production. One likely explanation for the lack of copulation in this paradigm could be that reduced locomotor ability of the males prohibits chasing the female, which is a requirement for successful courtship.

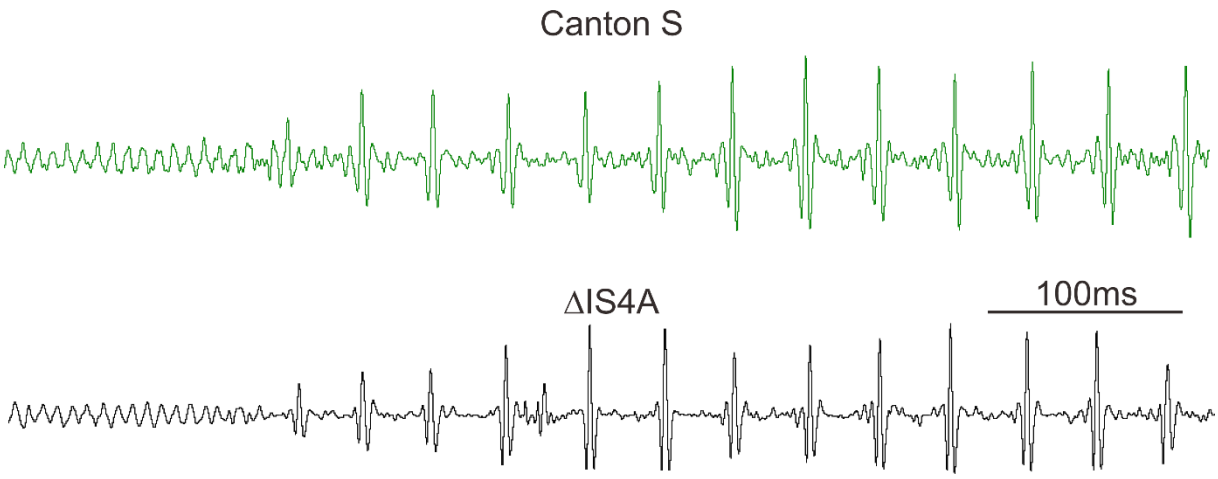

***Figure 11**: Canton and ΔIS4A animals do not show any obvious differences in song structure. Representative microphone recordings of courtship song of Canton S and ΔIS4A animals. The low amplitude part to the left is the so-called sine song, while the higher amplitude spikes show the pulse song.*

Contrary to this severe reduction in mating success of animals lacking IS4A, animals lacking the I-II A exon performed normal in these courtship analyses. The comparison of courtship success of ΔI-II A animals and the appropriate cac^{sfGFP} controls revealed no significant difference (Figure 12, Fisher's exact test $p>0.9999$).

Similarly, the time to copulation was not significantly different between ΔI-IIA animals and controls (Figure 12 B, unpaired t-test $p=0.431$). These findings confirm that a loss of I-II A does not affect the courtship success of the flies.

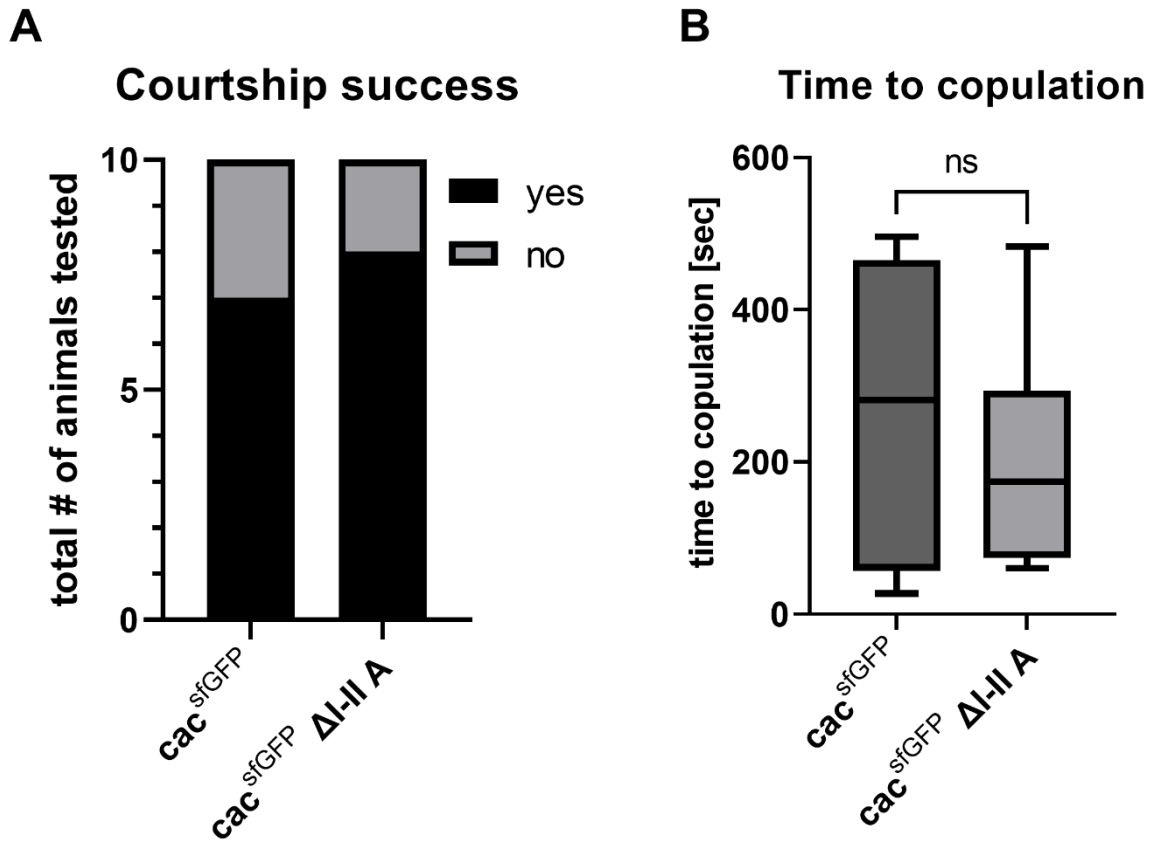

***Figure 12**: courtship success and time to copulation are unaffected by loss of exon I-II A : A: Courtship success of 10 animals of each cac^{sfGFP} and cac^{sfGFP} ΔI-II A observed for 10 minutes is not affected (Fishers exact test p>0.9999), B: time needed till copulation as a measure of successful courtship of the animals which mated in A (n of cac^{sfGFP} = 7; n of cac^{sfGFP} ΔI-II A = 8) is also not affected (unpaired t-test: p=0.431)*

To further analyze whether male courtship song patterns were affected in ΔI-IIA animals, I quantified sine song frequency (Figure 13 A) and the duration between subsequent song pulses (Figure 13 B, IPI) from microphone recordings. There was no statistically significant difference in either song parameter between ΔI-IIA and control animals (sine song frequency p=0.0715, unpaired T-test; IPI p= 0.0941, unpaired T-Test).

Taken together, neither the courtship song structure nor the resulting mating success is significantly affected by the loss of the I-IIA exon.

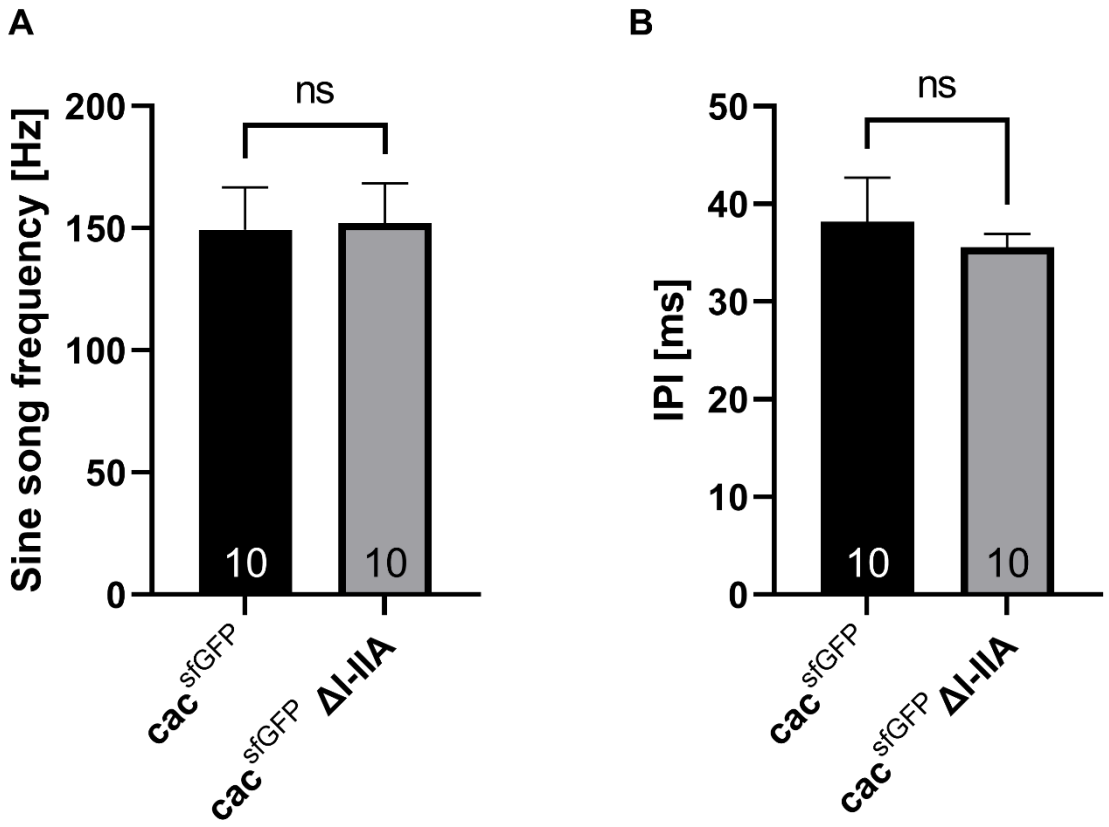

Figure 13: loss of I-IIA does not affect courtship song*: A: sine song frequency is unaffected by loss of I-IIA (unpaired t-test: p=0.715)* ***B:*** *Inter Pulse Interval (IPI)l is also not affected by loss of I-IIA (unpaired T-Test: p=0.0941) each cohort was composed of 10 recordings*

The motor behavioral tests confirm an essential role of the IS4 locus. ΔIS4A showed similar defects across all behaviors examined. The main function mediated by IS4A appears to be on the level initiating behavior and less on the correct execution of motor programs. However, the lack of IS4A also causes a severely reduced lifespan (Figure 5, see above). Moreover, animals homozygous for the other alternative IS4 exon, ΔIS4B, are not viable. Therefore, both alternative IS4 exons mediate critical functions in a non-redundant manner. By contrast, a lack of I-IIA does neither reduce lifespan nor motor performance. This indicates rather redundant functions of the alternative I-II exon, but additional non-redundant functions hidden to the life span and behavioral assays conducted in this thesis cannot be excluded.

To further scrutinize the non-redundant functions of the IS4A exon and the functions of the I-IIA exon on a cellular level, I next analyzed the cellular and the sub-cellular localization of the isoform reduced variants across different developmental stages. Then, I conducted functional tests on the cellular level by utilizing electro- and optophysiology.

3.3 Excision of specific alternative exons affects the localization of cacophony in the nervous system

I conducted immunohistochemistry with subsequent confocal laser scanning imaging experiments to test whether the general localization patterns of the cacophony proteins through the CNS, or whether the specific subcellular targeting of cacophony to specific compartments of identified motoneurons was affected by the exon excisions (see Methods). Immunocytochemistry was used to amplify the sfGFP tag tethered to the cacophony variants for better detection with a confocal laser scanning microscope, as well as to detect possible colocalization by applying antibodies for other proteins or structures of interest.

3.3.1 Loss of IS4B results in loss of cacophony in the larval VNC, but excision of other alternative exons does not cause differences of cacophony localization in the larval VNC

One of the behaviors analyzed was larval crawling, where a significant decrease in locomotion of the ΔIS4A larvae was observed (see above). Given that the larval motoneurons and premotor circuits for crawling are located in the ventral nerve cord (VNC), the localization of the different cacophony variants in larval VNC was examined.

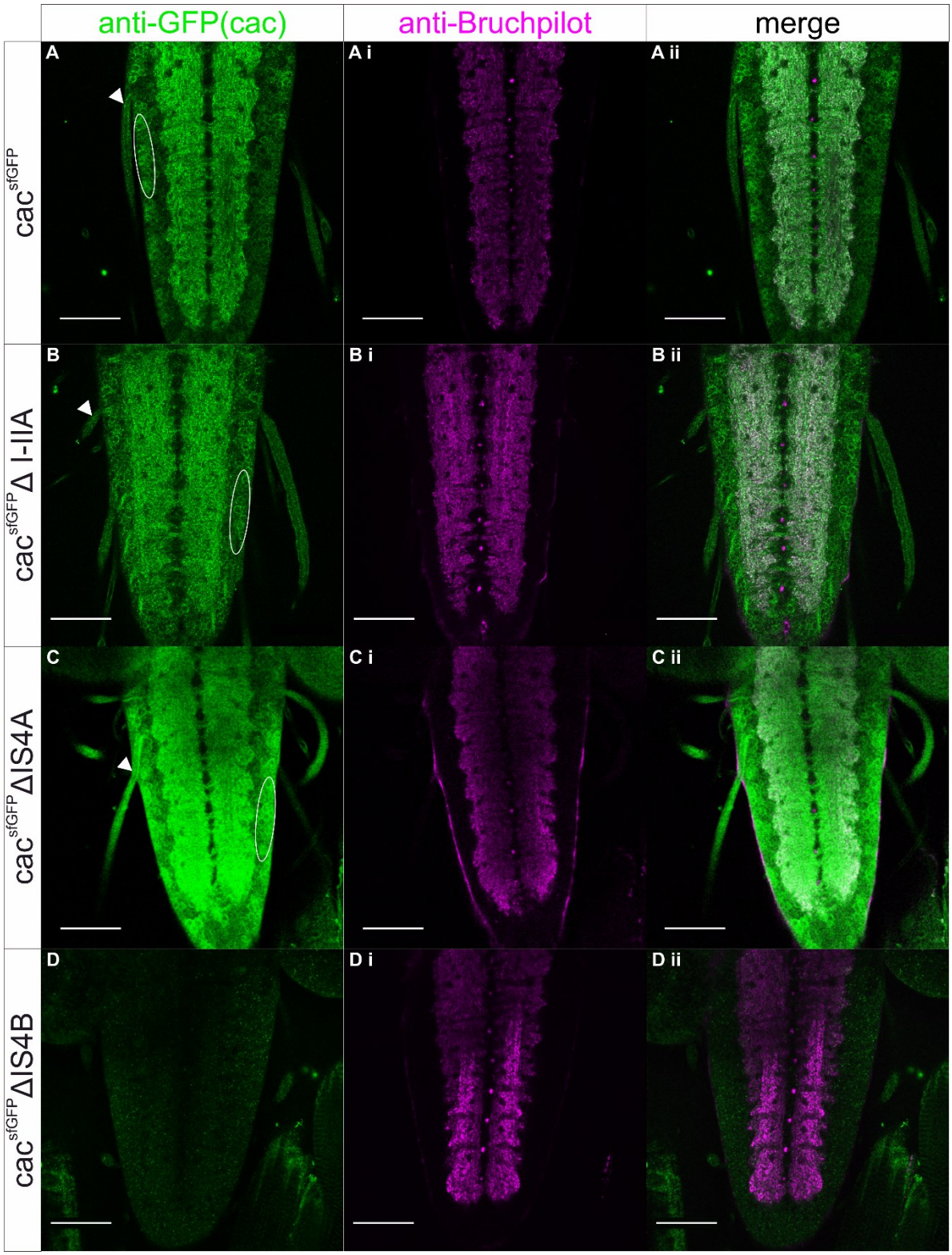

Figure 14: larval VNC cacophony label is not detectable above background in animals missing the IS4 B exon whilst normally distributed in the other exon excisions: ventral nerve cord (VNC) of L3 Drosophila *larvae; anti-GFP to localize the tagged cacophony (green, left column A-D) and anti-BRP to co-label for active zones (magenta, middle column Ai-Di) and merges of the two channels to visualize colocalization (right column Aii-Dii); white ellipses delineate somata expressing cacophony, arrowheads point to nerve roots also expressing cacophony A: positive control: cac^{sfGFP}; B: cac^{sfGFP} ΔI-IIA; C: cac^{sfGFP} ΔIS4A D: cac^{sfGFP} ΔIS4B; scalebar: 50µm.*

Representative images (Figure 14) demonstrate that absence of IS4A and I-IIA does not affect the localization of cacophony to the VNC neuropil regions (Figure 14, B, C). The neuropil regions were co-labelled with α-Bruchpilot (BRP, Figure 14 magenta) an active zone protein that is commonly used as a synaptic marker in *Drosophila* (Kittel et al., 2006). Similarly, in GFP tagged controls (cac^{sfGFP}) as well as in IS4A and I-IIA exon excision mutants, many larval motoneuron somata are GFP positive (Figure 14, A, B, C, white ellipses). Furthermore, the same is true for the segmental nerve roots of the VNC, which carry motoneuron axons to the body wall muscles as well as afferent sensory axons (Figure 14, A, B, C, white arrowheads). For the larval VNC I did not further distinguish the possibilities whether positive cacophony-sfGFP label in nerve roots was caused by sensory neuron axons, motoneuron axons, or both (but see below for the adult stage).

In contrast, the VNC of the animals lacking the IS4B exon show no label in the central neuropil of the VNC, motoneuron somata or nerve roots. Please note that these animals are homozygous lethal (compare Table 5/Figure 5), so that localization analysis in the VNC was conducted with heterozygous animals.

However, it is unlikely that heterozygosity is the cause for the absence of ΔIS4B label in the VNC, because inspection of heterozygous GFP tagged controls and heterozygous ΔIS4A clearly revealed positive label in the neuropil and in motoneurons (data not shown). In sum, there are no qualitative differences in VNC localization between tagged controls, ΔIS4A, and ΔI-IIA mutants. By contrast, ΔIS4B animals show no cacophony in the VNC. Therefore, the IS4B exon is required for normal cacophony localization in the VNC (Figure 14) and for viability (compare Table 5/Figure 5). By contrast, the significantly reduced life-span and larval motor performance in the ΔIS4A animals is not reflected in qualitatively different cac localization in the larval VNC and must thus be caused by different functional consequences of the IS4A exon excisions. In case of the ΔI-IIA animals, the qualitatively normal cacophony expression correlates with the normal crawling behavior, and therefore motor function (Figure 8). However, the different motor behavioral consequences of the IS4A and the I-IIA exon excisions are not a consequence of qualitatively different expression patterns in the VNC. Possible causes for the phenotypic differences are different channel properties or different interactions with other proteins that may result from different exon combinations (see

chapters on physiological analyses below) or aberrant subcellular localization hidden to this type of analysis.

3.3.2 The larval VNC expression patterns are recapitulated in adult VNC

Since many of the behaviors examined in this thesis are adult-specific, such as climbing, flight, and courtship, I conducted the equivalent analysis in the adult VNC. This allows for a comparison of expression patterns in the VNC to the behavioral phenotypes. Furthermore, first insights can be gleaned into whether cacophony undergoes developmental shifts in expression pattern by examining essentially the same structure in two different developmental stages.

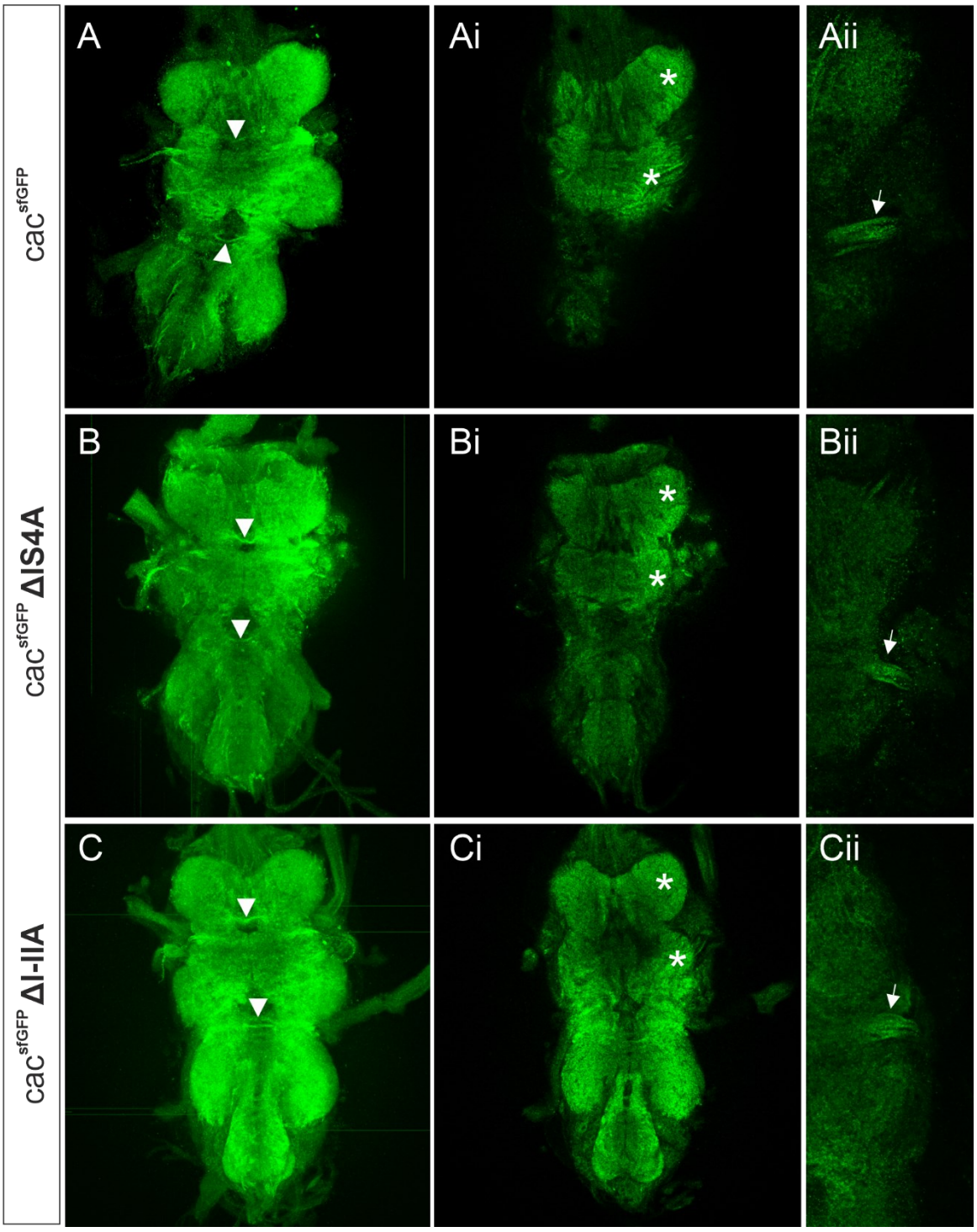

Figure 15: Adult VNCs showing cacophony label*: anti-GFP immunostaining of different genotypes:* ***A:*** *cac^{sfGFP},* ***B:*** *cac^{sfGFP} Δ IS4A,* ***C:*** *cac^{sfGFP} Δ I-IIA, left column (A-C) shows maximum projection views of confocal image stacks. Axonal bundles in VNC commissures are labeled by arrowheads,* ***i:*** *projection views of 8 optical sections highlighting part of the neuropil (asterisks);* ***ii:*** *magnification of the DLM motoneuron axon bundle(arrows) in segmental nerve roots leaving the VNC towards the flight muscles*

The qualitative distribution of cacophony in the adult VNC (Figure 15) is similar to that in larval VNC (Figure 14). Excision of IS4A (Figure 15 B) or I-IIA (Figure 15 C) does not affect the overall expression patterns of cacophony across the neuropile of the VNC as compared to sfGFP-tagged controls (Figure 15 A, example neuropil regions are labeled with white asterisks).

Moreover, axonal label is also present in the motoneurons innervating the DLMs as demonstrated by projection views of 8 optical sections (z-distance is 1µm) through the axonal bundles of these neurons in the nerve roots leaving the VNC towards the DLMs (Figure 15 Aii, Bii, Cii arrows). As in the larval VNC label for ΔIS4B could not be detected above background level (data not shown).

Taken together, ΔIS4B animals show no detectable cac expression in the larval or adult VNC and are homozygous lethal. ΔIS4A animals show reduced life span and impaired motor performance but cacophony localization to the adult and larval VNC is qualitatively similar to controls. ΔI-IIA animals show normal viability and lifespan, normal motor performance in the assays tested, and cacophony localization in the larval and adult VNC is qualitatively similar to controls but appears dimmer in the larval VNC. While life expectancy and motor performance are significantly reduced in ΔIS4A animals but not in I-IIA deficient mutants, the expression patterns of both variants show no obvious differences in the adult VNC. Therefore, the impairments of ΔIS4A animals are unlikely caused by erroneous expression in the VNC.

3.3.3 Cacophony expression pattens in the *Drosophila* brain are isoform specific

The similarities in cacophony expression patterns across the VNC in controls and animals lacking IS4A or I-IIA led to the conclusion that cacophony distribution in these parts of the nervous system was not likely the cause of the different behavioral phenotypes. Although the pattern generating networks for motor behavior are located in the VNC, many other aspects of motor control require higher brain parts. Therefore, I next analyzed the expression patterns of all genotypes in the brain by immunocytochemistry and subsequent CLSM.

3.3.3.1 IS4 B is required for cacophony expression in many but not all structures in the adult Drosophila central brain

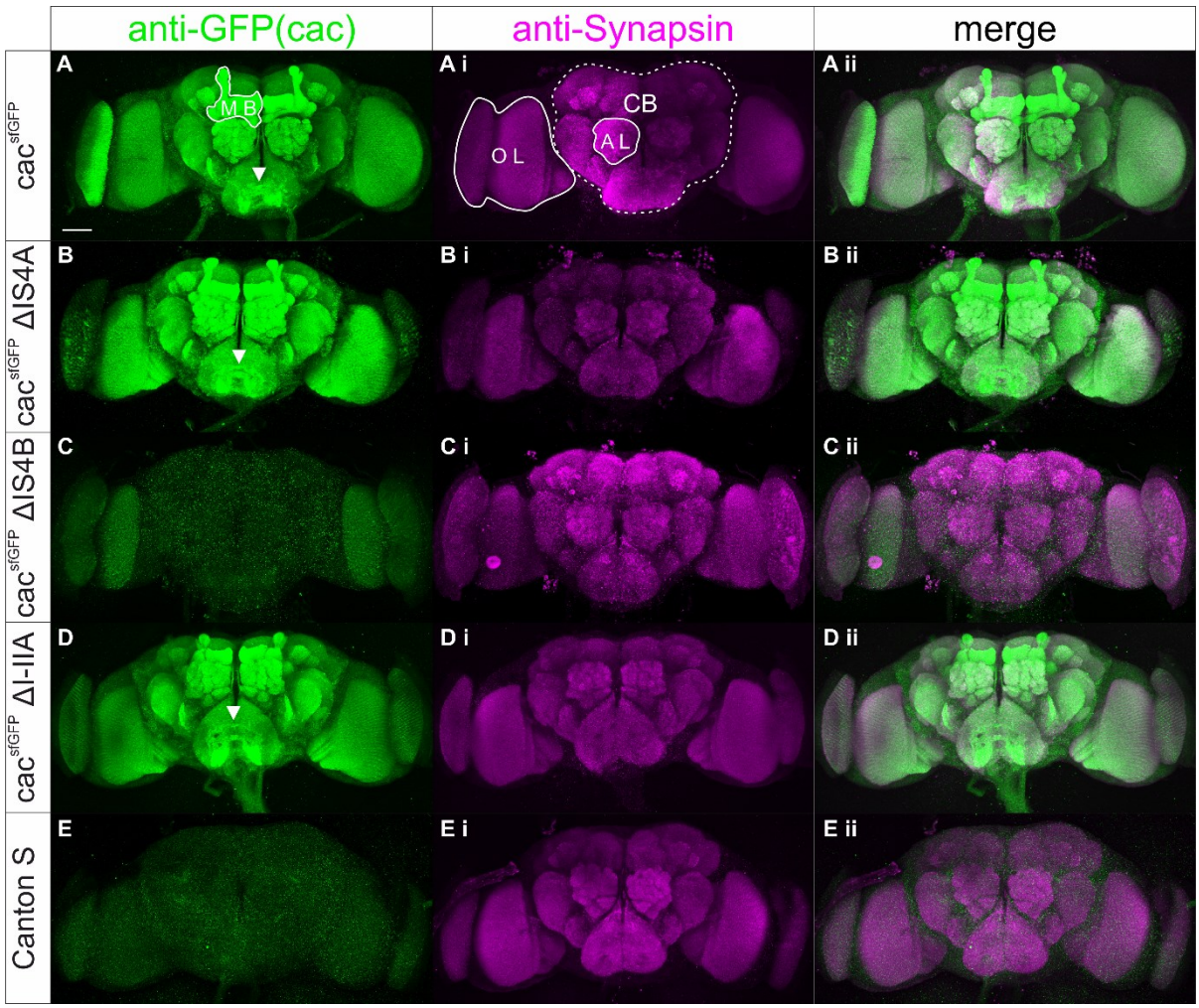

Figure 16: Maximum projection of whole mount adult Drosophila brains of different genotypes*; anti-GFP (cac): green, left column A-E, anti-Synapsin: magenta, middle column Ai-Ei, merge: right column Aii-Eii; A-Aii: cac^{sfGFP} positive control white line delineates mushroom body (MB); Ai: synapsin label shows prominent structures: optic lobes (white line, OL), central brain (dashed line, CB) and antennal lobes with typical glomeruli structure(white line, AL) B-Bii: cac^{sfGFP} ΔIS4A; C-Cii: cac^{sfGFP} ΔIS4B; D-Dii cac^{sfGFP} ΔI-IIA; E-Eii: Canton S, negative control; arrowheads in A,B and D point to axonal commissures in the central brain; scalebar in the top left panel equals 50µm for all images.*

Antibodies against GFP were used to amplify the label resulting from genomically tagged cacophony protein, while antibodies against synapsin were used as a co-label to visualize the synaptic neuropil areas. As exemplified by cac^{sfGFP} (Figure 16 A, Ai, Aii) cacophony is expressed in most of major neuropils in the *Drosophila* brain, such as the olfactory glomeruli of the antennal lobes (Figure 16 A-Aii, AL), the optical lobes (Figure 16 A-Aii, OL), and in many additional smaller structures. Moreover, strong cacophony label is also present in the mushroom body lobes (Figure 16 A-Aii, MB) which are comprised of Kenyon cell axons (Kenyon, 1896). Therefore, as in the VNC cacophony is present in nearly all synaptic neuropils as well as in axon bundles (Figure 16 A-Aii, MB and arrowheads). When comparing this broad expression

pattern in controls to the pattern of the animals lacking IS4A (Figure 16 B, Bi, Bii) or I-IIA (Figure 16 D, Di, Dii) most of these structures show qualitatively similar cacophony expression. However, clear differences can be observed in the optical lobes and will be further examined below. By contrast, animals without IS4B (Figure 16 C, Ci, Cii) lack cacophony expression across the entire central brain (compare Figure 16 A-Aii, CB). No label is detected above background, in the antennal lobes, the mushroom body, or the overall central brain neuropil regions. However, when comparing this to the native untagged cacophony of the Canton S flies (Figure 16 E, Ei, Eii), positive label in the Δ IS4B brains is clearly detected in the optic lobes and in the saddle, both of which will be further examined below. This indicates that cacophony isoforms including only IS4A but not IS4B are targeted exclusively to the optic lobes and the saddle but not any other brain or VNC part. This suggests that the IS4A exon restricts cacophony expression to these two distinct brain regions.

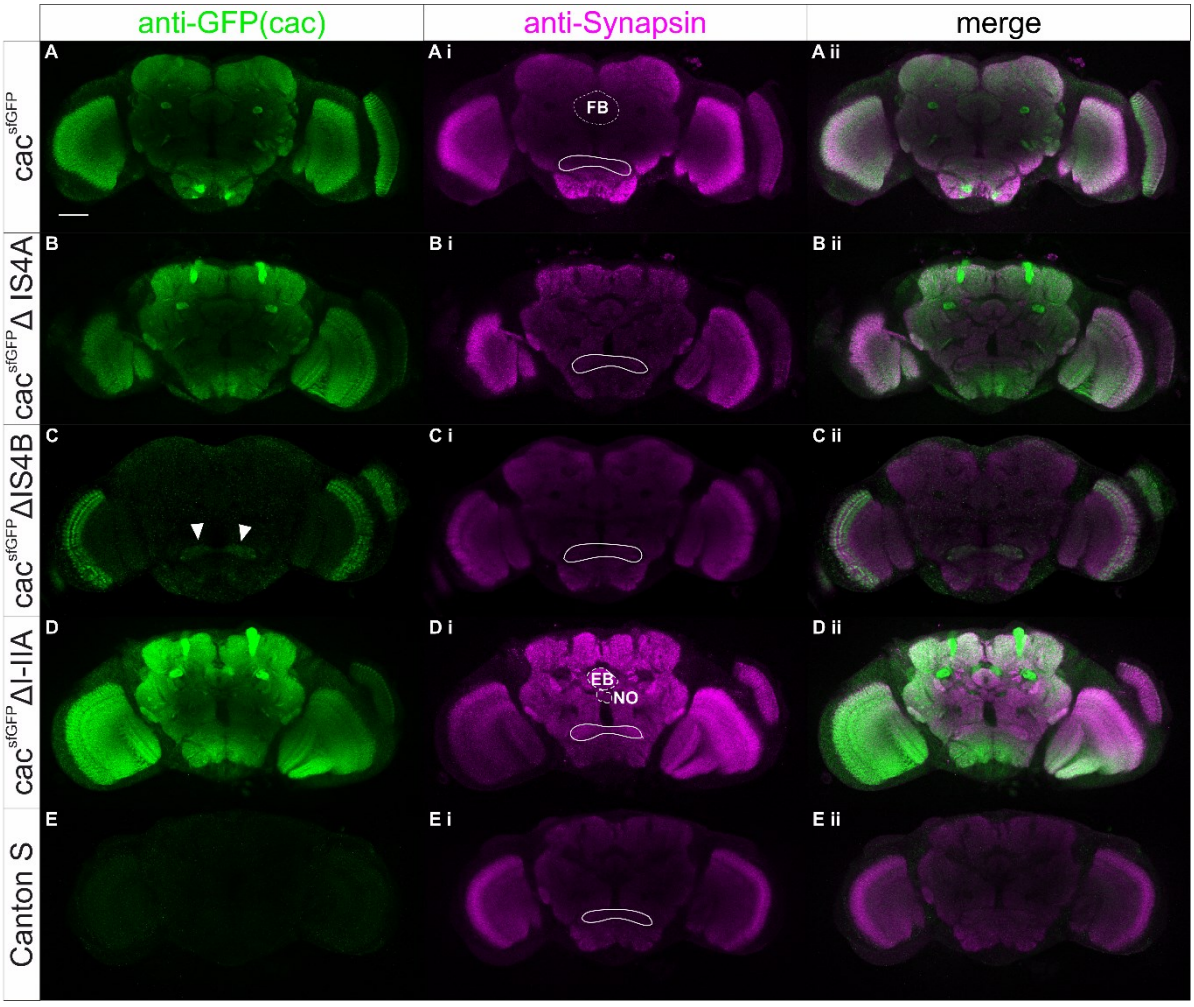

Figure 17: Single optical sections of confocal image stacks of whole mount adult Drosophila *brains of different genotypes; anti-GFP (cac): green, left column A-E, anti-Synapsin: magenta, middle column Ai-Ei, merge: right column Aii-Eii; A-Aii: cac^{sfGFP} positive control; B-Bii: cac^{sfGFP} ΔIS4A; C-Cii: cac^{sfGFP} ΔIS4B; D-Dii cac^{sfGFP} ΔI-IIA; E-Eii: Canton S, negative control; solid white line in middle column marks the saddle, C: arrowheads highlight the cacophony label in the saddle/antennal*

mechanosensory and motor center (AMMC)Ai&Di: dashed lines delineate parts of the central complex: fan-shaped body (FB, Ai) ellipsoid body (EB, Di) and noduli (NO, Di); Scalebar: 50µm

Examining individual optical section of the confocal stacks shown in Figure 17 allows for better visualization of cac expression pattern in ΔIS4 B animals. Here, label can only be seen in the saddle (Figure 17 C: arrowheads), specifically in its subsection with the antennal mechanosensory and motor center (AMMC) as well as in the optical lobes. The latter is further analyzed in a magnification in Figure 18. Furthermore, all parts of the central complex could be found in ΔIS4A and ΔI-IIA animals, but not in ΔIS4B (data not shown). All major central complex structures, such as the fan-shaped body (Figure 17 Ai, FB), the ellipsoid body (Figure 17 Di, EB) and the noduli (Figure 17 Di, NO) can be seen in some of the single optical slices in ΔIS4A and ΔI-IIA animals (not shown). Identification of the AMMC was achieved through comparison of the cac positive structure in ΔIS4B animals with a virtual fly hemibrain (Milyaev *et al.*, 2012). Whether cacophony label in the saddle is also present in the other two exon excision genotypes could not reliably be determined, because the significantly broader cacophony expression in brains of these flies reduces the contrast needed for reliable detection in the saddle, and no specific co-label for the saddle is available. Similarly, subtle differences among genotypes in cacophony expression patterns in other brain areas cannot be excluded. However, these data indicate that lethality of homozygous ΔIS4B animals is caused by a lack of cacophony expression in VNC and the central brain, but not by a complete absence of cacophony in the CNS. The cacophony isoforms that remain after IS4B excision are clearly expressed in distinct brain regions, indicating that the IS4 A exon restricts cac expression to few select brain parts.

3.3.4 Alternative exons for the IS4A locus induce complementary expression pattern in parts of the optic lobes

One other name for the *cacophony* mutation is *nightblind A* (nbA) due to early investigated *cacophony* mutants showing defects in phototaxis and orientation in low light conditions (Heisenberg and Götz, 1975; Smith *et al.*, 1998). Considering that I observed reduced flight initiation in some excision mutants, and flight is a visually guided behavior, impaired vision could be a possible explanation for reduced responsiveness. Therefore, the cacophony label in the optic lobes was examined in more detail.

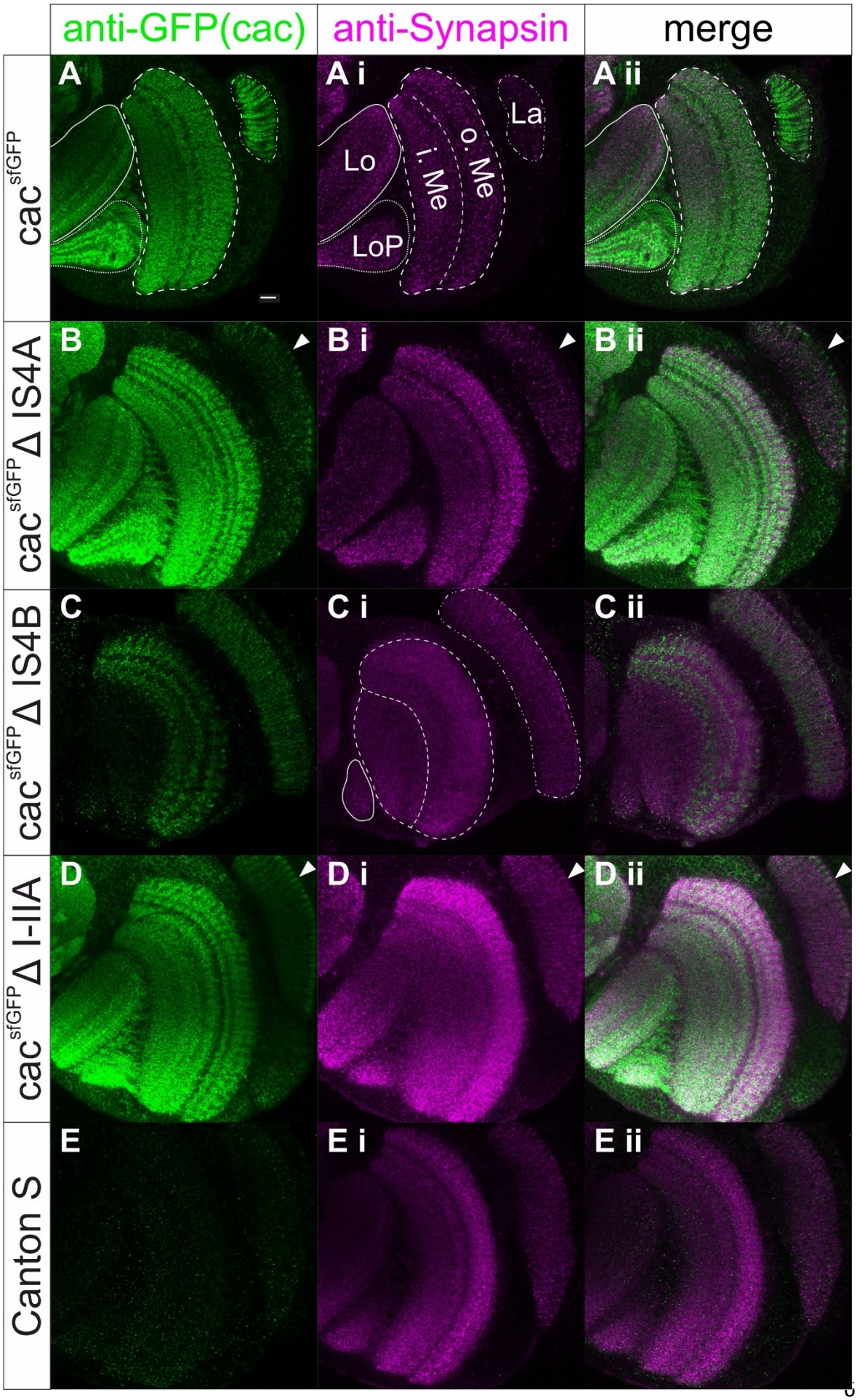
anti-GFP(cac)
anti-Synapsin
merge
cac^sfGFP
cac^sfGFP Δ IS4A
cac^sfGFP Δ IS4B
cac^sfGFP Δ I-IIA
Canton S
A
A i
A ii
B
B i
B ii
C
C i
C ii
D
D i
D ii
E
E i
E ii
La
Lo
i. Me
o. Me
LoP

Figure 18: Optical lobes and lamina show different expression patterns of cacophony based on the isoforms present: magnification of optical lobes and lamina of whole mount adult Drosophila *brains of different genotypes; anti-GFP (cac): green, left column A-E, anti-Synapsin: magenta, middle column Ai-Ei, merge: right column Aii-Eii; A-Aii: ca^{csfGFP} positive control; B-Bii: cac^{sfGFP} ΔIS4A; C-Cii: cac^{sfGFP} ΔIS4B; D-Dii cac^{sfGFP} ΔI-IIA; E-Eii: Canton S, negative control; optical lobes: medulla: inner Medulla(i. Me) & outer Medulla (o.Me)(dashed line) lobula plate (LoP, dotted line) lobula (Lo, solid line) and lamina (La, dots and dashes) arrowheads denote apical cac label in lamina; Scalebar: 10µm*

When comparing the label in the inner (compare Figure 18 Ai, i.Me) and outer medulla (compare Figure 18 Ai, o.Me) as well as the lobula (compare Figure 18 Ai, Lo) and lobula plate (compare Figure 18 Ai, LoP), no striking qualitative differences can be found between the tagged controls (Figure 18 A), ΔIS4A (Figure 18B) and ΔI-IIA (Figure 18D) animals. In contrast, in ΔIS4B animals label can only be found in the outer medullary layers (Figure 18). Meaning no label can be found in the lobula, lobula plate(see Figure 17C, since the image in Figure 18 C was chosen to better represent the lamina label) or the inner medulla (Figure 18 C), similar to the negative controls (Figure 18 E). When examining the lamina, ΔIS4A and ΔI-IIA animals both show a reduction in cacophony expression along the lamina cartridges and only show denser expression at the apical part (Figure 18 B, D, arrowheads) of the lamina. Moreover, this apical label is qualitatively different between ΔIS4A and ΔI-IIA. The lamina label in ΔI-IIA (Figure 18 D) animals shows a smooth but weak distribution along the lamina cartridges and an even bulbous label at the apical end of the lamina cartridges. By contrast, the label in the ΔIS4A (Figure 18 B) animals is sparser along the lamina cartridges and granular at the apical tips of the lamina. This ΔIS4A lamina label is in complementary to the label found in the ΔIS4B (Figure 18C) animals, where the label along the lamina cartridges is strong and even, while no label can be found at the apical part, as can be verified when examining the co-label with synapsin (Figure 18 Bi, arrowhead).

In sum, these findings show distinctly different expression patterns for all examined exon excision mutants in the lamina. Reinforcing the hypothesis that different isoforms differ in their localization. Notably, for animals lacking the I-IIA exon, this reduced expression pattern is the first observed difference to native cacophony, although these animals are not significantly affected in lifespan, vitality, motor behavior in adult and larval assays, or in localization across the VNC in larva and adult. This points to a highly specialized function of the I-IIA exon in the lamina.

Furthermore, cacophony incorporating the IS4A exon, as evidenced by examining the ΔIS4B animals, results in a narrow expression pattern. This pattern could not be found in any examined structure but the AMMC (Figure 17 C) and the lamina and outer medulla (Figure

18C). Specifically in the lamina the expression pattern of IS4B, as seen by examining the ΔIS4A animals, is complementary to that of IS4A. This indicates a strict division of labor in the optic system between two different exons encoding the same mutually exclusive part of the protein. In fact, IS4A appears to be the deciding factor for cacophony localization to the lamia cartridges.

To further ascertain which cell types are affected as a consequence of isoform reduction, co-labeling of specific cell types will be required. These experiments will be followed up by collaborators in the lab.

3.3.5 Reduced light responsiveness can be found in animals lacking cacophony in the lamina

Through a collaboration with Christopher Bell in the Ryglewski lab, we tested for physiological correlates of isoform specific *cac* expression in the visual neuropils. This has shown that the variants lacking broad lamina label for cacophony, ΔIS4 A and ΔI-II A, also show severely reduced responses to light stimuli as assessed with electroretinogram (ERGs, Figure 19). Here the extracellular sum potential of different parts of the *Drosophila* visual system can be recorded in response to a light stimulus. Briefly, the ERG consists of three main parts. First, the sum receptor potential (Figure 19) results from a sustained depolarization of the photoreceptors and can be seen as tonic downward response in the ERG that lasts as long as the light stimulus persists. The other two main parts of the ERG are the lamina ON and the lamina OFF responses, which are transient depolarizations of lamina neurons L1 and L2 in response to the receptor potential. Although the lamina ON response overlaps in time with the receptor potential, it is synaptically downstream of the receptor potential (Coombe and Heisenberg, 1986). Therefore, a lack or a reduction of the tonic receptor potential in the ERG indicates impaired phototransduction, whereas absent or reduced lamina ON- and/or OFF-responses indicate impaired synaptic transmission between photoreceptors and specific lamina interneurons, or impaired excitability of specific lamina interneurons.

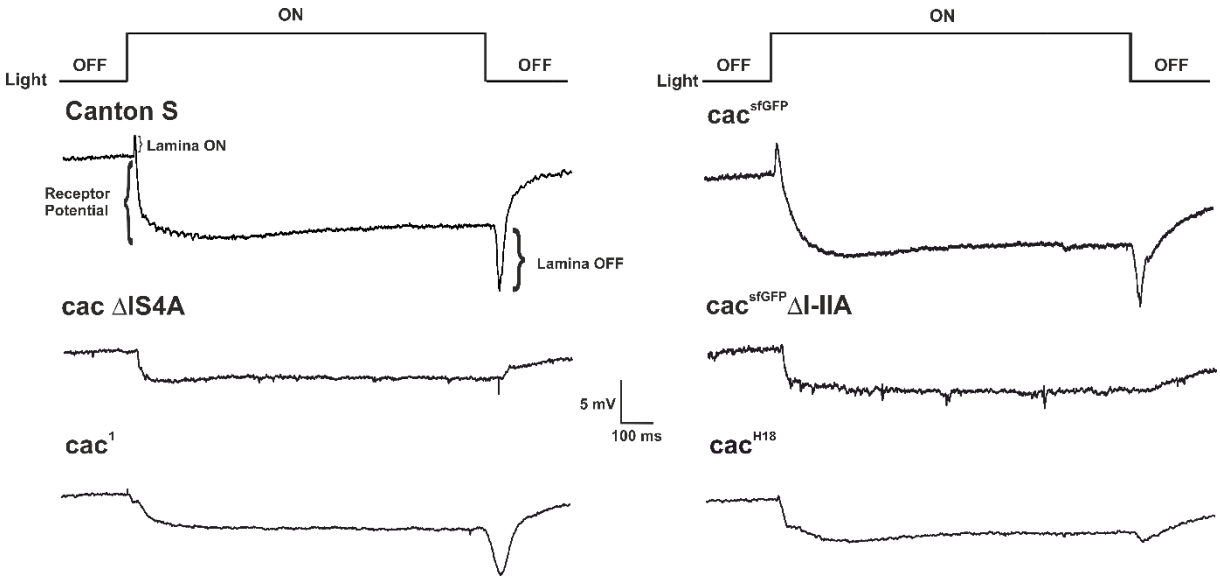

Figure 19: *lamina responses are abolished or reduced in variants missing cacophony in the lamina: representative ERG measurements, light on/off shows onset of light stimulus in recordings, lamina ON (peaks at onset of stimulus), lamina OFF (peaks at end of stimulus) and the receptor potential (depolarization over the course of the stimulus) for different cacophony genotypes and respective controls can be seen: cac^{sfGFP}, Canton S, cac ΔIS4A, cac^{sfGFP} ΔI-IIA, $elav^{C155}$-Gal4>UAS-cac^{1} and cac^{H18}, here cac^{1} is expressed pan neuronally in a cac null background. All receptor potentials are reduced when compared to controls. Lamina responses are abolished in the following genotypes cac ΔIS4A, cac^{sfGFP} ΔI-IIA, cac^{H18} while the lamina OFF response can still be observed in null mutants rescued by pan neuronal expression of cac^{1} (Data courtesy of Christopher Bell)*

Photoreceptor potentials as well as lamina ON- and OFF-responses are qualitatively similar in Canton S control flies and flies with genomically sfGFP tagged cacophony (cac^{sfGFP}). This indicates that the sfGFP tag does not interfere with visual function as assessed by ERG recordings. By contrast, the lamina ON- and OFF-responses are mostly abolished in ΔI-II A and ΔIS4 A animals. ΔI-IIA and ΔIS4A excision mutants also show smaller amplitude receptor potentials as compared to wildtype or cac^{sfGFP} controls. These data indicate that phototransduction is reduced and synaptic transmission to lamina or excitability of lamina neurons is impaired to below ERG detection level by the excision of either IS4A or I-IIA.

Even upon reducing the light stimulus intensity in Canton S animals to recapitulate the response amplitude in the ΔIS4A or ΔI-IIA animals, lamina ON and OFF responses were still reliably elicited in Canton S (Christopher Bell, personal communication).

The effects of loss of I-II A on the ERG can be partially replicated in the cacophony mutant cac^{H18}. This mutant contains a stop codon in the I-II A exon, and thus, is expected to at least partially mimic the ΔI-IIA phenotype (Smith *et al.*, 1998). In both, the cac^{H18} mutant as well as upon excision of I-IIA, the receptor potentials are smaller as compared to control, and the lamina ON-responses are missing. In I-IIA excision mutants the lamina OFF-response is also absent, but a small lamina OFF-response can be observed in cac^{H18}. Therefore, both

phenotypes are similar but not identical. Moreover, pan neuronal rescue of a cacophony null mutant with elav^{C155}-GAL4>UAS-cac^{1}, a specific isoform containing IS4 B and I-II B (Kawasaki, Collins and Ordway, 2002), rescues the lamina OFF-response, but not or only minimally the lamina ON-response.

The receptor potential is reduced in all examined mutants and exon excisions. Please note that none of the examined mutants has native expression of the IS4A and I-IIA variant at the same time. Consistent with this physiological result, my histological data show that lack of either of these exons reduces the cacophony label along the lamina cartridges.

Taking these findings together with the localization across the optic lobes and the behavioral data, specific functions for individual exons can be formulated. The I-IIA exon, although not needed for normal motor behavior and lifespan serves specific functions in the lamina. Excision of I-IIA is in part responsible for the reduced receptor response, as further underscored by comparison with the cac^{H18} animals. This reduced receptor potential could lead to the loss of the downstream located lamina responses, although correct lamina ON/OFF responses could also be an effect of regular I-IIA function. The latter seems more likely because reduced stimulus amplitude did not abolish Lamina ON and OFF responses in controls. Similarly, IS4A can only be found in the lamina and very few other sites throughout the nervous system, as evidenced from histology in ΔIS4B animals. IS4A is required for normal photoreceptor potentials. Similar to I-IIA, the role of IS4A for the lamina responses might be indirect due to a reduced receptor potential or an independent function of IS4A, again the latter seems more likely because reduced light intensity in controls did still yield lamina responses. These data, although qualitative at this point, clearly show that both IS4A and I-IIA likely mediate multiple specific functions in the visual system.

3.4 Subcellular localization of cacophony in controls and in exon excision mutants

The distribution of cacophony in different alternative exon excision mutants through the nervous system correlates with motor behavioral and/or sensory processing, and viability phenotypes. For example, the absence of cacophony in ΔIS4A and ΔI-IIA animals results in aberrant ERG signals (see Figure 19). In addition, it is known that voltage gated calcium channels mediate different functions in different subcellular compartments. For example, cacophony is needed for exocytosis at the chemical synapse, e.g. the larval NMJ (Kawasaki, et al.,2000; 2002; 2004, Krick *et al.*, 2021). Moreover, in adult DLM flight motoneurons,

cacophony channels are not only required at axon terminals for evoked synaptic release (Kawasaki, Felling and Ordway, 2000), but also in the somatodendritic domain (Ryglewski *et al.*, 2012; Ryglewski, Kilo and Duch, 2014), possibly to amplify excitatory synaptic input to dendrites, along the axon to shape action potentials (Heinrich and Ryglewski, 2020), and in the soma for activity dependent transcriptional control of dendrite growth during development (Vonhoff *et al.*, 2013). Therefore, different subcellular localizations of cacophony are essential for specific neuronal functions. To test whether alternative splicing is employed as a means to control subcellular cacophony localization, I next examined the consequences of alternative exon excisions on the subcellular expression patterns of cacophony in larval and adult motoneurons.

3.4.1 Exons I-IIA and IS4A are not required for somatic cacophony expression

As can be seen in Figure 20, cacophony is expressed in the somata of the identified motoneurons aCC and RP2 that innervate larval body wall muscles (Figure 20 white arrowheads). This holds true for ΔIS4A (Figure 20 D) and ΔI-IIA (Figure 20C) animals, but not for the animals lacking the IS4B exon, ΔIS4B animals (data not shown). Therefore, neither IS4A nor I-IIA are essential for somatic localization of cacophony in *Drosophila* larvae. In contrast, absence of label in ΔIS4B animals indicates a somatic function of cacophony isoforms containing the IS4B exon.

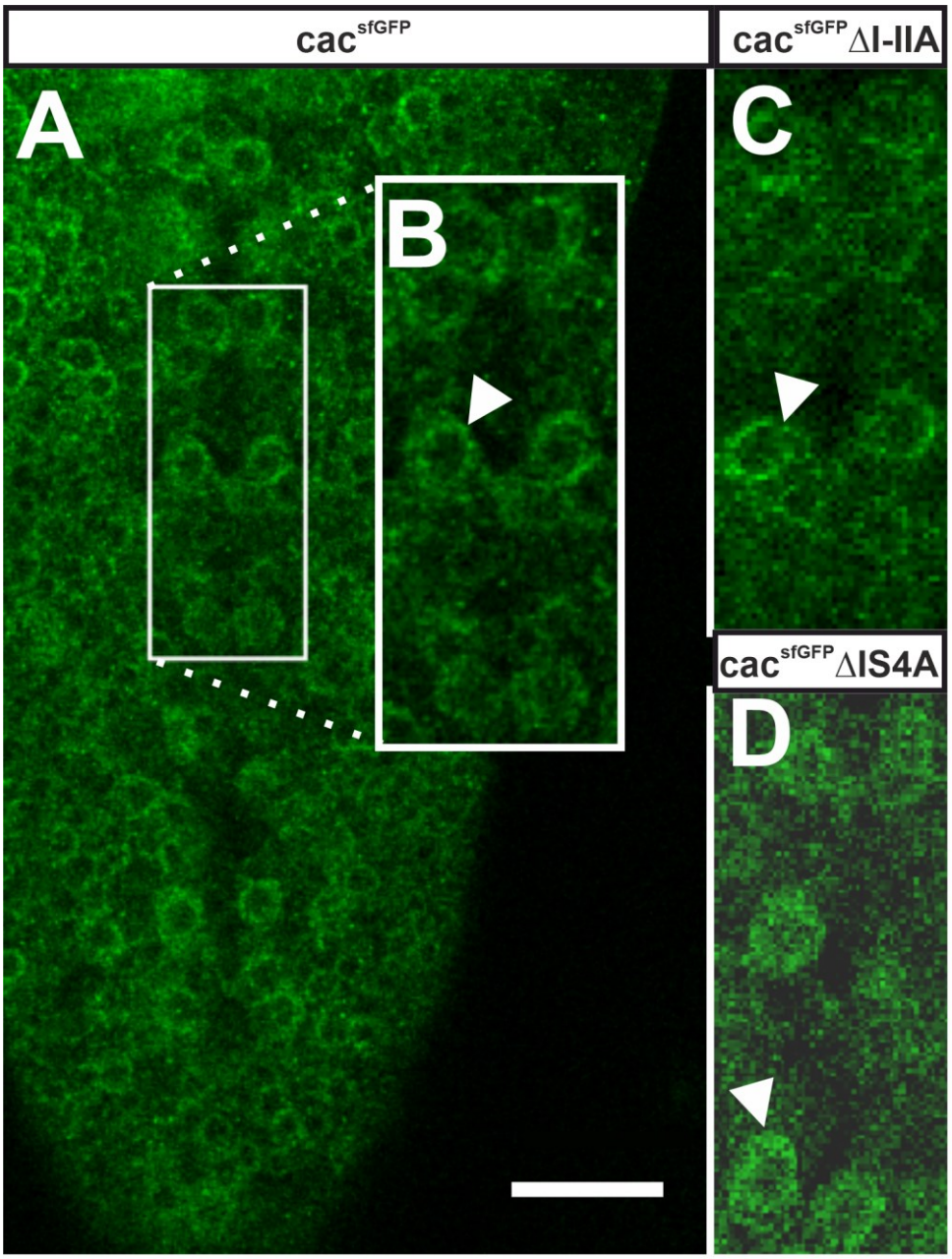

***Figure 20**: larval crawling motoneurons RP2/aCC show cacophony expression in animals missing IS4A or I-IIA. representative single optical sections of the abdominal part of the L3 VNC of cac^{sfGFP} (A, B), cac^{sfGFP}ΔI-IIA (C) and cac^{sfGFP}ΔIS4A (D). All show GFP label (cacophony) in the somata of aCC/RP2 motoneurons (white arrowheads). Differences in label intensity are due to different iterations of the experiment and do not reflect actual differences in expression strength. Scalebar: 25µm*

Additionally, to the positive cacophony label in identified motoneuron somata, ΔIS4A and ΔI-IIA mutants show positive label through all larval VNC neuropils (Figure 14). However, on the level of CLSM, I cannot unambiguously decide whether this label is attributed to the axon terminals, to dendrites of larval motoneurons and interneurons, or both. However, current clamp recordings from larval aCC and RP2 motoneurons in ΔIS4A and ΔI-IIA mutants show normal I/F relationships (Lea Deneke, personal communication). By contrast, hypomorphic mutants for cacophony in aCC and RP2 alter the I/F relationships, which was interpreted as a

consequence of altered somatodendritic cacophony function (Worrell and Levine, 2008). Therefore, it seems likely that neither ΔIS4A nor ΔI-IIA affect the somatodendritic localization of cacophony in larval motoneurons. Consequently, impaired motor behavior of ΔIS4A larvae is unlikely a consequence of altered somatodendritic cacophony localization.

3.4.2 Larval motor axons carry cacophony in animals lacking IS4A or I-IIA

Since the viable excision mutants generated in this thesis do not show any notable effects on somatic cacophony expression, I next examined the axons of these neurons, specifically, the nerve roots of the larval VNC.

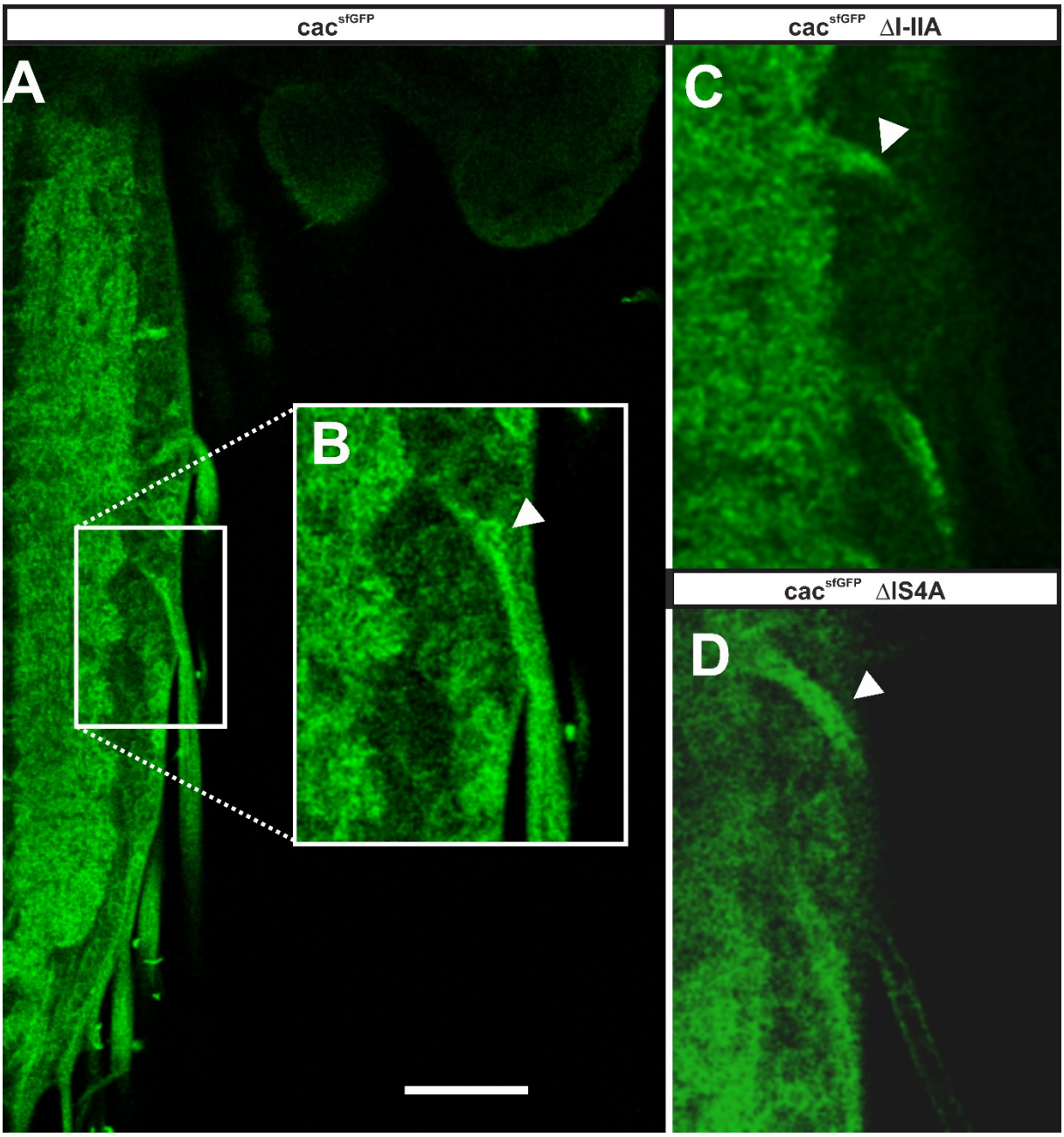

***Figure 21**: Nerve roots and axon bundles leaving the VNC of ΔIS4A, and ΔI-IIA animals are qualitatively not affected by loss of specific exons. Single optical sections of L3* Drosophila *larvae VNCs of cac^{sfGFP} (A, B), cac^{sfGFP}ΔI-IIA (C) and cac^{sfGFP}ΔIS4A (D) all show GFP label (cacophony) in the axon bundles highlighted by white arrowheads. Scalebar: 50µm*

The expression pattern of cacophony in the axons of the exon excision mutants ΔIS4A (Figure 21 D) and ΔI-IIA (Figure 21 C) is unaffected as compared to controls (Figure 21 A, B), at least on the qualitative level examined here. Furthermore, as stated above, without any counterlabel it can not be differentiated whether the axons seen in Figure 21 (white arrowheads) are projections of the motoneurons or other neurons in the same axon bundle. Despite theses experimental limitations, these data show that cacophony clearly localizes to

axons, also in animals lacking IS4A or I-IIA. The impaired locomotor behavior of the ΔIS4A larvae is therefore unlikely attributed to a loss of cacophony expression along the axon.

3.4.3 Loss of exon IS4 B abolishes synaptic cacophony in larval NMJ

A possible reason for the lethality of ΔIS4 B animals is the loss of essential functions of cacophony for exocytosis of neurotransmitters into the synaptic cleft of chemical synapses, since ΔIS4B mutants showed no cacophony positive label in VNC neuropil regions and in multiple neuropils of the central brain (see above). To rigorously test for cacophony localization to presynaptic active zones, the larval neuro muscular junction (NMJ), a commonly used model for glutamatergic synapses, was examined. It is well known that cacophony is required in presynaptic active zones at the *Drosophila* NMJ for evoked synaptic transmission (Gratz *et al.*, 2019; Krick *et al.*, 2021), but information on isoform specific cacophony localization to presynaptic active zones is not available in *Drosophila*. Isoform specific roles at the presynapse for the vertebrate homolog of cacophony, Ca_V2, have been recently identified (Heck *et al.*, 2019).

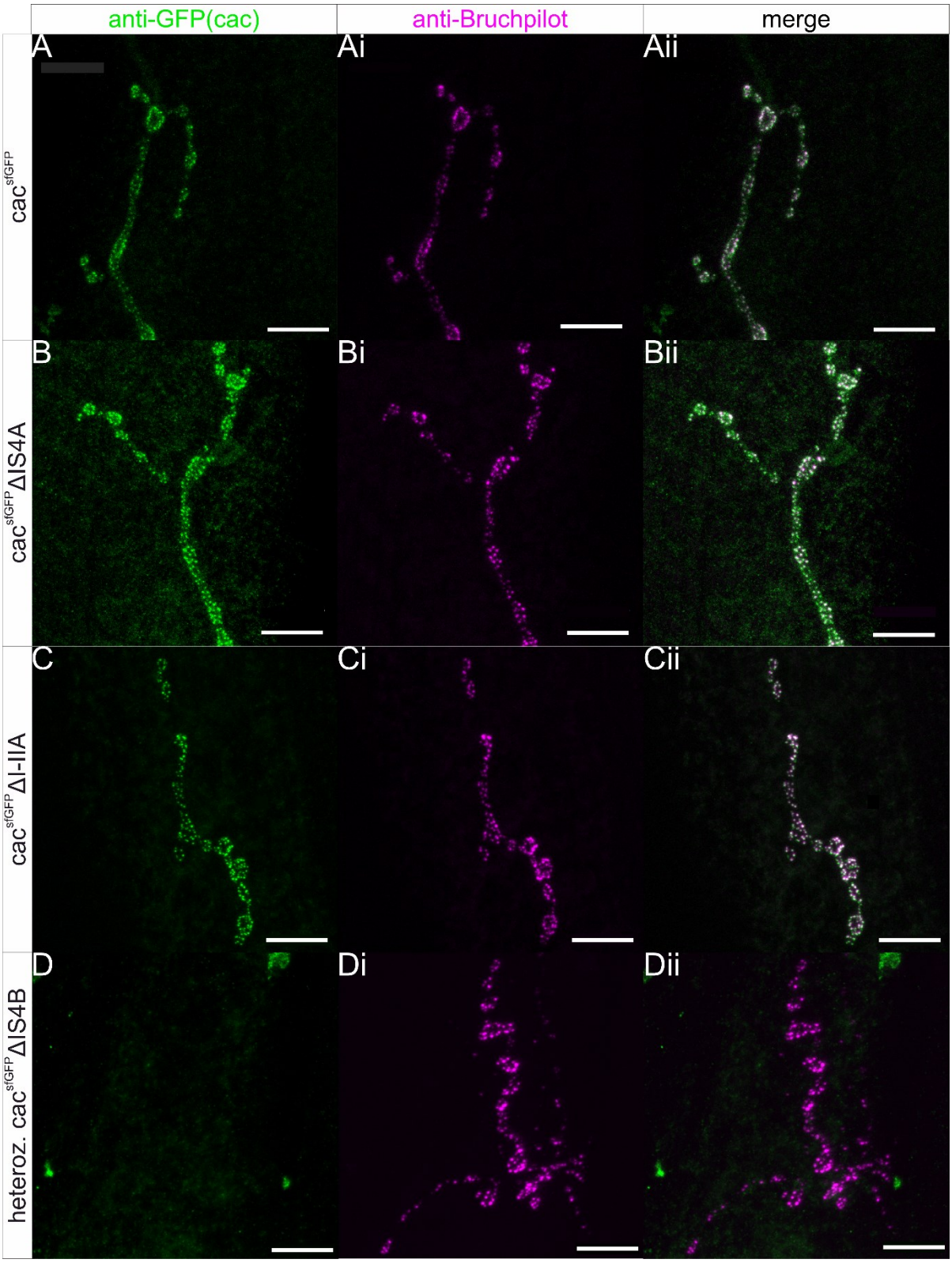

***Figure 22**: ΔIS4 B shows no cacophony label in NMJ AZ in contrast to controls as well as ΔIS4A and ΔI-IIA: Projection views of* Drosophila *larval (L3) NMJ abdominal segment 3 terminals on body wall muscle 4. α-GFP (green A-D) to label sfGFP tagged cacophony of the following genotypes: cac^{sfGFP} (A, Ai, Aii), cac^{sfGFP} ΔIS4A (B, Bi, Bii), cac^{sfGFP} ΔI-IIA (C, Ci, Cii) and cac^{sfGFP}ΔIS4B (D, Di, Dii). α-Brp (magenta, Ai- Di) label to identify active zones, scalebar: 10µm.*

Here (Figure 22), the boutons of motoneuron terminals at the 3rd instar larval NMJ on muscle 4 of abdominal segment 3 are examined. The sfGFP tagged cacophony channels are co-labeled

with the active zone marker bruchpilot (Kittel *et al.*, 2006). Bruchpilot and sfGFP label colocalize as can be seen in the cac^{sfGFP} control (Figure 22 Aii) as well as in both the ΔIS4A (Figure 22 Bii) and the Δ I-IIA (Figure 22 Cii) variants. Contrary to this no specific label of ΔIS4B can be seen at the active zones (Figure 22 D, Di, Dii). This effect is consistent across all screened animals. Please note that the animals lacking the IS4B exon were heterozygous over native untagged cacophony to produce viable animals. Therefore, the lack of cacophony expression in active zones in the ΔIS4 B animals could be caused by tagged protein levels below the detection threshold. Recent estimates of cacophony channel numbers in NMJ presynaptic zones yield about 10 channels per active zone (Martin Heine, personal communication). If expression of tagged channels from the ΔIS4B chromosome was equal to the expression of native untagged channels from the other chromosome, this would yield approximately 5 channels per active zone. I expect that I would have detected this signal with increased laser and detector intensity but tagged ΔIS4B label was always below detection threshold. Moreover, in exploratory experiments I expressed tagged ΔIS4A heterozygously over untagged native cacophony and could detect cacophony in active zones in these ΔIS4A animals, further supporting this hypothesis. The qualitatively similar label in ΔIS4A animals to controls offers no explanation for the reduction of locomotion observed in larval crawling assays (see Figure 8) based on availability of cacophony in the active zone. The variation in label of ΔI-IIA animals to controls or ΔIS4A animals are likely due to different imaging settings across several preparations.

3.4.4 Active zone density per bouton is unaffected by loss of specific cacophony exons

To exclude developmental effects of specific exon deficiencies on boutons and/or AZ numbers these parameters were separately assessed. To quantify any changes to the relations of the boutons and the active zone numbers, the general shape, and area of the terminals was mapped out using the neuronal marker HRP. The active zones themselves were then visualized using the synaptic marker BRP. Image stacks of the terminals were fed into a custom Python processing pipeline (see supplements), and based on the scripts by the Schenck lab (Nijhof *et al.*, 2016), the number of active zones and boutons were calculated.

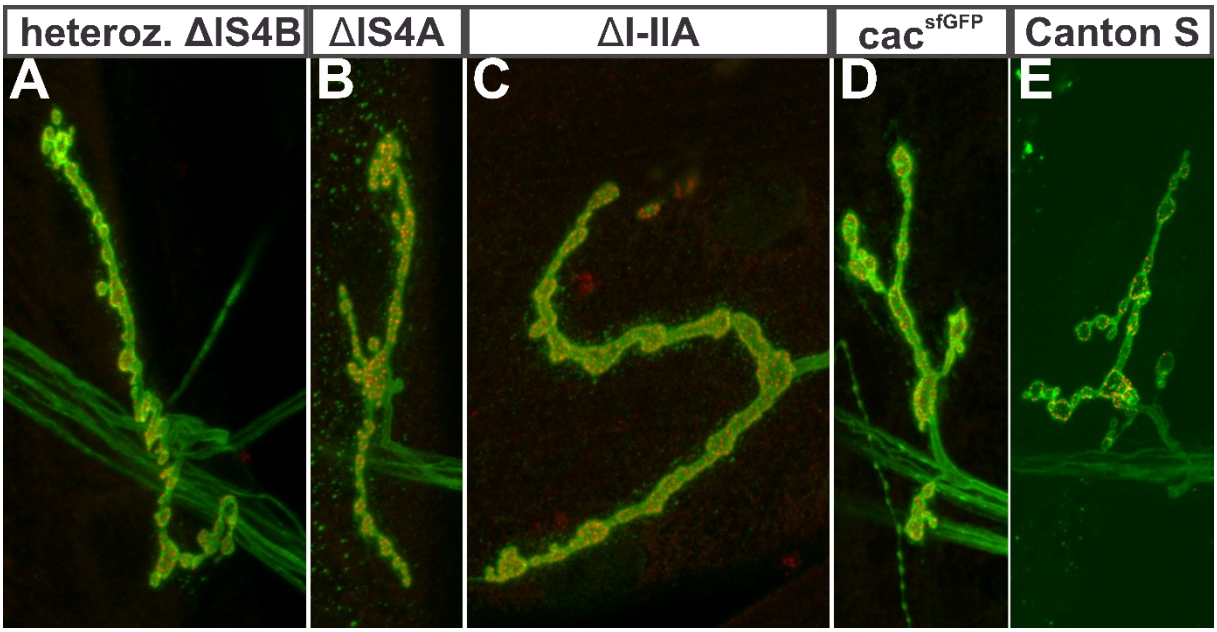

***Figure 23**: representative projection views of motoneuron terminals on muscle 4 of the larval body wall muscles. Merged images of two channels- anti-HRP (green) and anti-Brp (red). HRP a common axonal marker is used to outline the terminal, while brp is used to mark active zone. The following genotypes were assessed: A: cac^{sfGFP}ΔIS4B, B: cac^{sfGFP}ΔIS4A, C: cac^{sfGFP}ΔI-IIA, D: cac^{sfGFP} and E: Canton S.*

Figure 23 shows representative maximum projection views of the terminals on muscle 4 for the different examined genotypes. The differences in morphology are not genotype-specific, but part of the native variation of the terminals, as they occur across preparations and in all genotypes. This also holds true for the apparent increase in bouton diameter, which could otherwise be misconceived as a ghost bouton (Guangming *et al.*, 2020). Consequently, none of the examined variants showed a Gestalt unique to a specific exon excision.

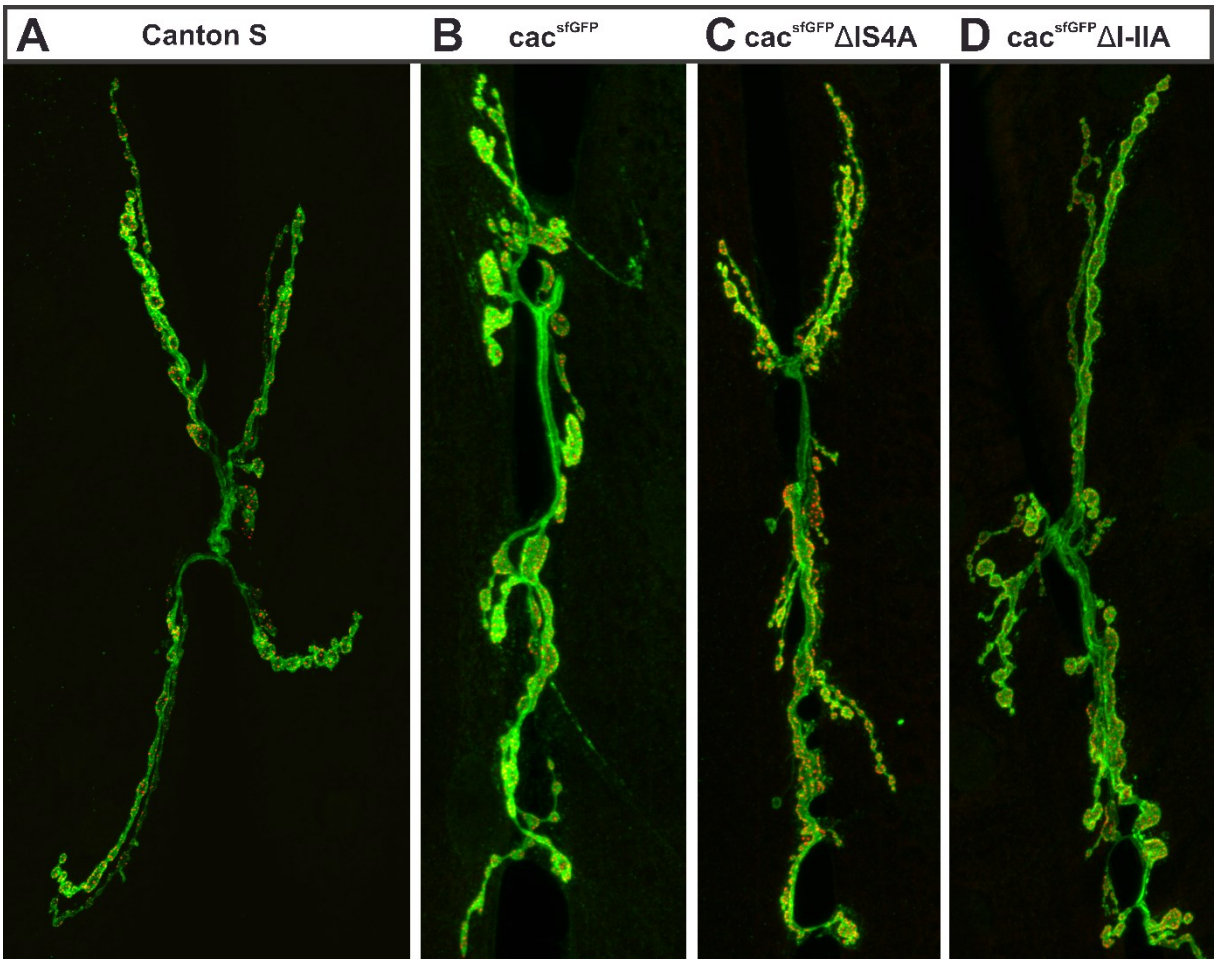

***Figure 24**: representative projection views of motoneuron terminals on muscle 6&7 of the larval body wall muscles. Merged images of two channels- anti-HRP (green) and anti-Brp (red). HRP a common axonal marker is used to outline the terminal, while brp is used to mark active zone. The following genotypes were assessed: A: Canton S, B: cac^{sfGFP}, C: cac^{sfGFP}ΔIS4A and D: cac^{sfGFP}ΔI-IIA.*

Similarly, Figure 24 shows the same kind of representative projection views, but this time of the terminals of muscles 6 and 7. For both muscle terminal regions the acquisition was done over multiple iterations of the experiment and thus the projection views vary slightly in intensity. This variation does not affect the downstream data analysis since the script marks individual active zones and boutons even with low intensity.

These data were then quantified. Figure 25 shows these data, namely the number of active zones, the number of boutons and active zones per bouton. These datasets were collected across the second and third abdominal segment.

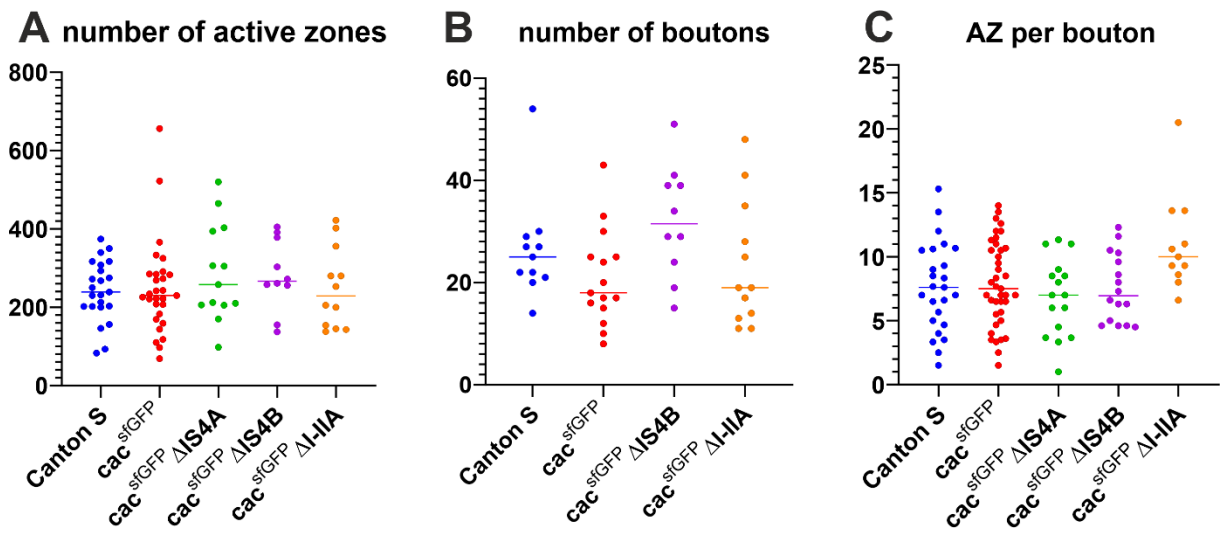

***Figure 25**: Active zone and bouton number are not affected in exon reduced mutants: genotypes for all tested animals were as follows: blue: Canton S, red: cac^{sfGFP}, green: cac^{sfGFP} ΔIS4A, violet: heterozygous cac^{sfGFP}ΔIS4B, orange: cac^{sfGFP} ΔI-IIA. A: no significant differences in number of active zones between the observed genotypes (since data were not normally distributed Kruskal-Wallis ANOVA: p=0.460) in terminals on muscle 4 of the second and third abdominal segment, B: no significant differences in number of boutons between the observed genotypes (Kruskal-Wallis, since data is not normally distributed ANOVA: p= 0.0716) in terminals on muscle 4 of the second and third abdominal segment. C: no significant differences in number of active zones per bouton can be observed (Kruskal- Wallis ANOVA, since data is not normally distributed p= 0.0772). Bars show median in all graphs. Number of replicates: A: Canton S: n=23, cac^{sfGFP}: n=29, cac^{sfGFP} ΔIS4A: n=13, cac^{sfGFP} ΔIS4B: n=10, cac^{sfGFP} ΔI-IIA: p= 12. B: Canton S: n=11, cac^{sfGFP}: n=15, cac^{sfGFP} ΔIS4B: n=10, cac^{sfGFP} ΔI-IIA: p=12. C: Canton S: n=25, cac^{sfGFP}: n=39, cac^{sfGFP} ΔIS4A: n=16, cac^{sfGFP} ΔIS4B: n=16, cac^{sfGFP} ΔI-IIA: p= 11*

The number of active zones of the terminals on muscle 4 is unaffected by the excision of either IS4A, I-IIA, or heterozygous loss of IS4B (Figure 25 A p= 0.460, Kruskal-Wallis ANOVA). Similarly, the number of boutons per terminal is also unaffected by the examined exon excisions (Figure 25, B p= 0.0716, Kruskal-Wallis ANOVA), but here ΔIS4A animals were not quantified. However, given the morphological similarities shown in Figure 24, no differences are expected. Furthermore, the comparison of the number of active zones per bouton also shows no significant differences across the tested groups for the genotypes measured in abdominal segment two and three (Figure 25 C, p= 0.0772, Kruskal-Wallis ANOVA).

These data show that the relations of active zones and boutons are unaffected by the loss of IS4A or I-IIA, thereby excluding gross morphological effects as a factor for further examination. Additionally, any behavioral differences observed are thus not a direct cause of erroneous arrangement at the AZ level. Therefore, any observed effects of the exon excisions are most likely due to other channel properties.

3.4.5 Loss of exon IS4A is reflected in altered of colocalization coefficients at the AZ

ΔIS4A mutant larvae show significant motor behavioral defects, but the morphology of the boutons was not significantly different. The number of active zones was similar to GFP tagged controls, and cacophony localized to active zones. To further quantify cacophony localization in active zones in the animals lacking the IS4A exon and respective sfGFP tagged controls, different coefficients of colocalization were measured: Pearson's coefficient of colocalization and Manders coefficient of colocalization.

The Manders coefficient is a measure of how much of the total of one label is overlapping, i.e., occupying the same pixel, with another label. In this case M1 denotes how much of the total cacophony label overlaps with any bruchpilot label while M2 shows how much of the total bruchpilot label overlaps with any cacophony label. Which is a different measure as the colocalization via the Pearson colocalization coefficient, which takes the labeling intensity into account.

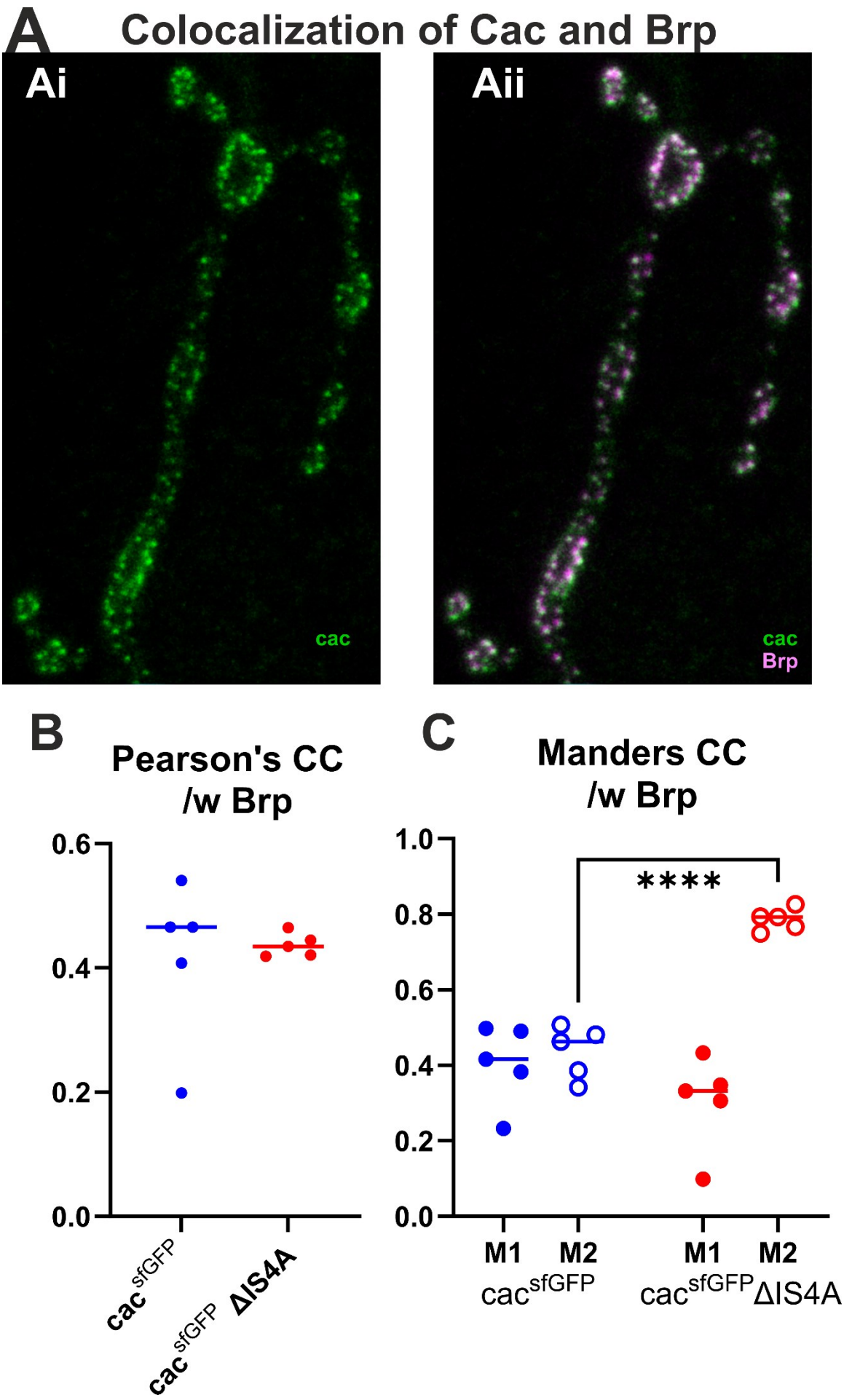
A
Colocalization of Cac and Brp
Ai
cac
Aii
cac
Brp
B
Pearson's CC
/w Brp
0.6
0.4
0.2
0.0
cac sfGFP
cac sfGFP ΔIS4A
C
Manders CC
/w Brp
1.0
0.8
0.6
0.4
0.2
0.0
****
M1
M2
M1
M2
cac sfGFP
cac sfGFP ΔIS4A

Figure 26**: loss of IS4A leads to increased Brp colocalization with cacophony in active zones on M4 and 6&7 and M12: A: representative optical stack of axon terminals on muscle 4 of the L3 abdominal segment 3 Ai: the same terminal, here cacophony is visualized by α-GFP Aii: overlap of α-GFP and α-Brp B: Pearson's coefficient of colocalization of cacophony and bruchpilot label (unpaired t-test: p=0.7303) C: M1 coefficient shows no significant differences in colocalization of the overall cacophony to brp label (p=0.208). M2 coefficient shows that ~80% of brp label overlap with cac^{sfGFP} label in Δ IS4A terminals which highly significantly differs from controls (~40% overlap, p<0.0001); Bars show mean number of assessed terminals, n for both groups was 5; comparisons were done using an unpaired t-test analysis since data was normally distributed (p >0.5 ns, p<0.0001*)*

The Pearson's coefficient of colocalization is not significantly different from the tagged controls (Figure 26 B unpaired t-test: p= 0.7303). When examining the Manders coefficient a shared thresholding value was assumed for all image stacks to reduce background, since all examined images were imaged in the same session and with the same settings and immunohistochemistry steps. Like with the Pearson's coefficient, the M1 coefficient is also not significantly different in the tested groups (Figure 26 C unpaired t-test: p=0.208). Strikingly, a highly significant (unpaired t-test: p<0.0001) different M2 denotes an increase in the overlap of total brp with the cacophony label in the Δ IS4A variants. In fact, while in controls ~40% of brp label overlaps with cac label, in terminals lacking IS4A ~80% of all brp label overlaps with cacophony label. Taken together these findings indicate a reduction of cacophony expression past the boundaries of the active zones, as delineated by brp. This is in agreement with a necessity of the alternative exon for the IS4 locus, IS4B, for the active zone localization of cacophony. The excision of IS4B caused complete absence of cacophony from presynaptic active zones. (Figure 22 D)

After examining the subcellular localization of cacophony in the different subcellular compartments in larvae, I also examined somatic, dendritic, and axonal localization in adult animals to address different effects on subcellular expression patterns in different stages of development. Furthermore, this allows to relate subcellular expression patterns to the observed defects in adult motor behaviors.

3.4.6 Lack of either exon IS4A or I-IIA does not affect somatodendritic cacophony expression in DLM motoneurons

To address cacophony expression in the somatodendritic component the uniquely identifiable motoneuron MN 5 (Consoulas et al., 2002) was used, because it allows for electrophysiological analysis of somatodendritic cacophony currents (Ryglewski *et al.*, 2012, and see below). This motoneuron innervates the fifth and sixth muscle fibers of the DLM flight muscles.

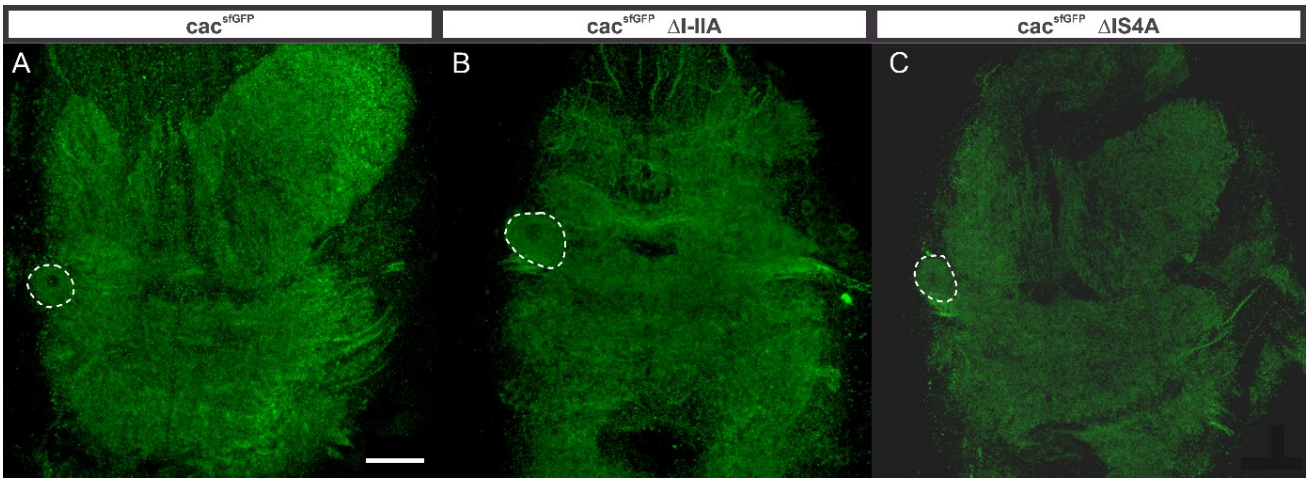

Figure 27: *representative stacks of ten optical sections across the thoracical part of the adult VNC showing the soma of MN5 on the left side of the VNC (white dashed line) of cac^{sfGFP}(A), cac^{sfGFP}ΔI-IIA (B)and cac^{sfGFP}ΔIS4A (C). scalebar: 50µm*

As can be seen in Figure 27, the somata of MN5 can be found and clearly identified in adult VNC preparations of sfGFP tagged cacophony (Figure 27 A) as well as the two exon excision mutants ΔI-IIA (Figure 27 B) and ΔIS4A (Figure 27 C). These qualitative data suggest that the expression of cacophony in the somata of MN5 is unaffected by the excision of the exons I-IIA or IS4A, again the ΔIS4B variant did not show cacophony expression (not shown).

3.4.7 Distribution of cacophony along the axon remains unchanged in ΔI-II A and ΔIS4 A, but loss of IS4B also results in loss of axonal cacophony

Next, the expression of cacophony along the axons of the motoneurons, MN1-5, leaving the adult VNC (Figure 15 Aii, Bii, Cii arrows) towards the DLM were examined.

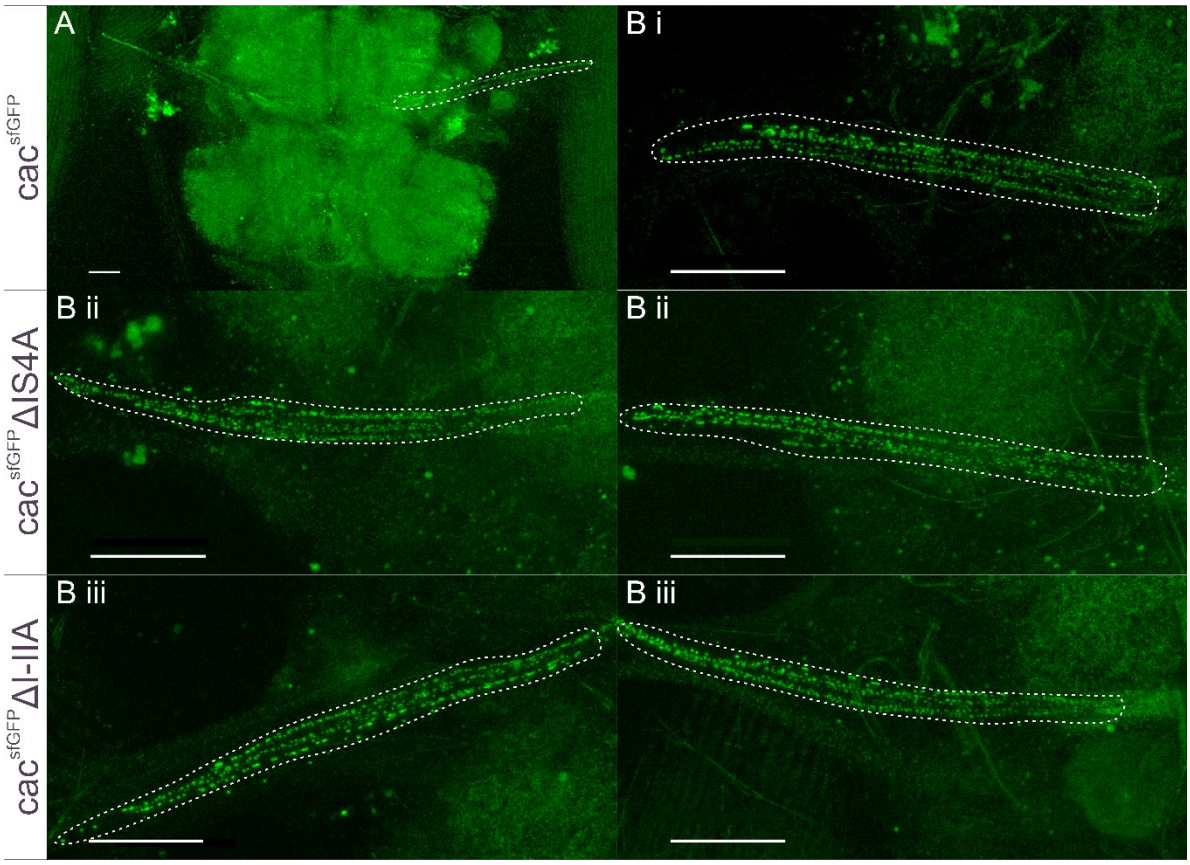

Figure 28: *loss of IS4 A or I-II A does not affect cacophony in the DLM motor axons: adult DLM MN axonal label of cacophony^{sfGFP} variants; scalebar: 25µm;* ***A:*** *cac^{sfGFP} upper two segments of the adult VNC with the axon bundle leaving the VNC toward the flight muscles,* ***B:*** *magnifications of only the axon bundles; one representative magnification for cac^{sfGFP} (B i) and two each for cac cac^{sfGFP} ΔIS4 (B ii) and cac^{sfGFP} ΔI-II A (B iii); scalebar: 25µm*

In Figure 28 A, the upper part of the VNC with the axon bundles of MN1-5 leaving the VNC can be seen. The B panels all show a magnification of the bundles. ΔIS4B animals showed no label in the axon (data not shown). Comparison of axon bundles reveals no difference, between ΔIS4A (Bii), ΔI-IIA (Biii), and the cac^{sfGFP} control (Bi). These findings show that the broad distribution of cacophony along the axon is not affected by the isoform reductions examined here, although no quantification of this data set was conducted. This excludes ΔIS4 B which did not show any label in the axon or the VNC, as mentioned above, thereby suggesting that cacophony expression in the axon region requires the IS4 B exon. Cacophony expression for the animals lacking IS4A or I-IIA is not affected. This is similar to the findings in larvae and the other subcellular motoneuron compartments examined so far.

Immunohistochemical detection of cacophony in the axons of the motoneurons MN1-5 could either be caused by functional cacophony channels in the axonal membrane or by transport of the channels to the axon terminals. Although these possibilities cannot be distinguished by CLSM based localization studies, it has been reported that functional cacophony channels are

expressed in MN1-5 (Heinrich and Ryglewski, 2020), and I confirmed this for IS4A and I-IIA excision mutants by functional imaging (see below). Therefore, the flight or courtship behavioral consequences that result from the excision of IS4A (see above) are unlikely caused by a failure to localize the remaining isoforms to the somatodendritic or the axonal compartment of DLM motoneurons.

To complete the analysis of the adult subcellular compartments, and to fully draw parallels to the larval expression pattern examination of the axon terminals of MN1-5 on the flight muscle fibers would have been the next step. This was not possible due to experimental difficulties. The adult flight muscle is a thick tissue bundle. Therefore, it is not possible to analyze the terminals using CLSM since the free working distance needed to examine these tissues cannot be reached. The presence of cacophony at the adult NMJ (Kawasaki, Felling and Ordway, 2000) is further underscored by the observation that selective knock out of cacophony in MN1-5 by employing a flippase strategy as well as expression of Δ IS4B over cacFLP-Stop only in MN1-5 causes loss of synaptic transmission to the DLM flight muscle and complete loss of flight and courtship song ability (personal communication Christopher Bell), two behaviors which are observed in animals lacking IS4A or I-IIA.

The expression pattern of cacophony in exon excision has been examined across the adult brain, the adult and larval VNC and across subcellular compartments in motoneurons for adult and larval *Drosophila*. These data show that in animals carrying the lethal excision of the IS4B cacophony is absent from many parts of the nervous system, despite distinct regions in the adult brain, namely the saddle and the visual system (compare Figure 17) This means that the remaining alternative exon IS4A, which can still be incorporated into cacophony proteins, does serve a function restricted to these brain regions. However, it cannot be excluded that in ΔIS4B mutants cacophony is still expressed throughout many parts of the nervous system, but at such low quantities that it cannot be reliably detected. Behavioral experiments with trans heterozygous ΔIS4A/ΔIS4B animals in fact provide evidence for this hypothesis (see below). In contrast, cacophony incorporating IS4B instead of IS4A, shown in the experiments with Δ IS4A animals, is abundant across the nervous system and can be found in every subcellular compartment in amounts qualitatively similar to controls. This reinforces the ubiquitous role of IS4B, loss of which is lethal. But IS4B by itself is not sufficient for normal life, as evidenced by the significantly reduced life expectancy of animals lacking IS4A. This effect and the strongly

affected motor behavioral performance in these animals cannot be sufficiently explained by the expression pattern of the remaining cacophony isoforms in these animals. Cacophony expression in animals missing I-IIA looks for the most part qualitatively similar to that of animals missing IS4A. The only noteworthy difference is the visual system. Here, animals missing I-IIA as well as animals missing IS4A show different cacophony expression pattens which can be related to reduced responsiveness to light stimuli as shown by the ERG recordings. Thus, the loss of the I-IIA exon can be compensated for by the remaining I-IIB exon in all examined parameters except visual processing.

In sum, although the localization analysis yielded clear evidence for isoform specific localization of cacophony through the nervous system as well as to specific subcellular compartments, these effects can explain the consequences on behavior and viability only partially. In particular, the severe consequences of ΔIS4A are not in accordance with obvious protein mis-localization, because in ΔIS4A animals, cacophony is abundantly expressed throughout most parts of the nervous system including synaptic terminals at the NMJ and throughout all subcellular compartments of motoneurons.

This suggests that in particular the excision of the IS4A exon might affect cacophony channel properties. Similar consequences of the I-IIA exon excision cannot be excluded although this manipulation caused performance defects only in the visual system. To pinpoint possible effects of the IS4A and I-IIA exons on cacophony channel function, I next conducted electro and optophysiological recordings from adult flight motoneurons, for which multiple functions of cacophony channels have been previously described (Ryglewski *et al.*, 2012; Ryglewski, Kilo and Duch, 2014; Heinrich and Ryglewski, 2020).

3.5 Exon excisions affect cacophony mediated channel properties

3.5.1 Loss of the exons IS4 A and I-IIA has opposite effects on calcium signals in the pupal *Drosophila* motoneuron 5

To test for the effects of alternative exon excisions on calcium influx electrophysiological and optophysiological studies were conducted. Since the distribution of the cacophony channels in DLM MNs was qualitatively similar for excisions of both IS4A and I-IIA (Figure 28) calcium imaging was conducted to investigate possible differences in channel calcium conductance between different isoforms. For this experiment, pupal stage P8/P9 animals were chosen due to relatively easy imaging access to the somatodendritic and axonal compartments of MN 5.

The cells were approached with whole cell voltage clamp method in current clamp mode, and current was injected into the cell to image calcium influx. The current injection was done either as a ramp current injection with a total amplitude of 1nA or triturated to induce two subsequent action potentials. The elicited calcium influx was visualized by targeted expression of the calcium indicator GCaMP6s only in DLM MNs. The fluorescence difference was examined across different subcellular compartments (compare **Figure 29** G) as well as for the two different stimulation protocols, a ramp current injection with 1nA maximum amplitude (Figure 29 A,C,E) and two subsequent action potentials (Figure 29 B,D,F).

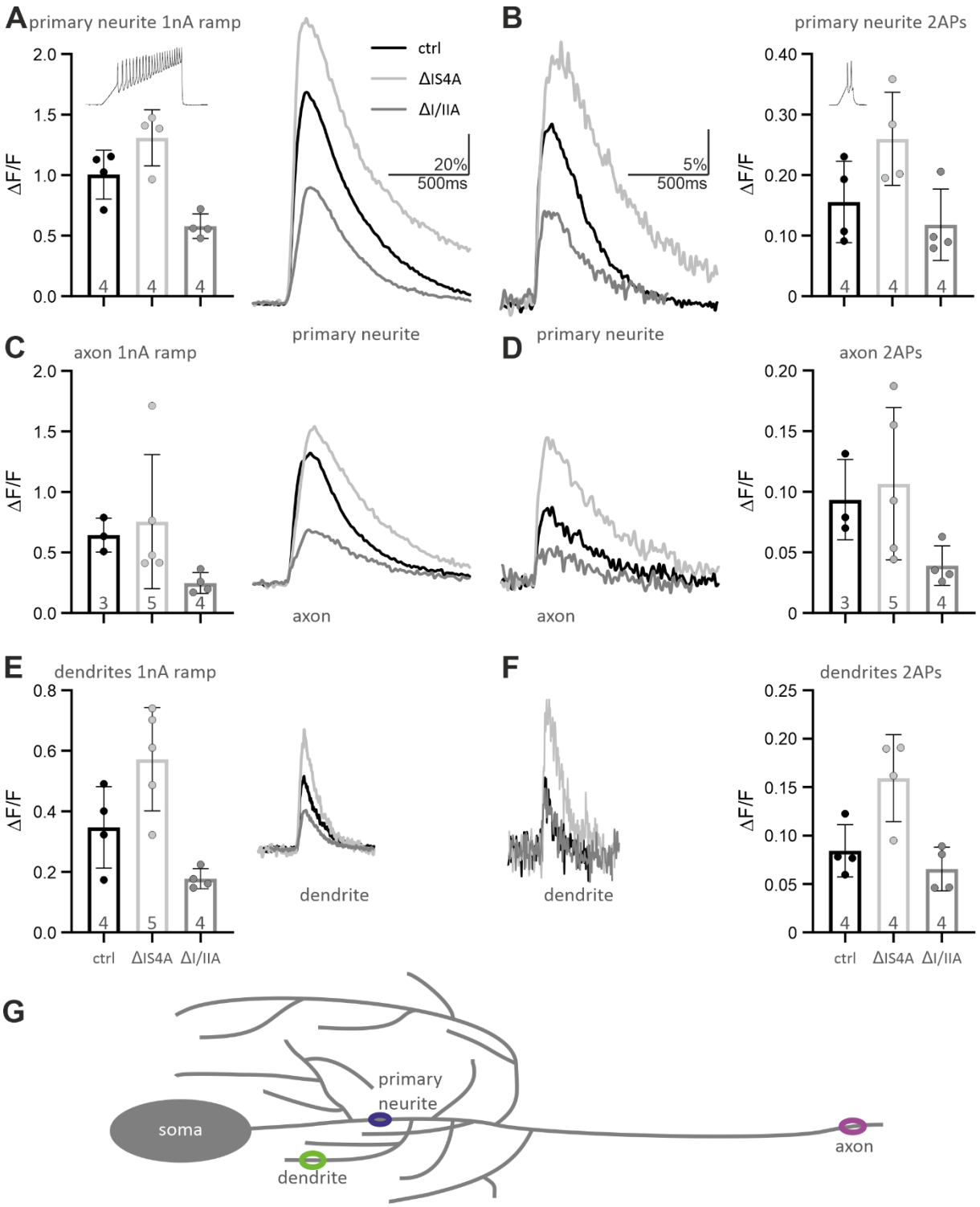

***Figure 29**: loss of IS4 A leads to increased calcium signal, while ΔI-II A leads to reduced signal in all compartments: Calcium imaging of pupal MN5 with a focus on different compartments: dendrites, primary neurite and axon. For imaging, exon excision mutants expressed the genetic calcium indicator GCaMP6s in MN1-5. A, C, E: injection of a 1nA ramp into the soma to elicit a response, B, D, F: injection of current evoking 2 action potentials into the soma. G: cartoon of MN5 with exemplary recording areas of primary neurite (blue), dendrite (green) and axon (magenta) delineated. T-tests were performed to check for possible differences in the calcium signals. A: region of interest was set to the primary neurite CS vs ΔI-IIA p=0.0094, ΔIS4A vs ΔI-IIA p=0.0012. B: region of interest was set to the primary neurite, ΔIS4A vs ΔI-IIA p=0.0264. C: region of interest was set to the axon. CS vs Δ I-IIA p=0.0054. D: region of interest was set to the axon. CS vs Δ I-IIA p=0.0335. E: region of interest was set to the dendrites. ΔIS4A vs ΔI-IIA p=0.0028. F: region of interest was set to the dendrites. CS vs ΔIS4A p=0.00287 ΔIS4A vs ΔI-IIA p= 0.0097. All not denoted comparisons were not significant. In every panel light gray denotes ΔIS4A, dark gray denotes ΔI-IIA and black the control animals, in this case Canton S (CS). The fluorescence change in comparison to baseline fluorescence is shown (Δ F/F). Diagrams show means with SD as whiskers.*

First, the dendritic calcium responses upon the stimulus (Figure 29 E,F) are shorter than the ones observed in the primary neurite (Figure 29 A,B) or the axon (Figure 29 C,D) and the response toward only two APs (Figure 29 B,D,F) is expectedly weaker than the response towards the 1nA ramp (Figure 29 A,C,E). Second, across all the examined compartments and both stimulus protocols a larger amplitude calcium response is observed in ΔIS4 A animals as compared to controls. In contrast, the ΔI-IIA animals showed smaller amplitude calcium signals than the controls. This is further supported by comparing the calcium responses individually. Specifically, in recordings from the primary neurite, significant differences between the Δ IS4A and Δ I-IIA animals (Figure 29 A t-test p= 0.0012, Figure 29B t-test p= 0.0264) can be seen. Furthermore, the ramp stimulus reveals significant differences between Canton S and Δ I-IIA in the primary neurite (Figure 29A p= 0.0094). When examining the axon both protocols reveal significant differences for Δ I-IIA when compared to controls. (Figure 29 C, p=0.0054 and Figure 29 D, p=0.0335). Similar to the primary neurite, the dendritic calcium signals are significantly different when comparing Δ IS4A and Δ I-IIA (Figure 29 E, p= 0.0028 and Figure 29 F, p=0.0097), while for the stimulus of two AP's, a significant difference can also be observed when comparing Δ IS4A to Canton S (Figure 29F, p=0.0287).

Thus, these data show that loss of IS4A leads to higher calcium influx through cacophony channels. By contrast, the opposite effect can be observed for animals missing I-IIA.

For both scenarios, decreased calcium signal amplitudes upon I-IIA excision and increased calcium signal amplitudes upon IS4A excision, additional experiments are required to determine whether the effects are caused by altered channel densities, kinetics, activation voltages, or conductances. However, the qualitative data on channel density along the axons and the somatic compartment renders altered channel densities unlikely. To address possible consequences of exon excision on calcium current kinetics, or amplitudes, and/or activation voltages I next conducted somatic whole cell patch clamp recordings from MN5.

3.5.2 Both, loss of I-II A and IS4A induces APs with double peaks upon somatic stimulation in pupal MN5

Whole cell patch clamp recordings from pupal stage P8/P9 MN5 somata were conducted in ΔIS4A and ΔI-IIA animals. The somata were identified by their distinct shape and characteristic localization on the dorsal surface of the VNC. Pupal MN5s display a distinct calcium

component in their action potentials, which can be blocked by bath application of cadmium (300µm), leaving only the fast sodium component of the AP (Figure 30A, demarked in top current ; see also Ryglewski, Kilo and Duch, 2014).

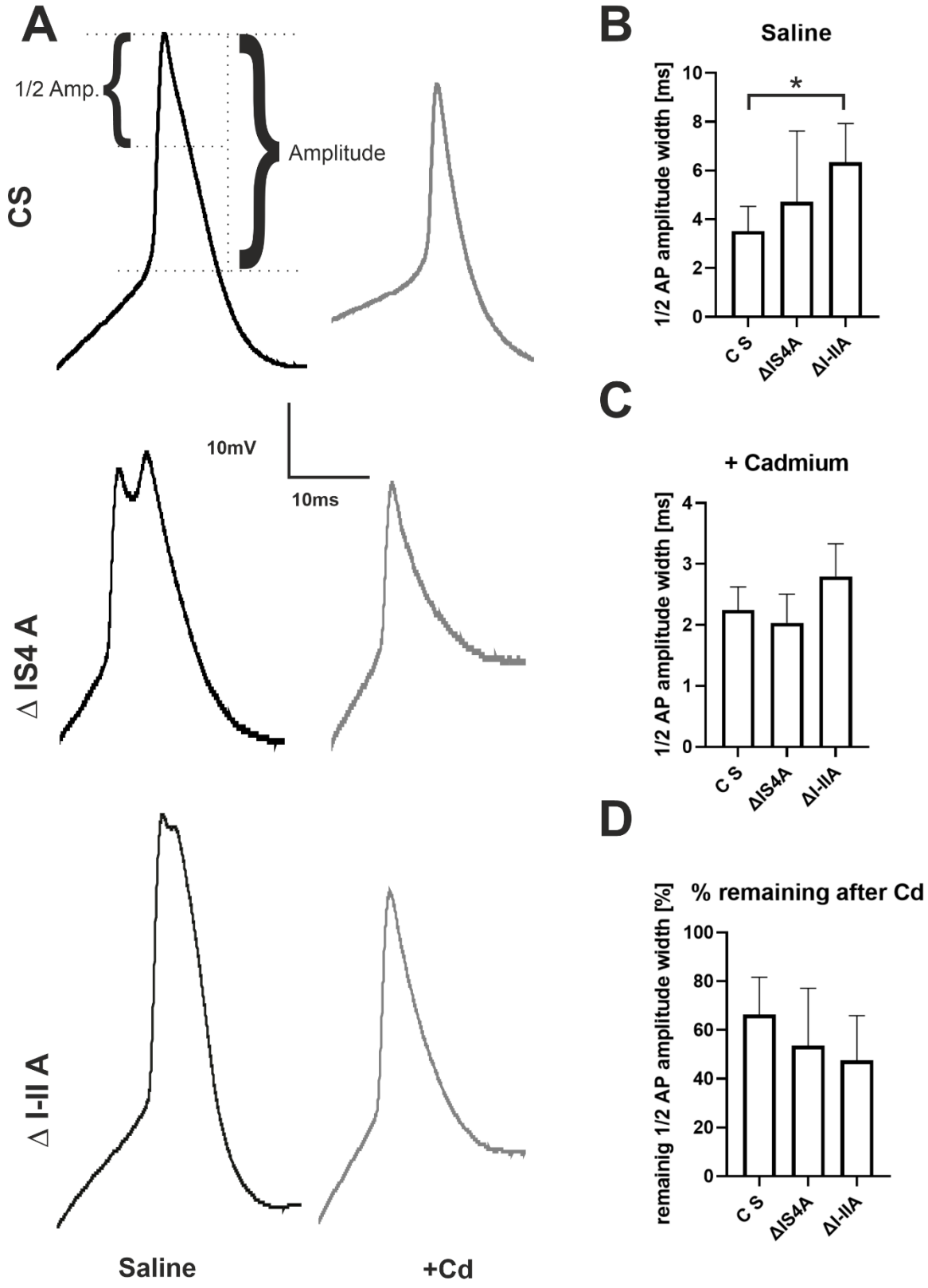

***Figure 30**: loss of either alternative exons (IS4 A and I-II A) leads to more pronounced calcium dependent action potential shoulder or to double spikes, but does not significantly affect AP width and cadmium induced loss of shoulder: A: Pupal action potential shape before and after application of cadmium in CS, ΔIS4 A and ΔI-II A animals, measurements of the half AP amplitude were taken when considering the AP as firing threshold to max amplitude B: half amplitude width of action potential at membrane potential around -10mV does not show significant differences between genotypes (p=0.12 ANOVA),*

unpaired t-test between CS and ΔI-IIA p= 0.0101, C: half AP amplitude width after application of the channel blocker cadmium is also not significantly different (p = 0.06 ANOVA, since data is not normally distributed) D: remaining width of AP after application of calcium channel blocker cadmium (300µM for 2 minutes) also is not significantly affected in the exon excision animals(ANOVA: p=0.33), (animals tested: CS: n=5; ΔIS4A n=5; ΔI-IIA n=5)

ΔIS4 A (Figure 30 A middle traces) and ΔI-IIA (Figure 30 A lower traces) animals show a broadening of the calcium shoulder as well as a tendency towards double spikes. These spikes occur in 5 out of 5 recordings for the Δ I-IIA animals and 3 out of 5 animals in the ΔIS4A animals. In contrast, none of the 5 recorded Canton S animals showed excessively broadened action potentials or a propensity for double spikes. Half action potential amplitude width in regular saline was not significantly different across the genotypes (Figure 30 B, ANOVA: p=0.12). After application of cadmium, a calcium channel blocker, the remaining action potential width is measured (Figure 30 C). Then the remaining parts of the base width are calculated using both widths, before and after cadmium application (Figure 30 D). Similarly, the measurements after application of cadmium are also not significantly different (ANOVA p= 0.06). Lastly, relative reduction of AP width by application of cadmium is also not significantly different between groups (ANOVA p= 0.33). Although multiple comparisons did not show significant differences between the tested groups an individual comparison between the Canton S and ΔI-IIA animals shows a significant difference (t-test p=0.0101) in AP width in saline. This supports the qualitative findings of broadened calcium dependent AP shoulders.

In sum, both exon excisions show an increased predisposition towards double spikes and possibly broadened AP width. Even though, recording quality in these experiments can vary and thus affect the amplitude, the reduction of action potential amplitude width suggests a strong tendency of both isoform reductions examined towards permitting a stronger calcium influx. The increase in propensity for double spikes in both examined genotypes could be due to altered gating properties, of the cacophony variants remaining. These properties could be for example lowered activation thresholds or extended opening times of the channel. Whether these effects originate in a simple lack of cacophony or whether a specific channel function is responsible cannot be determined with these data alone.

3.5.3 IS4A and I-IIA do not affect cacophony mediated calcium current amplitude in pupae

Whole cell voltage clamp measurements from pupal stage eight (P8) animals were performed from the soma of MN5, to assess the calcium currents mediated by cacophony in more detail

and to address the possibly altered channel kinetics further. In this developmental stage the cacophony VGCC only mediates a high voltage activated current (Ryglewski, Kilo and Duch, 2014).

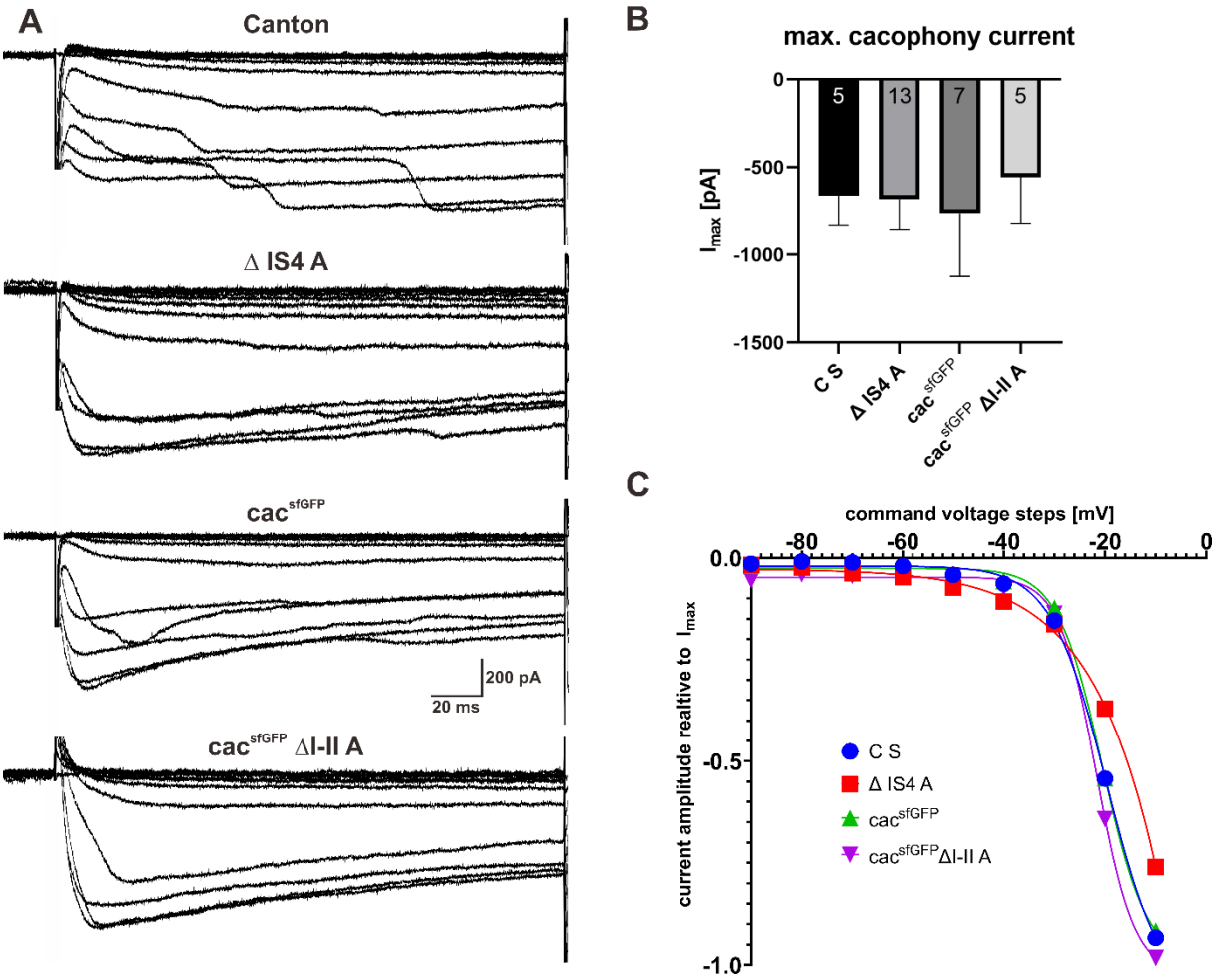

***Figure 31**: maximum pupal current amplitude is not affected by removal of IS4 A or I-II A, but loss of IS4A hints at reduced activation threshold: A:representative voltage clamp recordings from the pupal MN5 soma; B: maximum current per genotype is not affected; number of replicates per genotype: CS: 5; ΔIS4 A:13 ; cac^{sfGFP} :7 ;cac^{sfGFP} ΔI-II A: 5; ANOVA: p=0.54 C: I-V plot of the relative pupal cac current amplitude at different command voltages, each normalized to maximum within genotypes. Datapoints represent mean, curves fitted with the previously mentioned equation (see methods), error bars not shown for clarity, replicate numbers constituting the mean are the same as in B*

The representative currents shown in Figure 31A depict no qualitative differences, across the tested groups. The variation seen in the currents is due to the size of the recorded cell and consistent throughout all recordings regardless of genotype. Space clamp problems can, for example, lead to the staircase-like currents seen in the Canton S and ΔIS4A recordings. Furthermore, the current amplitudes were not significantly altered across the groups tested (Figure 31 B ANOVA: p=0.54), as can be seen in the representative recordings of the currents of the different genotypes (Figure 31 A). Comparing the activation range reveals a tendency of IS4A cacophony current activation around -50mV to -40mV in contrast to regular -30mV

(IV-plot, current amplitudes normalized to max within each genotype, Figure 31 C). These findings in pupae already hint at increased excitability due to the lower activation threshold of the HVA cacophony mediated pupal calcium current, which has been shown to mediate all current at this developmental stage (Ryglewski, Kilo and Duch, 2014). These recordings were further preferable due to the ease of access to MN5. To provide further parallels to the behavioral data acquired adult recordings of the same motoneuron were also conducted in adults in the following.

3.5.4 Loss of IS4A produces lowers HVA threshold in adult *Drosophila* MN5

Since some of the experiments performed already gave a clear indication that the composition of cacophony isoforms changes during development for a given compartment, further voltage clamp recordings were performed in adult *Drosophila*, but in the same uniquely identifiable Motoneuron, MN5. Somatodendritic HVA and LVA calcium current in the adult MN5 is mediated by cacophony (Ryglewski *et al.*, 2012).

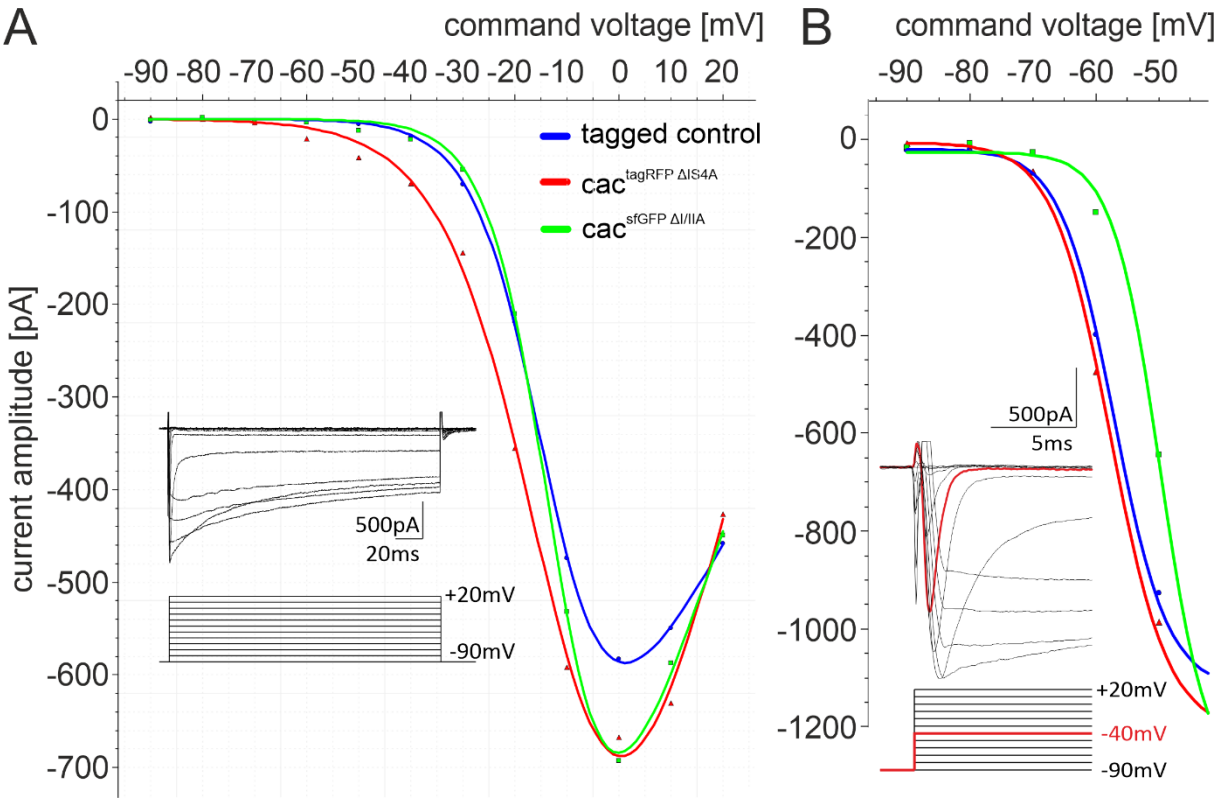

***Figure 32**: ΔIS4 A animals show higher HVA excitability while ΔI-IIA animals show a delay in LVA response: A: high voltage activated current portion of cacophony currents measured from the soma of adult MN5 shows higher excitability in ΔIS4A animals, insets show representative recordings and stimulus protocol; B: Low voltage activated portion of the calcium currents, insets show representative recordings and stimulus protocol. curves fitted with the previously mentioned equations (see methods). Number of recordings per datapoint is 4 for all genotypes. Error bars not shown for clarity.*

Similar to the pupal MN5 (see above), the adult high voltage activated calcium current in ΔIS4A activates 10 to 20 mV more negative (between -60 and -50mV) as compared to controls and ΔI-IIA (Figure 32A). Interestingly, the activation voltage of the low voltage activated part of the cacophony mediated current does not seem to be affected by the loss of the IS4A exon (Figure 32B). These findings taken together suggest a specific role for the IS4 A exon affecting the voltage sensing properties of high voltage activated response mediated by cacophony, furthermore this function seems to hold true across multiple developmental stages. Interestingly, in both pupal and adult high voltage activated currents loss of I-IIA does not seem to influence activation voltage but does seem to increase the activation threshold for the adult low voltage activated current (Figure 32B).

Taken together these findings suggest that the increased calcium influx observed in the calcium imaging recordings (**Figure 29**) and the change of AP shape (**Figure 30**) might be due to a higher likelihood of the remaining cacophony channels in ΔIS4A animals opening at more negative membrane potentials. Note, that excisions done in the germline, as is the case here affect all cells expressing cacophony, so that decreased activation threshold of cacophony channels in ΔIS4A animals may lead to nervous system wide hyper excitability.

3.5.5 Epilepsy like phenotype in variant with decreased activation threshold in adults

Increased excitability and increased calcium influx upon stimulation may be elicited by the lowered activation voltage and could be a reason for the strong motor defects of ΔIS4A animals and their reduced lifespan. Therefore, an assay for putative hyperexcitability was conducted. In this vortex assay the animals are put into a vial and put onto a regular benchtop vortex to induce strong stress and increased synaptic input on the fly (Saras and Tanouye, 2016). After the vortex period the recovery time until the flies attempted wall climbing was measured for the first, fourth and eight fly, of the ten tested flies per experiment. These numbers were chosen, since preliminary experiments showed that some of the flies never recovered from the vortex in the allotted time and the initially chosen ten out of ten flies became an unreliable measurement. Aside from the regular negative controls such as Canton S some genotypes with known hyperexcitability mutations were used as a positive control. In this case a mutant of the voltage gated sodium channel *para* was used. Namely *bang sensitive* ($para^{bss1}$ and $para^{bss2}$). These mutants harbor a gain of function mutation of the *para* voltage gated sodium channel lowering their activation threshold (Parker *et al.*, 2011).

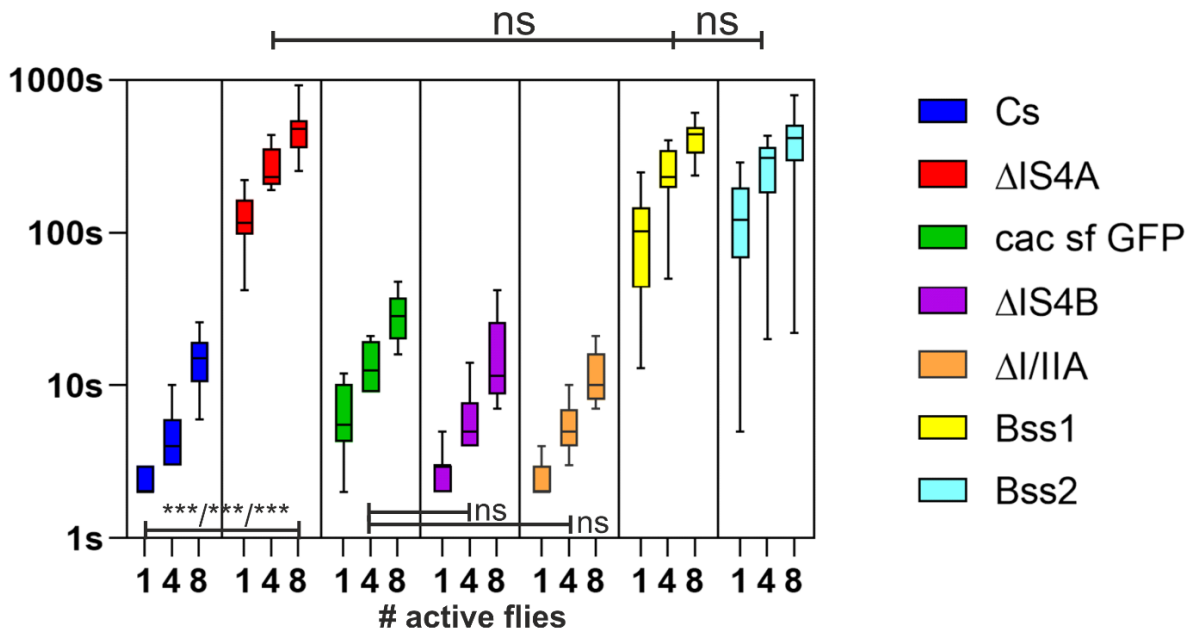

Figure 33**: Delay in climbing due to vortex induced paralysis measured in ΔIS4 A animals mimics epilepsy phenotype: time measured to the first (1), fourth (4) and eighth (8) fly of ten per vial climbing. The means for the CS flies are CS (1)=2.4 s CS (4)= 4.8 s, CS (8)=15.1 s; for ΔIS4 A: ΔIS4 A (1)= 128.9 s ΔIS4 A (4)= 274 s ΔIS4 A (8)= 485.3 s; for cac ^{sfGFP}: cac ^{sfGFP} (1)=6.6 s, cac ^{sfGFP} (4)= 13.8 s, cac ^{sfGFP} (8)= 16.8 s; for ΔIS4 B: ΔIS4 B (1)= 2.8 s, ΔIS4 B (4)= 6.4 s, ΔIS4 B (8)= 16.8 s; for ΔI-II A: ΔI-II A (1)= 2.5 s, ΔI-II A (4)= 5.6 s, ΔI-II A (8)=12.1 s; the two positive controls: Bss^1: Bss^1 (1)=107.8 s, Bss^1 (4)= 249.7 s, Bss^1 (8)= 426 s; for Bss^2: Bss^2 (1)= 130.4 s, Bss^2 (4)=266.1 s, Bss^2 (8)=416.2 s; for all genotypes 100 flies were tested except for cac^{sfGFP} in which case 80 animals were tested. Kruskal-Wallis-ANOVA with Dunn's post-hoc test for multiple comparisons: Kruskal-Wallis ANOVA: p=<0.0001, Dunn's: CS (1) vs ΔIS4A (1) p=0.0001, CS (4) vs ΔIS4A (4) p<0.0001, CS (8) vs ΔIS4A (8) p=0.0002, (p < 0.05*; p < 0.01**; p < 0.001)*

As shown in Figure 33, the response of the flies after the vortex shock varies greatly. The figure shows the time it took for the first, fourth and eighth fly to start climbing the wall of the vial. Each vial housed 10 flies, 5 males and 5 females, which showed no gender specific differences and were therefore pooled in the following. In all genotypes 100 animals were tested, only for cac^{sfGFP} 80 animals were used. The CS flies showed a quick righting behavior and subsequent short latency to attempted climbing of 2.4 s for the first fly, 4.8 s for the fourth and 15.1 s for the eighth fly (median). The ΔIS4A animals show a strong contrast to this in their recovery times: the first fly took on average 128.9 seconds, the fourth fly 274 seconds and the eighth fly 485.3 seconds (median). This strong delay is due to an epilepsy or seizure like behavior of the fly which incapacitates them for quite some time, not unlike the bss^1 and bss^2 phenotypes until they regain control over their body. Although, in contrast to these two genotypes the ΔIS4A animals show reduced overall activity even before the vortex experiment, thereby further impacting their overall performance. The cac^{sfGFP} animals show a similar behavior to

the CS animals with a mean delay to the first fly of 6.6 s to the fourth 13.8 s and 29.3 s for the eighth (median). The timeframe observed in the ΔIS4B animals is about the same with a median time needed for the first fly of about 2.7 seconds, 6.4 seconds for the fourth and 16.8 for the eighth. The behavior of the ΔI-IIA animals presents in the same fashion. With the first fly needing 2.5 seconds on average, the fourth 5.6seconds and the eighth 12.1 seconds. The *bss* mutants both exhibit a phenotype similar to the ΔIS4A animals. Specifically, the mean time it takes for the first fly of the bss1 genotype to attempt climbing up the vial was about 107.8 seconds, for the fourth it was on average 249.7 seconds and for the eighth fly it was 426 seconds. For the bss2 mutant the phenotype is even slightly more severe. With a median time for the first fly of 130.4 seconds, the fourth of 266.1 seconds and the eighth with an average time of 416.2 seconds. These observations are reflected in the significant differences in between the ΔIS4A, bss1, bss2 animals when compared to the remaining genotypes (overall Kruskal-Wallis ANOVA $p<0.0001$). Here, no differences among the first flies for ΔIS4A, bss1 and bss2 can be observed (Dunn's: $p>0.9999$ for all comparisons), while significant differences were observed in comparison of these groups with the control groups (e.g.: Dunn's: Canton S (1) vs ΔIS4A (1) $p=0.0001$, Canton S (1) vs bss1(1) $p= 0.0005$). The control groups were also not statistically different form one another (Dunn's Canton S (1) vs cac^{sfGFP} (1) $p>0.9999$). The same holds true for the ΔI-IIA animals which do not show significant differences to controls (e.g.: Canton S (1) vs ΔI-IIA (1): $p>0.9999$). The heterozygous ΔIS4B animals also do not show any statistically significant differences to the controls (Dunn's Canton S (1) vs ΔIS4B (1) $p>0.9999$), thereby excluding any dominant negative effects of the ΔIS4B.

These strong epilepsy-like phenotypes could be a direct behavioral consequence of the lower activation threshold shown above, as is the case for the para mutants and their increased excitability. In contrast, the loss of I-IIA does not affect the performance of these animals in the vortex assay, further supporting a strong redundancy in between the alternative exons of the I-IIA locus, aside from the visual system.

3.5.6 Locomotive defects of loss of IS4A can be alleviated by trans-heterozygous expression of ΔIS4B

Although the ΔIS4B animals did show a distinct cacophony expression pattern, albeit limited to the saddle and parts of the visual system (see above) their function could not be easily assessed due to their lethal nature. Since the animals examined were usually heterozygous

ΔIS4B over wildtype cacophony on the other X-chromosome. Trans-heterozygous animals expressing ΔIS4B over ΔIS4A were tested to check whether the remaining cacophony expressed in ΔIS4B animals mediates a function, and this function is sufficient to rescue the various defects described above resulting from a loss of IS4A. The expectation was that, since in a trans-heterozygous animal expressing ΔIS4A over ΔIS4B all cacophony exons are present, the flies show normal behavior. In addition, the possibility of misprocessing of IS4A variants in ΔIS4A animals, could be tested with trans-heterozygous expression. Therefore, a locomotion assay was performed to test this hypothesis. Flies were put in a regular fly vial and banged on the tabletop, then their climbing speed up the vial, following negative geotaxis, was assessed. This climbing assay is a common test for escape behavior and negative geotaxis and addresses different effects than the vortex assay just examined. The vortex assay examines the recovery time the flies need after excessive stimulation on the vortex. Therefore, the vortex assay examines 10 flies per iteration. In contrast, the climbing assay conducted in the following looks at the climbing speed, following a single tap on the tabletop. Thus, the stimulus is not lengthy or intensive enough to elicit the hyperexcited/ epileptic behavior assessed in the vortex assay. In addition, climbing speed is independent of when the flies actually started climbing. As cacophony is located on the X-chromosome, all flies tested here were female to be able to produce trans-heterozygotes in which one X-chromosome is missing IS4A while the other is missing IS4B.

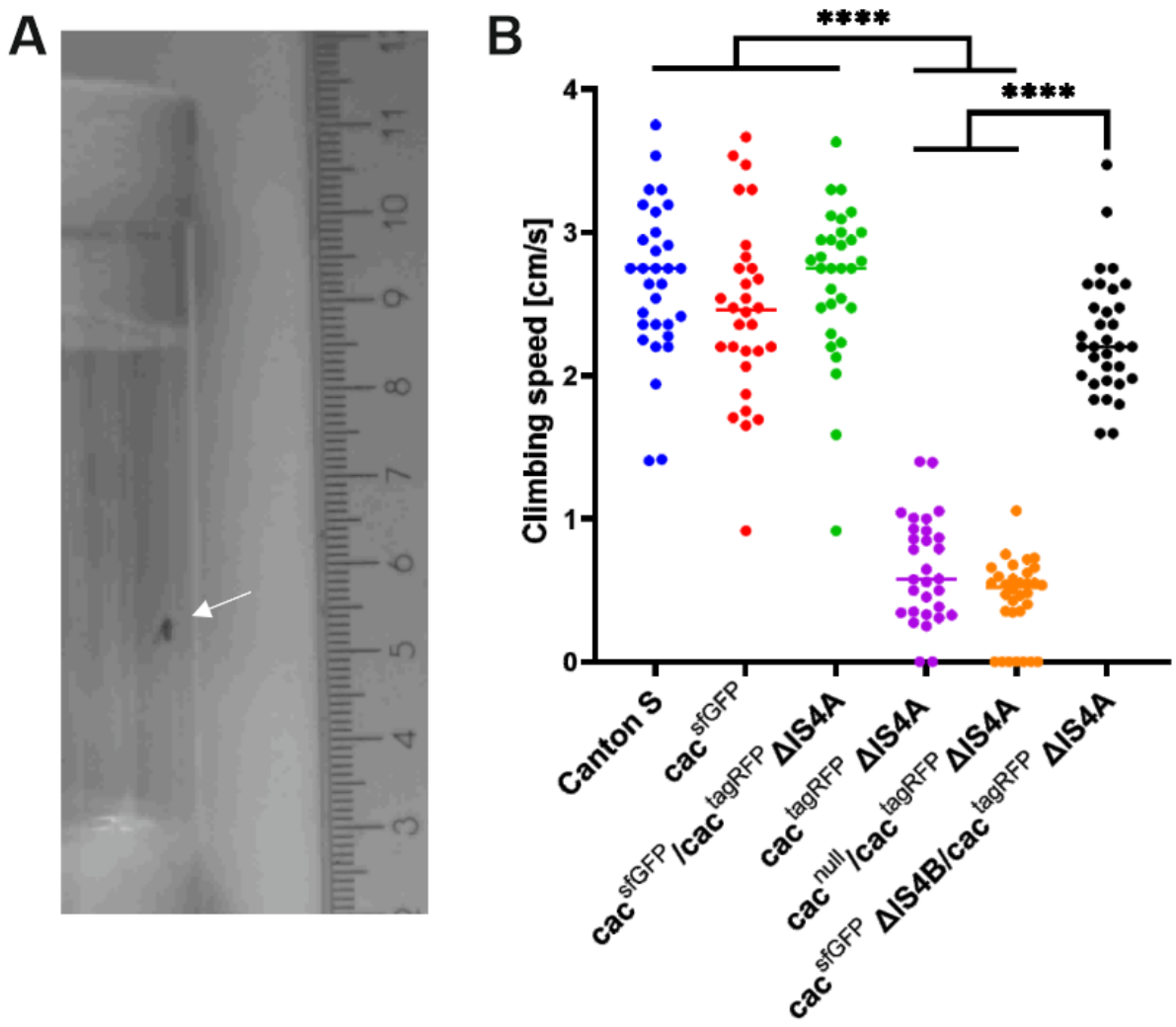

Figure 34: *ΔIS4B chromosome rescues ΔIS4A induced reduction in climbing speed:* ***A:*** *representative image of a fly performing the climbing assay.* ***B:*** *climbing speed of the tested genotypes is significantly different (Kruskal-Wallis ANOVA: p=<0.0001). post hoc tests are Dunn's multiple comparisons: controls (Canton S, cac^{sfGFP}, cac^{sfGFP}/ cac^{tagRFP} ΔIS4A) are not significantly different from one another (all p-values for these comparisons are p>0.9999). Homozygous cac^{tagRFP} ΔIS4A and, cac^{null}/ cac^{tagRFP} ΔIS4A are both highly significantly different form all controls (all p-values for these comparisons are p<0.0001). The trans-heterozygous animals (cac^{sfGFP}ΔIS4B/ cac^{tagRFP} ΔIS4A) are significantly different from the other two test groups (Homozygous cac^{tagRFP} ΔIS4A, cac^{null}/ cac^{tagRFP} ΔIS4A) with p-values of p>0.9999 for both comparisons. By contrast cac^{sfGFP}ΔIS4B/ cac^{tagRFP} ΔIS4A show no significant differences in climbing speed when compared to the controls (cac^{sfGFP}ΔIS4B/ cac^{tagRFP} ΔIS4A vs Canton S: p= 0.4085, cac^{sfGFP}ΔIS4B/ cac^{tagRFP} ΔIS4A vs cac^{sfGFP}: p>0.9999, cac^{sfGFP}ΔIS4B/ cac^{tagRFP} ΔIS4A vs cac^{sfGFP}/ cac^{tagRFP} ΔIS4A: p= 0.21). number of animals tested per genotype Canton S: n=31, cac^{sfGFP}n=30, cacsfGFP/ cac^{tagRFP} ΔIS4A n=31, cac^{tagRFP} ΔIS4A n= 30, cac^{null}/ cac^{tagRFP} ΔIS4A n =32, cac^{sfGFP}ΔIS4B/ cac^{tagRFP} ΔIS4A n=33. Bars denote median since data was not normally distributed. Only significant comparisons are shown (p> 0.05 ns, p<0.0001 ****)*

When comparing the overall variance of the groups tested in this assay a highly significant difference can be found (not all data distributed normally, therefore: Kruskal-Wallis ANOVA: p<0.0001). The different control groups all show climbing behavior with similar median speeds (Canton S: 2.75 cm/s, cac^{sfGFP}: 2.46 cm/s and cac^{sfGFP}/cac^{tagRFP}ΔIS4A: 2.75cm/s). These also do not show any significant differences amongst one another (p-values for Dunn's multiple comparisons all. p>0.9999). The two ΔIS4A groups (medians: homozygous cac^{tagRFP} ΔIS4A: 0.5773, cac^{null}/ cac^{tagRFP} ΔIS4A: 0.5221) similarly are also not different to one another (Dunn's:

p>0.999). But expectedly they are highly significantly different form the controls (Dunn's p<0.0001 for all comparisons). The trans-heterozygous cac^{sfGFP}ΔIS4B/ cac^{tagRFP} ΔIS4A animals show climbing speeds like that of the negative controls (median: 2.2cm/s) and are consequently not significantly different in multiple comparisons with these groups (Dunn's: cac^{sfGFP}ΔIS4B/ cac^{tagRFP} ΔIS4A vs Canton S: p= 0.4085, cac^{sfGFP}ΔIS4B/ cac^{tagRFP} ΔIS4A vs cac^{sfGFP}: p>0.9999, cac^{sfGFP}ΔIS4B/ cac^{tagRFP} ΔIS4A vs cac^{sfGFP}/ cac^{tagRFP} ΔIS4A: p= 0.21). In contrast they are highly significantly different to the positive controls (Dunn's p<0.0001 for both comparisons).

These data clearly show that the IS4A exon remaining on the X-chromosome of the ΔIS4B animals are sufficient to rescue the otherwise severe defects of ΔIS4A, thereby proving that the remaining cacophony in the ΔIS4B animals does mediate a function, since no differences to wildtype and matched controls could be detected. Furthermore, the rescue of ΔIS4A in this assay strongly indicates that the lack of IS4A is in fact responsible for the defects found in the ΔIS4A animals and not some unknown secondary effects, further supporting the data acquired in this thesis.

In Sum, I could show that loss of IS4A indeed leads to different channel properties. Taking the largely unaffected expression pattern into account this strongly indicates that these altered channel properties cause the impaired motor behaviors, as well as the stunted life expectancy of the animals lacking the IS4A exon.

In contrast, although the loss of I-IIA did result in perturbed processing along in the visual system, no other effects observed led to a significant difference in the assessed behaviors and channel properties. Thereby I conclude that the function of the I-IIA exon can for the most part be either compensated for by I-IIB, is strictly limited to the visual system, or mediates another function which was not addressed with the assays conducted in this thesis.

I could show that IS4B is in fact essential for survival of *Drosophila*, broadly expressed across the nervous system, and the relevant exon mediating the essential presynaptic functions of cacophony. But, the more refined motor functions and behaviors, such as flight initiation, require IS4A as well.

Possible mechanisms by which the IS4A exon and its resulting cacophony isoforms could interact with the bulk of cacophony throughout the nervous system carrying IS4B will be further explored below (see Discussion).

4 Discussion

Differential splicing is one mean to increase the number of proteins encoded by one gene. In fact, a single gene can produce proteins with completely different properties (Dinges *et al.*, 2017). Although uncommon for differential splicing of ion channel RNA, the production of isoforms that function as membrane channels and isoforms that function as transcription factors has been suggested for eag (Hegle, Marble and Wilson, 2006) channels. Concerning the two alternative exon pairs of the *Drosophila* Ca_v2 channel, there was no evidence that the production of isoforms with functions different than calcium channels. This was also not expected, since all annotated IS4 and I-II exon isoforms contain all pore forming transmembrane domains, the voltage sensor, and other typical features of voltage gated calcium channels. Nonetheless, many voltage gated calcium channel isoforms are produced across species. In humans new Ca_v1 channel isoforms are still being discovered (Clark *et al.*, 2020). Additionally, evidence that correct HVA channel splicing is critical for normal brain function is accumulating (Heck *et al.*, 2021). In principle, HVA channel isoforms could mediate redundant, exclusive, or cooperative functions: Redundant functions would mean that multiple isoforms with similar biophysical properties are present in the same brain areas and subcellular compartment. True redundancy would indicate that identical isoforms operate as fail-safe solutions for each other, but any two HVA channel isoforms analyzed here are structurally different. Multiple structurally different elements with similar functions are defined as degenerate solutions (Edelman and Gally, 2001; Drion, O'Leary and Marder, 2015), and ion channel degeneracy has been proposed to mediate increased operational bandwidth or increase functional robustness in addition to redundancy (Goaillard and Marder, 2021). Exclusive functions of distinct isoforms means that only this one isoform can mediate a specific calcium channel function. This could either be caused by isoform-specific expression in distinct brain parts, or in specific subcellular compartments, or alternatively, by unique biophysical properties of certain isoforms, or by unique interactions with other proteins. Examples of voltage gated calcium channel isoforms with distinct functions have been observed (Pan and Lipscombe, 2000; Lin, McDonough and Lipscombe, 2004; Lipscombe, Andrade and Allen, 2013; Heck *et al.*, 2019). However, systematic *in vivo* analyses across brain parts, subcellular compartments, and calcium channel functions are sparse. Cooperative function means that two different calcium channel isoforms are required to operate together to mediate a specific

function of a neuron. To the best of my knowledge, this has not been suggested before. This thesis provides evidence for all three, degenerate, exclusive, and cooperative functions of the *Drosophila* Ca_v2 channel alterative exons IS4 and I-II. I-IIA and B isoforms show similar expression patterns and functions in the larval and the adult ventral nerve cord, thus indicating degenerate function. By contrast, in the visual system, one isoform shows differential localization and is required for normal ERG, thus indicating an exclusive function. IS4 exon isoforms show exclusive and cooperative functions. Only one splice isoform localizes to the presynaptic active zone and is required for synaptic transmission and survival, thus clearly mediating an exclusive function. Strikingly, both IS4 isoform are required cooperatively for normal motor fitness and live expectancy. Below, I will continue to discuss these results for each of the two alternative exons.

4.1 I-II locus

4.1.1 I-II mediates predominantly redundant functions

Examination of the I-II B variant showed no significant differences in comparison to the controls, aside from the impaired ERG responses and the increased calcium signal in pupal animals further discussed below. Thus, for the most part I-IIB appears to serve redundant functions to I-IIA which is missing in the ΔI-IIA animals. There have been hypotheses (Kawasaki et al., 2002) arguing for a putative variant of cacophony, lacking both otherwise mutually exclusive exons for the I-II locus. Although this could possibly explain the narrow specific function of the exons responsible for the I-II locus, there has been no conclusive evidence as to whether this variant occurs. As such, none of the 18 annotated cacophony isoforms lacks both exons. Therefore, this avenue of explanation seems unlikely and in the similar expression patterns and function of the exons encoding the I-II locus seem to be actual redundancies. Of note, initial observations of the newly generated animals lacking the I-IIB locus suggest no severe defects, further supporting the high redundancy across the I-II splice isoforms. Similar strong redundancies have been reported for several other voltage gated channel genes and proteins (Goaillard and Marder, 2021). This can serve multiple purposes for the animals, firstly it reduces the susceptibility to genome damage, by duplicating the number of loci which would need to be affected by perturbations to leave lasting damage. Secondly, these redundancies also offer a possible location for further genomic changes some of which might be beneficial in nature without simultaneously losing all other previous gene functions, since the alternative

exon in this case would still be available. Lastly, as discussed below, alteration in the channel properties can, for instance, alter the activation thresholds of these channels resulting in a broader working range for continuous performance. This working range can then be narrowed down by expression of only specific splice isoforms to tailor the channel makeup to specific needs in parts of the nervous system. Whether the degenerate effect observed in the I-II variants is also applicable to other tissues or compartments cannot be concluded from the data presented here. In addition, I detected one exclusive function of I-IIA discussed in the following.

4.1.2 I-IIA mediates exclusive functions in the visual system on a level of interaction with accessory subunits

Δ I-IIA animals, animals capable of expressing only the I-IIB exon variant and thus able to interact with the β- as well as the βγ G-protein subunit show some distinct properties, beyond the broadly redundant functions they share with I-IIB. Firstly, like the animals lacking IS4A expression, they showed lowered cacophony expression in lamina and outer medulla. Here, the phenotype observed between lack of I-IIA and lack of IS4A is alike to a degree which cannot exclude a sort of bleed over from the other alternative exon. Meaning that the single exon excisions examined in this thesis always also affect the number of possible isoforms incorporating the alternative exons for the other locus. For example, in this case removal of I-IIA also leads to less isoforms incorporating IS4A and vice versa. Here, simultaneous exon excision at both loci, which has been enabled by the work done by me in this thesis, will be needed to thoroughly distinguish the function of specific exons.

Loss of the I-IIA exon also causes distinct decreases in calcium influx in several subcellular compartments but at the same time a stronger tendency towards double spikes in pupal current clamp recordings than in ΔIS4A animals. The apparent reduction in calcium signals might be due to a variation in voltage dependent kinetics mediated by subunit binding. Similarly, a possible explanation for the increased likelihood of double spikes in animals lacking I-IIA could be the altered voltage dependent inactivation of the channels, as a result of altered coupling. Here, in animals missing I-IIA, the remaining I-IIB exon is thought to be able to couple with either the β- subunit and/or the G-protein βγ subunit (reviewed by Buraei & Yang, 2010). This can be inferred from the α interaction domain (AID) being present in both amino acid sequences for the I-II locus. But only the I-IIB variant also contains the binding site for G protein

βγ subunits, as evidenced by the presence of the typical QxxER amino acid sequence, here in exon I-IIB with the variation QQIER, analogous to the mammalian $Ca_v2.1$ family variant of this sequence. G protein βγ and β subunits can bind to the α_1-subunit simultaneously, as well as individually, thereby possibly affecting the voltage dependent activation as well as inactivation (Buraei and Yang, 2010). A possible explanation for the increase in spiking as mentioned above, could be the lack of splice isoforms of cacophony expressing only the AID sequence (I-IIA) and thus preferentially binding β-subunits. Thereby reducing the number of unbound β-subunits, enabling the I-IIB containing splice variants to bind G protein βγ subunits. This variation in binding could then lead to a more balanced assembly of cacophonies with different gating properties as modulated by the subunits. Further alterations in binding preferences with accessory subunits as a result of the reduced isoform diversity could also include interactions with the α2δ accessory subunit. This subunit has been shown to affect location and properties of cacophony (Heinrich and Ryglewski, 2020). Determining which cacophony splice isoforms interact with which accessory subunits will be key to unravelling the intricate regulation of voltage gated calcium channel properties, but this was not the focus of this study.

4.2 IS4 locus

Both exon excisions of one of the IS4 exons lead to reduced vitality, either a lethal phenotype (lack of IS4B) or to a strongly reduced life expectancy and many different behavioral defects such as decreased ability to initiate flight, reduced sensory response and reduced locomotion, all of which are essential for survival outside of laboratory conditions. Thus, in contrast to the I-II locus, the functions of either alternative exon of IS4 are distinctly necessary for specific behaviors and therefore exclusive to the individual alternative exon.

4.2.1 IS4B is essential and mediates calcium currents with lowered activation threshold in the adult VNC

The IS4B exon was determined to mediate an essential function (see chapter 3.1.2.1), as evidenced by the lethal phenotype observed when removing this exon from the genome. In animals which could only express cacophony incorporating IS4B (ΔIS4A animals) cacophony could be found across all examined subcellular compartments (see chapter 3.4) and in nearly all parts of the nervous system (see chapter 3.3.). The only distinct regions lacking cacophony expression in animals containing only this isoform were parts of the visual system, yet life span and motor abilities were significantly reduced. IS4A must therefore mediate an essential

function. When examining the known functions of cacophony, its arguably most essential function is mediating exocytotic vesicle release at the active zone of chemical synapses (Kawasaki *et al.*, 2004). Here animals expressing only cacophony containing IS4B could be shown to have a stronger colocalization with brp in the active zone, by a relative reduction of cacophony in the periactive zone in comparison to the active zone (see chapter 3.4.5 Loss of exon IS4A is reflected in altered of colocalization coefficients at the AZ). Thereby highlighting the relevance of IS4B for cacophony in the active zone, furthermore synaptic transmission in TEVC recordings is not altered (personal communication Christopher Bell). These data are in agreement, with similar findings on cacophony colocalization with brp (e.g. Krick et al., 2021). Furthermore, somatodendritic cacophony currents in animals with exon choice reduced towards only expressing IS4B at the IS4 locus also showed an increase in excitability. This can be attributed to cacophony, since previous work has shown that cacophony is the main VGCC in the examined MNs somatodendritic domain (Ryglewski *et al.*, 2012). Specifically, the high voltage activated current mediated by cacophony (see chapter 3.5.4 Loss of IS4A produces lowers HVA threshold in adult *Drosophila* MN5) was reduced in its activation threshold. This finding could be confirmed in pupa and adult, each with distinct somatodendritic calcium currents. These findings strongly indicate that the cacophony remaining in animals lacking IS4A is susceptible to smaller depolarizations. In this case the excision of IS4A removes the exon which carries an additional positive charge in its voltage sensing domain, when compared to IS4B. This effect is in accordance with reports of others (Beyl *et al.*, 2016), stating that reduction of positive charges in the voltage sensor of the first homologous repeat of voltage gated calcium channels do in fact lower the activation voltage toward more hyperpolarized activation thresholds.

The increased lethality of animals lacking IS4A might very well be due to the increase in excitability observed in these animals. Previous studies could already show that cacophony mediated calcium influx can lead to cytotoxicity in cultured *Drosophila* neurons (Wiemerslage and Lee, 2015). Thus, loss of IS4A in a pan neuronal manner could lead to increased neurodegenerative effects resulting in premature death as observed in ΔIS4A. This in turn means that Cacophony incorporating IS4A has neuroprotective function for the animals in general. Likewise, the increase in seizure susceptibility observed in the ΔIS4A animals is likely also related to the decrease in activation thresholds. Others could show that temperature sensitive variants of the cacophony channel (cac^{TS2}) are less susceptible to seizures mediated

by the gain of function mutation of the voltage gated sodium channel para, bss1. Upon reaching restrictive temperatures cac^{TS2} becomes seizure susceptible itself, although it goes along with a reduction of transmitter release and reduced neuronal excitability (Saras and Tanouye, 2016). Here the authors hypothesize that a tighter coupling to the neurotransmitter vesicles might be responsible for increased seizure susceptibility in animals with lower channels density. Although no clear reduction in channel density became evident in this study, no quantification was done at a resolution which would be sufficient to determine these differences in channel quantity.

Lastly, animals expressing only the IS4B exon did show an increase in double action potentials in pupal current clamp recordings. Here the width of the half amplitude of the characteristic action potential is not significantly increased, while there are several double spike events (compare chapter 3.5.2) these effects do not translate to a stronger decrease in half AP width when abolishing the calcium component. Beyl et al. further showed that other gating properties are unaffected by these changes in amino acid charge in the voltage sensing domain (Beyl *et al.*, 2016) which seems also true for the data obtained in this thesis. The only thing they found was an increase in the activation slope. Although this parameter was not determined in this thesis, it could explain the increase in calcium dependent action potentials observed in the current clamp recordings, while no significant broadening of the calcium shoulder could be observed.

4.2.2 IS4A operates in sensory processing and is necessary for regular life expectancy

As described, IS4B mediates many specific functions, contrary to the functions of IS4A they are harder to grasp due to the lethal phenotype of the animals lacking IS4B. Nonetheless IS4A, although found only very sparsely in the nervous system (see chapters 3.3 and 3.4) mediates exclusive functions for the animals. The loss of IS4A leads to severely reduced life expectancy when only IS4B remains as the only possibility for the IS4 site in the mRNA (see chapter 3.1.2.1). Furthermore, the expression pattern of the IS4A exon is very sparse across the NS. The only strong expression could be found in the AMMC and parts of the visual system. In the lamina the expression pattern is the opposite of its mutually exclusive sister-exon for the IS4 locus, IS4B (compare chapter 3.3.4). These defects caused by the loss of IS4A can be extended to the examined motor behaviors, a reduction in mobility. These defects manifest in adult flight initiation, locomotion while courtship and reduced larval crawling distance. Interestingly,

others also suggest that the isoform diversity has a profound effect on larval locomotion cacophony (Hazelett *et al.*, 2012; Chang *et al.*, 2014; Lembke *et al.*, 2019). Specifically, the Morten lab could show that the so called ''exon 7'' is relevant for normal larval locomotion. This C-terminally located exon is present in all but one of the 18 currently annotated mRNAs for cacophony. This single mRNA transcript incorporates the B variant for the IS4 locus and the A variant for I-II. Thereby the only animals tested in this thesis capable of producing this transcript are the animals missing IS4A. Thereby recapitulating the crawling phenotype found in ΔIS4a animals in the animals examined in Lembke et al. This is assuming that excision of an alternative exon does not preclude splice isoform expression otherwise part of the wildtype isoform pool, the conceivable effects of have which not been examined in this thesis. This possible disruption of splice regulation could have been circumvented by employing homology directed repair because of the CRISPR induced double strand breaks, instead of homologous end joining. For example, by providing a repair template containing the other alternative exon e.g., exchanging IS4A with IS4B, leaving only IS4A as a possible exon to be incorporated, regardless of surrounding regulation. This approach would on the one hand be more sensitive to the surrounding intronic landscape, but on the other hand more susceptible to creating artificial gene products and misexpression in unintended cell compartments.

Nonetheless, not only locomotion is affected in animals lacking IS4A, but also their response to externally stimuli is reduced. These stimuli include visual stimuli, such as lamina responses to light pulses, which are completely abolished in animals lacking IS4A, as well as motor responses toward air puffs, normally sufficient to elicit flight in controls. Parts of the neuronal pathways producing these behaviors are located in the two areas with the most prominent IS4A expression. The AMMC, receiving sensory input from the Johnston organ which detects air blasts and similar cues (Mamiya and Dickinson, 2015). And the lamina as well as the outer medulla, important parts in the visual system, processing the information from the photoreceptor cells (e.g. Zhu, 2013). Thus, IS4A fulfills a crucial role in at least two structures downstream from receptors receiving external cues. Whether these defects are due to a lack of highly specialized channel properties of cacophony incorporating IS4A needed in exactly these tissues cannot be concluded from the data presented in this thesis. Although, expression of a cacophony transgene did not rescue the response as demonstrated by the pan neuronal expression of cac^{1}. This indicates that the specific properties of cacophony carrying IS4A are needed to fulfill the function in the visual system. Others could show that cacophony mediates

the exocytosis in the axon terminals of photoreceptors, which are found in the lamina and medulla (Astorga *et al.*, 2012). Thus, loss of the necessary cacophony variant mediating this could explain the absence of cacophony expression in lamina and medulla as well as the aberrant ERGs, as the lamina-ON/OFF fraction of the ERG is originating from the synaptic interaction between photoreceptor and lamina. Alternative splicing dependent effects on ion channel function in sensory cells has been described already, for example in chick hair cells, where splice isoforms of a potassium channel mediate dedicated functions (Fettiplace and Fuchs, 1999).

4.2.3 IS4 splice isoforms cooperate to generate physiological function

The above mentioned possible fine tuning of the isoform constellations at specific sites is one example for cooperative functions of the cacophony channels. Here the functional division of labor discussed for IS4A and IS4B cooperatively produces the wildtype channel properties observed. Specifically, although sparsely expressed, IS4A splice isoforms fine tune the excitability mediated by the broadly expressed IS4B splice isoforms to more depolarized and thus less excitable levels, protecting the neuron from excessive channel activity due to normally subthreshold membrane voltage changes. Thereby, IS4A functions as a fine throttle or break of sorts for the higher excitability of the more abundant cacophony channels incorporating IS4B. Thereby the incorporation of only a small number of IS4A carrying cacophony channels could provide an easily implemented but strong mechanism to fundamentally alter excitability of a neuron. For example, lack of the throttle (IS4A carrying cacophony) could increase the excitability of the somatodendritic area of a neuron, such as shown here for MN5. A scenario in which this effect could be beneficial for the animals could be during the arborization phase of the dendritic tree, where a reduced activation threshold of cacophony could promote activity dependent dendritic growth. Thereby making it easier for the dendrites to form synaptic connections with sparsely firing partners which might, after formation of a dendritic tree incorporate the throttling IS4A channels, resulting in a reevaluation of the synaptic interaction at another developmental stage and potential pruning of excess connections. Single channel voltage clamp could yield insights into whether this effect of throttling is on the level of individual channels or accumulated across as observed so far by whole cell voltage clamp. Another although similar possibility to mediate this throttling effect could be the interaction with other proteins such as accessory subunits in certain splice isoforms. As interaction of cacophony with different isoforms of the α2δ subunit could be

shown to have significant effects on location and channel properties (Heinrich and Ryglewski, 2020).

4.4 Outlook

This study provided a first systematic assessment of distinct splice isoforms generated by the individual exclusion of alternative exons at two distinct sites in the cacophony VGCC. The individual splice isoforms exhibit redundant/degenerate, exclusive and in on instance cooperative functions. These findings show that not only individual isoforms but also their influence on one another needs to be considered. Furthermore, this study highlights the necessity to further investigate splice isoform specific interactions with accessory subunits. Therefore, utilizing the tools and findings provided by this thesis, a further dissection of the exon specific properties will be possible. For example, by further reduction of isoform diversity towards more detailed subsets or by probing for interaction partners with specific isoforms, such as the α2δ and other accessory subunits. Lastly developmental defects, for example on dendritic tree growth could also play a role for the defective locomotor behavior, so far unaddressed. RNAi induced knockdowns of cacophony in MN5 could be shown to severely decrease dendritic tree growth and complexity (Ryglewski, Kilo and Duch, 2014). These broad developmental phenotypes could potentially be narrowed down to splice isoform specific impairments affecting dendritic growth, utilizing the tools generated in this thesis.

References:

Adams, P. J. *et al.* (2009) “CaV2.1 P/Q-type calcium channel alternative splicing affects the functional impact of familial hemiplegic migraine mutations: Implications for calcium channelopathies,” *Channels*, 3(2), pp. 110–121. doi: 10.4161/chan.3.2.7932.

Ashcroft, F. M. (2006) “From molecule to malady,” *Nature*, 440(7083), pp. 440–447. doi: 10.1038/nature04707.

Astorga, G. *et al.* (2012) “TRP, TRPL and Cacophony Channels Mediate Ca2+ Influx and Exocytosis in Photoreceptors Axons in Drosophila,” *PLoS ONE*. Edited by A. G. Obukhov, 7(8), p. e44182. doi: 10.1371/journal.pone.0044182.

Atwood, H. L. and Karunanithi, S. (2002) “Diversification of synaptic strength: Presynaptic elements,” *Nature Reviews Neuroscience*, 3(7), pp. 497–516. doi: 10.1038/nrn876.

Bainbridge, S. P. and Bownes, M. (1981) “Staging the metamorphosis of Drosophila melanogaster,” *Journal of Embryology and Experimental Morphology*, Vol.66(1967), pp. 57–80. doi: 10.1242/dev.66.1.57.

Beyl, S. *et al.* (2016) “Upward movement of IS4 and IIIS4 is a rate-limiting stage in Cav1.2 activation,” *Pflugers Archiv European Journal of Physiology*, 468(11–12), pp. 1895–1907. doi: 10.1007/s00424-016-1895-5.

Bier, E. *et al.* (2018) “Advances in engineering the fly genome with the CRISPR-Cas system,” *Genetics*, 208(1), pp. 1–18. doi: 10.1534/genetics.117.1113.

Blanchette, M. (2005) “Global analysis of positive and negative pre-mRNA splicing regulators in Drosophila,” *Genes & Development*, 19(11), pp. 1306–1314. doi: 10.1101/gad.1314205.

Brembs, B. *et al.* (2007) “Flight initiation and maintenance deficits in flies with genetically altered biogenic amine levels,” *Journal of Neuroscience*, 27(41), pp. 11122–11131. doi: 10.1523/JNEUROSCI.2704-07.2007.

Brent, J. R., Werner, K. M. and McCabe, B. D. (2009) “Drosophila Larval NMJ Dissection,” *Journal of Visualized Experiments : JoVE*, 24(24). doi: 10.3791/1107.

Brooks, A. N. *et al.* (2011) “Identification and experimental validation of splicing regulatory elements in Drosophila melanogaster reveals functionally conserved splicing enhancers in

metazoans," *RNA*, 17(10), pp. 1884–1894. doi: 10.1261/rna.2696311.

Buraei, Z. and Yang, J. (2010) "The β subunit of voltage-gated Ca2+ channels," *Physiological Reviews*, 90(4), pp. 1461–1506. doi: 10.1152/physrev.00057.2009.

Buraei, Z. and Yang, J. (2013) "Structure and function of the β subunit of voltage-gated Ca 2 + channels," *Biochimica et Biophysica Acta - Biomembranes*, 1828(7), pp. 1530–1540. doi: 10.1016/j.bbamem.2012.08.028.

Cain, S. M. and Snutch, T. P. (2011) "Voltage-gated calcium channels and disease," *BioFactors*, 37(3), pp. 197–205. doi: 10.1002/biof.158.

Castells-Nobau, A. *et al.* (2017) "Two algorithms for high-throughput and multi-parametric quantification of drosophila neuromuscular junction morphology," *Journal of Visualized Experiments*, 2017(123). doi: 10.3791/55395.

Cens, T. *et al.* (2006) "Voltage- and calcium-dependent inactivation in high voltage-gated Ca 2+ channels," *Progress in Biophysics and Molecular Biology*, 90(1–3), pp. 104–117. doi: 10.1016/j.pbiomolbio.2005.05.013.

Chang, J. C. *et al.* (2014) "Motor neuron expression of the voltage-gated calcium channel cacophony restores locomotion defects in a Drosophila, TDP-43 loss of function model of ALS," *Brain Research*, 1584, pp. 39–51. doi: 10.1016/j.brainres.2013.11.019.

Christel, C. and Lee, A. (2012) "Ca2+-dependent modulation of voltage-gated Ca2+ channels," *Biochimica et Biophysica Acta (BBA) - General Subjects*, 1820(8), pp. 1243–1252. doi: 10.1016/j.bbagen.2011.12.012.

Clark, M. B. *et al.* (2020) "Long-read sequencing reveals the complex splicing profile of the psychiatric risk gene CACNA1C in human brain," *Molecular Psychiatry*, 25(1), pp. 37–47. doi: 10.1038/s41380-019-0583-1.

Clark, M. Q. *et al.* (2016) "Functional Genetic Screen to Identify Interneurons Governing Behaviorally Distinct Aspects of Drosophila Larval Motor Programs," *G3 (Bethesda, Md.)*, 6(7), pp. 2023–2031. doi: 10.1534/G3.116.028472.

Consoulas, C., Restifo, L. L. and Levine, R. B. (2002) "Dendritic Remodeling and Growth of Motoneurons during Metamorphosis of Drosophila melanogaster," *Journal of Neuroscience*,

22(12), pp. 4906–4917. doi: 10.1523/jneurosci.22-12-04906.2002.

Coombe, P. E. and Heisenberg, M. (1986) “The structural brain mutant vacuolar medulla of drosophila melanogaster with specific behavioral defects and cell degeneration in the adult,” *Journal of Neurogenetics*, 3(3), pp. 135–158. doi: 10.3109/01677068609106845.

Dinges, N. *et al.* (2017) “Comprehensive Characterization of the Complex lola Locus Reveals a Novel Role in the Octopaminergic Pathway via Tyramine Beta-Hydroxylase Regulation,” *Cell Reports*, 21(10), pp. 2911–2925. doi: 10.1016/j.celrep.2017.11.015.

Dolphin, A. C. (2013) “The α2δ subunits of voltage-gated calcium channels,” *Biochimica et Biophysica Acta - Biomembranes*, 1828(7), pp. 1541–1549. doi: 10.1016/j.bbamem.2012.11.019.

Dolphin, A. C. (2016) “Voltage-gated calcium channels and their auxiliary subunits: physiology and pathophysiology and pharmacology,” *Journal of Physiology*, 594(19), pp. 5369–5390. doi: 10.1113/JP272262.

Dolphin, A. C. and Lee, A. (2020) “Presynaptic calcium channels: specialized control of synaptic neurotransmitter release,” *Nature Reviews Neuroscience*, 21(4), pp. 213–229. doi: 10.1038/s41583-020-0278-2.

Doudna, J. A. and Charpentier, E. (2014) “The new frontier of genome engineering with CRISPR-Cas9,” *Science*, 346(6213), pp. 1258096–1258096. doi: 10.1126/science.1258096.

Drion, G., O’Leary, T. and Marder, E. (2015) “Ion channel degeneracy enables robust and tunable neuronal Firing rates,” *Proceedings of the National Academy of Sciences of the United States of America*, 112(38), pp. E5361–E5370. doi: 10.1073/pnas.1516400112.

Du, X. *et al.* (2013) “XSecond cistron in CACNA1A gene encodes a transcription factor mediating cerebellar development and SCA6,” *Cell*, 154(1), p. 118. doi: 10.1016/j.cell.2013.05.059.

Edelman, G. M. and Gally, J. A. (2001) “Degeneracy and complexity in biological systems,” *Proceedings of the National Academy of Sciences of the United States of America*, 98(24), pp. 13763–13768. doi: 10.1073/pnas.231499798.

Fettiplace, R. and Fuchs, P. A. (1999) “Mechanisms of hair cell tuning,” *Annual Review of*

Physiology, 61(1), pp. 809–834. doi: 10.1146/annurev.physiol.61.1.809.

Gaitanidis, A. *et al.* (2019) "Longitudinal assessment of health-span and pre-death morbidity in wild type Drosophila," *Aging*, 11(6), pp. 1850–1873. doi: 10.18632/aging.101880.

Ganetzky, B. and Wu, C. F. (1982) "Indirect Suppression Involving Behavioral Mutants with Altered Nerve Excitability in DROSOPHILA MELANOGASTER," *Genetics*, 100(4), pp. 597–614. doi: 10.1093/GENETICS/100.4.597.

Goaillard, J. M. and Marder, E. (2021) "Ion Channel Degeneracy, Variability, and Covariation in Neuron and Circuit Resilience," *Annual Review of Neuroscience*, 44, pp. 335–357. doi: 10.1146/annurev-neuro-092920-121538.

Gratz, S. J. *et al.* (2013) "Genome engineering of Drosophila with the CRISPR RNA-guided Cas9 nuclease," *Genetics*, 194(4), pp. 1029–1035. doi: 10.1534/genetics.113.152710.

Gratz, S. J. *et al.* (2014) "Highly specific and efficient CRISPR/Cas9-catalyzed homology-directed repair in Drosophila," *Genetics*, 196(4), pp. 961–971. doi: 10.1534/genetics.113.160713.

Gratz, S. J. *et al.* (2019) "Endogenous tagging reveals differential regulation of Ca 2+ channels at single AZs during presynaptic homeostatic potentiation and depression," *The Journal of Neuroscience*, 39(13), pp. 3068–18. doi: 10.1523/JNEUROSCI.3068-18.2019.

Greenspan, R. J. and Ferveur, J. F. (2000) "Courtship in Drosophila," *Annual review of genetics*, 34, pp. 205–232. doi: 10.1146/ANNUREV.GENET.34.1.205.

Guangming, G. *et al.* (2020) "Neurexin and Neuroligins Maintain the Balance of Ghost and Satellite Boutons at the Drosophila Neuromuscular Junction," *Frontiers in Neuroanatomy*, 14(June), pp. 1–16. doi: 10.3389/fnana.2020.00019.

Hazelett, D. J. *et al.* (2012) "Comparison of parallel high-throughput RNA sequencing between knockout of TDP-43 and its overexpression reveals primarily nonreciprocal and nonoverlapping gene expression changes in the central nervous system of drosophila," *G3: Genes, Genomes, Genetics*, 2(7), pp. 789–802. doi: 10.1534/g3.112.002998.

Heck, J. *et al.* (2019) "Transient Confinement of CaV2.1 Ca2+-Channel Splice Variants Shapes Synaptic Short-Term Plasticity," *Neuron*, 103(1), pp. 66-79.e12. doi:

10.1016/j.neuron.2019.04.030.

Heck, J. *et al.* (2021) “More than a pore: How voltage-gated calcium channels act on different levels of neuronal communication regulation,” *Channels*, 15(1), pp. 322–338. doi: 10.1080/19336950.2021.1900024.

Hegle, A. P., Marble, D. D. and Wilson, G. F. (2006) “A voltage-driven switch for ion-independent signaling by Ether-à-go-go K+ channels,” *Proceedings of the National Academy of Sciences of the United States of America*, 103(8), pp. 2886–2891. doi: 10.1073/pnas.0505909103.

Heinrich, L. and Ryglewski, S. (2020) “Different functions of two putative Drosophila α2δ subunits in the same identified motoneurons,” *Scientific Reports*, 10(1), pp. 1–17. doi: 10.1038/s41598-020-69748-8.

Heisenberg, M. and GÖtz, K. G. (1975) “The use of mutations for the partial degradation of vision inDrosophila melanogaster,” *Journal of Comparative Physiology ? A*, 98(3), pp. 217–241. doi: 10.1007/BF00656971.

Ikeda, K. and Koenig, J. H. (1988) “Morphological identification of the motor neurons innervating the dorsal longitudinal flight muscle of Drosophila melanogaster,” *Journal of Comparative Neurology*, 273(3), pp. 436–444. doi: 10.1002/cne.902730312.

Ikeda, K., Koenig, J. H. and Tsuruhara, T. (1980) “Organization of identified axons innervating the dorsal longitudinal flight muscle ofDrosophila melanogaster,” *Journal of Neurocytology*, 9(6), pp. 799–823. doi: 10.1007/BF01205020.

Kadas, D. *et al.* (2017) “Dendritic and axonal L-type calcium channels cooperate to enhance motoneuron firing output during Drosophila larval locomotion,” *Journal of Neuroscience*, 37(45), pp. 10971–10982. doi: 10.1523/JNEUROSCI.1064-17.2017.

Kawasaki, F. *et al.* (2004) “Active Zone Localization of Presynaptic Calcium Channels Encoded by the cacophony Locus of Drosophila,” *Journal of Neuroscience*, 24(1), pp. 282–285. doi: 10.1523/JNEUROSCI.3553-03.2004.

Kawasaki, F., Collins, S. C. and Ordway, R. W. (2002) “Synaptic calcium-channel function in Drosophila: Analysis and transformation rescue of temperature-sensitive paralytic and lethal mutations of Cacophony,” *Journal of Neuroscience*, 22(14), pp. 5856–5864. doi:

10.1523/jneurosci.22-14-05856.2002.

Kawasaki, F., Felling, R. and Ordway, R. W. (2000) “A temperature-sensitive paralytic mutant defines a primary synaptic calcium channel in Drosophila,” *Journal of Neuroscience*, 20(13), pp. 4885–4889. doi: 10.1523/jneurosci.20-13-04885.2000.

Kenyon, F. C. (1896) “The brain of the bee. A preliminary contribution to the morphology of the nervous system of the arthropoda,” *Journal of Comparative Neurology*, 6(3), pp. 133–210. doi: 10.1002/cne.910060302.

Kittel, R. J. *et al.* (2006) “Bruchpilot promotes active zone assembly, Ca2+ channel clustering, and vesicle release,” *Science*, 312(5776), pp. 1051–1054. doi: 10.1126/science.1126308.

Klugbauer, N. *et al.* (2000) “A family of γ-like calcium channel subunits,” *FEBS Letters*, 470(2), pp. 189–197. doi: 10.1016/S0014-5793(00)01306-5.

Kondo, S. and Ueda, R. (2013) “Highly Improved gene targeting by germline-specific Cas9 expression in Drosophila,” *Genetics*, 195(3), pp. 715–721. doi: 10.1534/genetics.113.156737.

Krick, N. *et al.* (2021) “Separation of presynaptic Cav2 and Cav1 channel function in synaptic vesicle exo- And endocytosis by the membrane anchored Ca2+ pump PMCA,” *Proceedings of the National Academy of Sciences of the United States of America*, 118(28), p. e2106621118. doi: 10.1073/pnas.2106621118.

Kulkarni, S. J. and Hall, J. C. (1987) “Behavioral and cytogenetic analysis of the cacophony courtship song mutant and interacting genetic variants in Drosophila melanogaster,” *Genetics*, 115(3), pp. 451–460. doi: 10.1093/GENETICS/115.3.461.

Lembke, K. M. *et al.* (2019) “Deletion of a specific exon in the voltage-gated calcium channel gene cacophony disrupts locomotion in Drosophila larvae,” *Journal of Experimental Biology*, 222(1). doi: 10.1242/jeb.191106.

Liao, P., Zhang, H. Y. and Soong, T. W. (2009) “Alternative splicing of voltage-gated calcium channels: From molecular biology to disease,” *Pflugers Archiv European Journal of Physiology*, 458(3), pp. 481–487. doi: 10.1007/s00424-009-0635-5.

Lin, Y., McDonough, S. I. and Lipscombe, D. (2004) “Alternative splicing in the voltage-sensing region of N-Type Ca v2.2 channels modulates channel kinetics,” *Journal of*

Neurophysiology, 92(5), pp. 2820–2830. doi: 10.1152/jn.00048.2004.

Lipscombe, D., Andrade, A. and Allen, S. E. (2013) "Alternative splicing: Functional diversity among voltage-gated calcium channels and behavioral consequences," *Biochimica et Biophysica Acta - Biomembranes*, 1828(7), pp. 1522–1529. doi: 10.1016/j.bbamem.2012.09.018.

Lipscombe, D. and Lopez Soto, E. J. (2019) "Alternative splicing of neuronal genes: new mechanisms and new therapies," *Current Opinion in Neurobiology*, 57(1), pp. 26–31. doi: 10.1016/j.conb.2018.12.013.

Lohmann, C., Myhr, K. L. and Wong, R. O. L. (2002) "Transmitter-evoked local calcium release stabilizes developing dendrites," *Nature*, 418(6894), pp. 177–181. doi: 10.1038/nature00850.

Mamiya, A. and Dickinson, M. H. (2015) "Antennal Mechanosensory Neurons Mediate Wing Motor Reflexes in Flying Drosophila," *Journal of Neuroscience*, 35(20), pp. 7977–7991. doi: 10.1523/JNEUROSCI.0034-15.2015.

Milyaev, N. *et al.* (2012) "The virtual fly brain browser and query interface," *Bioinformatics*, 28(3), pp. 411–415. doi: 10.1093/bioinformatics/btr677.

Nijhof, B. *et al.* (2016) "A New Fiji-Based Algorithm That Systematically Quantifies Nine Synaptic Parameters Provides Insights into Drosophila NMJ Morphometry," *PLoS Computational Biology*. Edited by L. J. Graham, 12(3), p. e1004823. doi: 10.1371/journal.pcbi.1004823.

Pan, J. Q. and Lipscombe, D. (2000) "Alternative splicing in the cytoplasmic II-III loop of the N-type Ca channel α(1B) subunit: Functional differences are β subunit-specific," *Journal of Neuroscience*, 20(13), pp. 4769–4775. doi: 10.1523/jneurosci.20-13-04769.2000.

Parker, L. *et al.* (2011) "Drosophila as a model for epilepsy: bss is a gain-of-function mutation in the para sodium channel gene that leads to seizures," *Genetics*, 187(2), pp. 523–534. doi: 10.1534/genetics.110.123299.

Peixoto, A. A., Smith, L. A. and Hall, J. C. (1997) "Genomic organization and evolution of alternative exons in a Drosophila calcium channel gene," *Genetics*, 145(4), pp. 1003–1013. doi: 10.1093/genetics/145.4.1003.

Ryglewski, S. *et al.* (2012) “Ca v2 channels mediate low and high voltage-activated calcium currents in Drosophila motoneurons,” *Journal of Physiology*, 590(4), pp. 809–825. doi: 10.1113/jphysiol.2011.222836.

Ryglewski, S. *et al.* (2014) “Dendrites are dispensable for basic motoneuron function but essential for fine tuning of behavior,” *Proceedings of the National Academy of Sciences of the United States of America*, 111(50), pp. 18049–18054. doi: 10.1073/PNAS.1416247111.

Ryglewski, S. and Duch, C. (2012) “Preparation of Drosophila central neurons for in situ patch clamping,” *Journal of visualized experiments : JoVE*, (68). doi: 10.3791/4264.

Ryglewski, S., Kilo, L. and Duch, C. (2014) “Sequential acquisition of cacophony calcium currents, sodium channels and voltage-dependent potassium currents affects spike shape and dendrite growth during postembryonic maturation of an identified Drosophila motoneuron,” *European Journal of Neuroscience*, 39(10), pp. 1572–1585. doi: 10.1111/ejn.12517.

Saras, A. and Tanouye, M. A. (2016) “Mutations of the Calcium Channel Gene cacophony Suppress Seizures in Drosophila,” *PLoS Genetics*. Edited by S. Petrou, 12(1), p. e1005784. doi: 10.1371/journal.pgen.1005784.

von Schilcher, F. (1977) “A mutation which changes courtship song inDrosophila melanogaster,” *Behavior Genetics 1977 7:3*, 7(3), pp. 251–259. doi: 10.1007/BF01066278.

Von Schilcher, F. (1976) “The behavior of cacophony, a courtship song mutant in Drosophila melanogaster,” *Behavioral Biology*, 17(2), pp. 187–196. doi: 10.1016/S0091-6773(76)90444-2.

Smith, L. A. *et al.* (1996) “A Drosophila calcium channel α1 subunit gene maps to a genetic locus associated with behavioral and visual defects,” *Journal of Neuroscience*, 16(24), pp. 7868–7879. doi: 10.1523/jneurosci.16-24-07868.1996.

Smith, L. A. *et al.* (1998) “Courtship and visual defects of cacophony mutants reveal functional complexity of a calcium-channel α1 subunit in Drosophila,” *Genetics*, 149(3), pp. 1407–1426. doi: 10.1093/genetics/149.3.1407.

Sternberg, S. H. and Doudna, J. A. (2015) “Expanding the Biologist’s Toolkit with CRISPR-Cas9,” *Molecular Cell*, 58(4), pp. 568–574. doi: 10.1016/j.molcel.2015.02.032.

Striessnig, J. (2016) “Voltage-gated calcium channels – from basic mechanisms to disease,” *Journal of Physiology*, 594(20), pp. 5817–5821. doi: 10.1113/JP272619.

Vonhoff, F. *et al.* (2013) “Temporal coherency between receptor expression, neural activity and AP-1-dependent transcription regulates Drosophila motoneuron dendrite development,” *Development*, 140(3), pp. 606–616. doi: 10.1242/dev.089235.

Wiemerslage, L. and Lee, D. (2015) “Role of Drosophila calcium channel cacophony in dopaminergic neurodegeneration and neuroprotection,” *Neuroscience Letters*, 584, pp. 342–346. doi: 10.1016/j.neulet.2014.11.004.

Williamson, W. R. and Hiesinger, P. R. (2010) “Preparation of Developing and Adult Drosophila Brains and Retinae for Live Imaging,” *Journal of Visualized Experiments*, (37), pp. 3–8. doi: 10.3791/1936.

Worrell, J. W. and Levine, R. B. (2008) “Characterization of voltage-dependent Ca2+ currents in identified drosophila motoneurons in situ,” *Journal of Neurophysiology*, 100(2), pp. 868–878. doi: 10.1152/jn.90464.2008.

Wu, J. *et al.* (2016) “Structure of the voltage-gated calcium channel Cav1.1 at 3.6 Å resolution,” *Nature*, 537(7619), pp. 191–196. doi: 10.1038/nature19321.

Zamponi, G. W. *et al.* (2015) “The physiology, pathology, and pharmacology of voltage-gated calcium channels and their future therapeutic potential,” *Pharmacological Reviews*. Edited by D. R. Sibley, 67(4), pp. 821–870. doi: 10.1124/pr.114.009654.

Zhu, Y. (2013) “The Drosophila visual system: From neural circuits to behavior,” *Cell Adhesion and Migration*, 7(4), pp. 333–344. doi: 10.4161/cam.25521.

5. Appendix

Salines, buffers and gels

Solution	Reagents/Formulation/Supplier
Saline (adult extracellular, AP recordings, current clamp, calcium imaging)	128 mM NaCl 2 mM KCl 1.8 mM $CaCl_2$ 4 mM $MgCl_2$ 5 mM HEPES ~35.5 mM Sucrose pH adjusted to 7.24-25 using NaOH
Intracell saline (current clamp recordings)	140mM K Gluconate 2mM $MgCl_2$ 11mM EGTA 10mM HEPES 2mM ATP-Mg Adjust pH with KOH
TEA extracellular saline (Calcium current recordings, voltage clamp)	93.2mM NaCl 5mM KCl 4mM $MgCl_2$ 1.8mM $CaCl_2$ 1.8mM $BaCl_2$ 30mM TEA-Cl 2mM 4-AP 5mM HEPES ~35.5mM Sucrose Adjust pH to 7.24 with NaOH, target mOsm: ~300
Cs Intracell saline (voltage clamp recordings)	144mM CsCl 0.5mM $CaCl_2$ 2mM ATP-Mg 5mM EGTA 10mM HEPES

	20mM TEA-Br 0.5mM 4-AP Adjust pH to 7.24 with CsOH
5X TBE	54 g Tris-Base 27,5 g Boric acid 20 ml 0,5 M EDTA Fill to 1l with H_2O
stacking gel (5%)	2,7 ml H_2O 670 µl Acrylamid (30%) 500 µl 1M Tris-HCl Puffer, pH=6.8 20 µl SDS (20%) 40 µl APS (10%) 4 µl TEMED
running gel (5%)	3,4 ml H_2O 1,7 ml Acrylamid (30%) 1,6 ml 1,5 M Tris-HCl Puffer, pH=8.8 50 µl SDS (20%) 100 µl APS (10%) 10 µl TEMED
6x SDS buffer	7 ml 4x Tris-HCl/SDS, pH=6,8 3,6 ml Glycerol 1 g SDS 0,93 g DTT 1 mg Bromphenolblau Fill to 10ml with H_2O 25µl sample buffer per tube
10x SDS-Tris-Glycine Electrophoresis buffer for 1l	30,3 g Trisbase 144,4 g Glycine 10 g SDS Fill to 1l with H_2O
Calcium imaging saline (intra)	140mM K-gluconate

	2mM Mg-ATP 2mM MgCl2 10mM phosphocreatine di tris, 0.3mM Na2GTP 10mM HEPES pH adjusted to 7.24 with 1N KOH
Squishing buffer	10 mM Tris-Cl pH 8,2 1 mM EDTA 25 mM NaCl
1x TBST	900 ml H_2O 100 ml 10x TBS 1000 µl Tween-20

Other chemicals and reagents used

Reagent/chemical	Origin/ supplier
PBS (Tablets, 1 per 1l ddH_2O)	Sigma # P4417
α-brp (mouse)	Hybridoma Bank nc82
α-chicken (goat) – Alexa488	Life technologies A11039
α-GFP (rabbit)	Life technologies A11122
α-mouse (donkey) Alexa 647	Jackson ImmunoResearch 715-605-150
α-rabbit (donkey) Alexa568	Invitrogen A10042
α-rabbit (donkey) Alexa488	Invitrogen A21206
α-HRP (rabbit)	Jackson ImmunoResearch 323-005-021
α-SynORF (mouse)	Hybridoma Bank 3C11
Triton X-100	Sigma Aldrich T8787
Tris-Base	Carl Roth 5429.3
TEMED	BIO-RAD 1610801
SDS	Carl Roth 2326.1
Acrylamid (30%)	BIO-RAD 1619154
Skim milk powder	Carl Roth T145.2

Ratios of antibody combinations for the different imaging experiments

Method	Primary antibodies	Secondary antibodies
Larval immuno (VNC and NMJ)	α-GFP (rabbit) 1:400 α-brp (mouse) 1:400	α-rabbit (donkey) Alexa 488 α-mouse (donkey) Alexa 647 both 1:750
Bouton/AZ counting	α-HRP (rabbit) 1:500 α-brp (mouse) 1:400	α-rabbit (donkey) Alexa 568 α-mouse (donkey) Alexa 647 Both 1:750
Brain immune (whole brain and optical lobes)	α-GFP (rabbit) 1:400 α-SynORF (mouse) 1:200	α-rabbit (donkey) Alexa488 α-mouse (donkey) Alexa 647 both 1:750
Western	α-GFP (rabbit) 1:1000 (top part of the membrane) α-Actin mouse 1:1000 (bottom part of the membrane)	α-rabbit lgG (goat) HRP conjugate 1:10000 α-mouse (goat) HRP conjugate 1:5000

Programs used, version and application

Program	Version	Used for
Snapgene Viewer	Up to version 6	Cloning, plasmid maps, planning of molecular biology
Serial cloner	2.6.1	Cloning, plasmid maps, planning of molecular biology, restriction digests
FIJI	Up to v1.53c	Image analysis
PRISM	9.1	Data analysis

Clampex/fit	10.7	Electrophysiological analysis/acquisition
Labchart	Version 7	Courtship recordings
Spike 2	7.20	Flight, song data analysis
Tracker	5.1.5.	Crawling data analysis

Plasmid maps and sequences

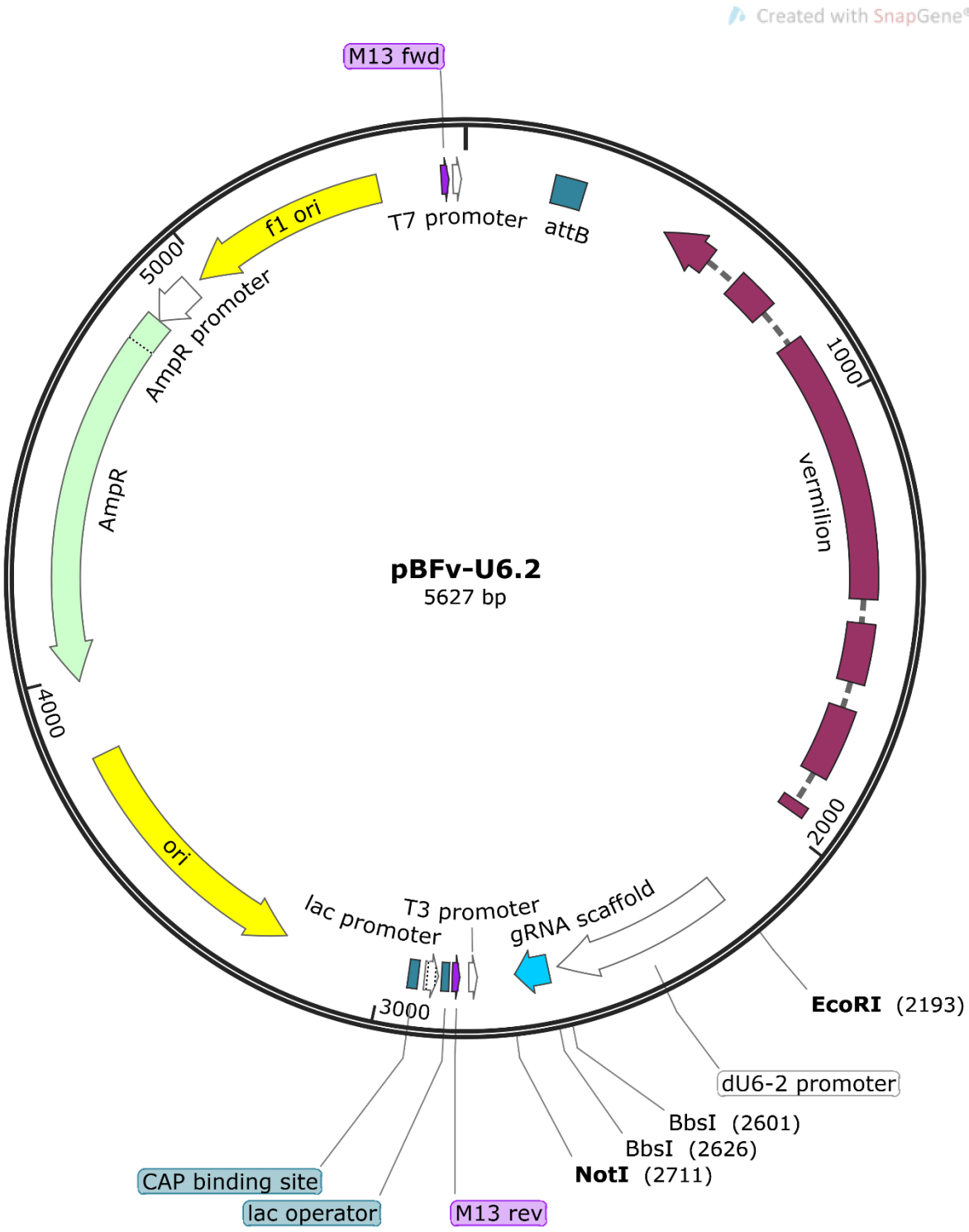

Figure 35: map of unaltered pBFv-U6.2 and sequence below

GGTACCTCGACATGCCCGCCGTGACCGTCGAGAACCCGCTGACGCTGCCCCGCGTATCCGCACCCGCCGACGCCGTCGCA

CGTCCCGTGCTCACCGTGACCACCGCGCCCAGCGGTTTCGAGGGCGAGGGCTTCCCGGTGCGCCGCGCGTTCGCCGGGAT

CAACTACCGCCACCTCGACCCGTTCATCATGATGGACCAGATGGGTGAGGTGGAGTACGCGCCCGGGGAGCCCAAGGGC

ACGCCCTGGCACCCGCACCGCGGCTTCGAGACCGTGACCTACATCGTCGACAAGCTTGGATTTATTTTGTTATGTTATATGT

ATTATATGTCAGACATAAAGAAAAGGAACACATCAAATGTGATAACAAAGACTAAACAAGTAATTTTATTACACCAAAACG
ACAAAACAGTAGGCAGAACAAACAACGCATAGCCAAACATTGACGAATTGGATACCCTGCCGATTGTCAGACACTTTTGTT
GATCAGTTTCTTGCGAATGGTCTCGTCCAGCGGTGGAATCGCCTCGCGGGGAATCAGAAAAGTGGACAGATTGAACAGAT
CCAGAAACACCTTGTACCGATCACTGAAACCAAAAAAAAACAAAGGGAGAACAGTTTGAGTTCATTGATCCCCGATATAAT
CACATCTGCGATGATCACCTGAGAGTGGAGCGCAGATATTGATATCCAGACGAGCCACCAGTGCCCAACTGTTGGGATCC
AATCATGCGTTGCACCATGATCACGTGATTGTCTGCGGCGGGAATAGAAAGTATTTGGTTAGGAAAACCAGTCTTAAACAT
AAGATATATTTATAAAAGAGTATCAAAGAATGCAATACTTACATCTCCACTTGGTTATTAACGAGTCGATGTCCATGAGCA
GGGTGAGCAACTGGTGTGGTTGGCTGAACCTGGGTTCATCCCTATAGAAGGTGATCATGATGGCTCCCTGAAGGGCACGA
TGGCTAAACCGGCGATCCCCACGACGCACCAGTGCATCGTGCACTGCCGGATCAAAGATGGAGCGATACACCTCGCGTCG
CTTCTCAATGTCCATGAGGCGGTAGTTTTTCGCCTTCTCCACGGGCTCCTCCATGGCGCTCTGTACCTGCGCCTCCAGGAAT
CGATCGACGCTCTCCTGAAACTTGGCCCAGAAGTTGAAGCCACTCTCCTCCAGTCCGGGCGTCCTCTCCAGCCATCGCTGC
ACTAGCTCCAGTAGCGAGGGATCTTTCTCCGAGTTGCGAATCGAGTTCCGCGCCTCCTCGTCGCTAAAGACATCCGAGTAC
TTCTGGTTGTATCTCACCCGCTGCTCTGTCAGAACTCCCAGCTTGTTCTCGATCAAACGGAACTGCAGCGACTGAAAACCAG
ATGCGGGTGCCAGGTACTTGCGGAAGTCCATGAAGTCTAGCGGGGTCATGGTCTCCAGAATGGGCACTTGGTCCACCAGG
AGCTGTACAAAGGAAGTTATAAACGGATTTTGGTAAGAGATTCAGAAAGCACTCACTTTTAGAATCAGAACCACTCGGTTC
AGTCGCTTGACAATCTCCAGCGTCTTGGTTTCATCGATGACCTCTGCATCCAACATGTCTCGTATGGAGTCGAACTCAAAGA
TGATCTGCTTGAACCAAAGCTCGTAGGCTGTGGCGAAGGTACTTAAATGCCATTGAGTGTTGTCATCAAAGTTGTAAACCT
ACTCACCCTGGTGCGTGATGATGAACAGATGCTCATCGTGCACGGGTCGCTTGTCCTCCTCGGACAGCATACACTGGGCAT
CCAGCAGTTTGTCCAGCATCAGATACTCTCCATAGATTTTGCCCACTTCCGTGGTTAATGGCACCGCCGAATCATCGTGATC
GTTTCTGTATGGGTTTGAATTGAATCGCAGAACTGAAGATCGATTGGCATTCCTGGACAGCACGTGCTGGTGCTCACCCGT
TTCCTGCATAGGGACAGCTCATGGTGCACAGCTCAGATCAGATCGTGACTCCTCGAGCGGCGGATGCTGGCGAACTGATC
TCCGCCAGCGGACCGGAGATGAGACCCCAGCGAACCGATAACAGAGCGAGAGAGCTCCAGTTCCGACTGATTGCACAGT
CGGTGATCTGGGCGATGGGCACTGCCAGATAGGCTGGGAATTATCAATCACTTGAGGTGAAAGTGCGGCGCACACAAAT
CCAAGCTTGATATCGAATTCCCTGCAGGTTCGACTTGCAGCCTGAAATACGGCACGAGTAGGAAAAGCCGAGTCAAATGC
CGAATGCAGAGTCTCATTACAGCACAATCAACTCAAGAAAAACTCGACACTTTTTTACCATTTGCACTTAAATCCTTTTTTAT
TCGTTATGTATACTTTTTTTGGTCCCTAACCAAAACAAAACCAAACTCTCTTAGTCGTGCCTCTATATTTAAAACTATCAATTT
ATTATAGTCAATAAATCGAACTGTGTTTTCAACAAACGAACAATAGGACACTTTGATTCTAAAGGAAATTTTGAAAATCTTA
AGCAGAGGGTTCTTAAGACCATTTGCCAATTCTTATAATTCTCAACTGCTCTTTCCTGATGTTGATCATTTATATAGGTATGT
TTTCCTCAATACTTCGGGTCTTCGAGTTGAAGACCTGTTTTAGAGCTAGAAATAGCAAGTTAAAATAAGGCTAGTCCGTTAT
CAACTTGAAAAAGTGGCACCGAGTCGGTGCTTTTTTTGCGGCCGCGCATGCACTTGGCTTTCCACCGTTGGTATCGATTCTC
TGGGACGATGAGTCGAGCTCCAGCTTTTGTTCCCTTTAGTGAGGGTTAATTGCGCGCTTGGCGTAATCATGGTCATAGCTG
TTTCCTGTGTGAAATTGTTATCCGCTCACAATTCCACACAACATACGAGCCGGAAGCATAAAGTGTAAAGCCTGGGGTGCC
TAATGAGTGAGCTAACTCACATTAATTGCGTTGCGCTCACTGCCCGCTTTCCAGTCGGGAAACCTGTCGTGCCAGCTGCATT
AATGAATCGGCCAACGCGCGGGGAGAGGCGGTTTGCGTATTGGGCGCTCTTCCGCTTCCTCGCTCACTGACTCGCTGCGCT
CGGTCGTTCGGCTGCGGCGAGCGGTATCAGCTCACTCAAAGGCGGTAATACGGTTATCCACAGAATCAGGGGATAACGCA
GGAAAGAACATGTGAGCAAAAGGCCAGCAAAAGGCCAGGAACCGTAAAAAGGCCGCGTTGCTGGCGTTTTTCCATAGGC
TCCGCCCCCCTGACGAGCATCACAAAAATCGACGCTCAAGTCAGAGGTGGCGAAACCCGACAGGACTATAAAGATACCAG
GCGTTTCCCCCTGGAAGCTCCCTCGTGCGCTCTCCTGTTCCGACCCTGCCGCTTACCGGATACCTGTCCGCCTTTCTCCCTTC

GGGAAGCGTGGCGCTTTCTCATAGCTCACGCTGTAGGTATCTCAGTTCGGTGTAGGTCGTTCGCTCCAAGCTGGGCTGTGT
GCACGAACCCCCCGTTCAGCCCGACCGCTGCGCCTTATCCGGTAACTATCGTCTTGAGTCCAACCCGGTAAGACACGACTT
ATCGCCACTGGCAGCAGCCACTGGTAACAGGATTAGCAGAGCGAGGTATGTAGGCGGTGCTACAGAGTTCTTGAAGTGG
TGGCCTAACTACGGCTACACTAGAAGGACAGTATTTGGTATCTGCGCTCTGCTGAAGCCAGTTACCTTCGGAAAAAGAGTT
GGTAGCTCTTGATCCGGCAAACAAACCACCGCTGGTAGCGGTGGTTTTTTTGTTTGCAAGCAGCAGATTACGCGCAGAAA
AAAAGGATCTCAAGAAGATCCTTTGATCTTTTCTACGGGGTCTGACGCTCAGTGGAACGAAAACTCACGTTAAGGGATTTT
GGTCATGAGATTATCAAAAAGGATCTTCACCTAGATCCTTTTAAATTAAAAATGAAGTTTTAAATCAATCTAAAGTATATAT
GAGTAAACTTGGTCTGACAGTTACCAATGCTTAATCAGTGAGGCACCTATCTCAGCGATCTGTCTATTTCGTTCATCCATAG
TTGCCTGACTCCCCGTCGTGTAGATAACTACGATACGGGAGGGCTTACCATCTGGCCCCAGTGCTGCAATGATACCGCGAG
ACCCACGCTCACCGGCTCCAGATTTATCAGCAATAAACCAGCCAGCCGGAAGGGCCGAGCGCAGAAGTGGTCCTGCAACT
TTATCCGCCTCCATCCAGTCTATTAATTGTTGCCGGGAAGCTAGAGTAAGTAGTTCGCCAGTTAATAGTTTGCGCAACGTTG
TTGCCATTGCTACAGGCATCGTGGTGTCACGCTCGTCGTTTGGTATGGCTTCATTCAGCTCCGGTTCCCAACGATCAAGGCG
AGTTACATGATCCCCCATGTTGTGCAAAAAAGCGGTTAGCTCCTTCGGTCCTCCGATCGTTGTCAGAAGTAAGTTGGCCGC
AGTGTTATCACTCATGGTTATGGCAGCACTGCATAATTCTCTTACTGTCATGCCATCCGTAAGATGCTTTTCTGTGACTGGT
GAGTACTCAACCAAGTCATTCTGAGAATAGTGTATGCGGCGACCGAGTTGCTCTTGCCCGGCGTCAATACGGGATAATACC
GCGCCACATAGCAGAACTTTAAAAGTGCTCATCATTGGAAAACGTTCTTCGGGGCGAAAACTCTCAAGGATCTTACCGCTG
TTGAGATCCAGTTCGATGTAACCCACTCGTGCACCCAACTGATCTTCAGCATCTTTTACTTTCACCAGCGTTTCTGGGTGAG
CAAAAACAGGAAGGCAAAATGCCGCAAAAAAGGGAATAAGGGCGACACGGAAATGTTGAATACTCATACTCTTCCTTTTT
CAATATTATTGAAGCATTTATCAGGGTTATTGTCTCATGAGCGGATACATATTTGAATGTATTTAGAAAAATAAACAAATAG
GGGTTCCGCGCACATTTCCCCGAAAAGTGCCACCTAAATTGTAAGCGTTAATATTTTGTTAAAATTCGCGTTAAATTTTTGTT
AAATCAGCTCATTTTTTAACCAATAGGCCGAAATCGGCAAAATCCCTTATAAATCAAAAGAATAGACCGAGATAGGGTTGA
GTGTTGTTCCAGTTTGGAACAAGAGTCCACTATTAAAGAACGTGGACTCCAACGTCAAAGGGCGAAAAACCGTCTATCAG
GGCGATGGCCCACTACGTGAACCATCACCCTAATCAAGTTTTTTGGGGTCGAGGTGCCGTAAAGCACTAAATCGGAACCCT
AAAGGGAGCCCCCGATTTAGAGCTTGACGGGGAAAGCCGGCGAACGTGGCGAGAAAGGAAGGGAAGAAAGCGAAAGG
AGCGGGCGCTAGGGCGCTGGCAAGTGTAGCGGTCACGCTGCGCGTAACCACCACACCCGCCGCGCTTAATGCGCCGCTAC
AGGGCGCGTCCCATTCGCCATTCAGGCTGCGCAACTGTTGGGAAGGGCGATCGGTGCGGGCCTCTTCGCTATTACGCCAG
CTGGCGAAAGGGGGATGTGCTGCAAGGCGATTAAGTTGGGTAACGCCAGGGTTTTCCCAGTCACGACGTTGTAAAACGA
CGGCCAGTGAGCGCGCGTAATACGACTCACTATAGGGCGAATTG

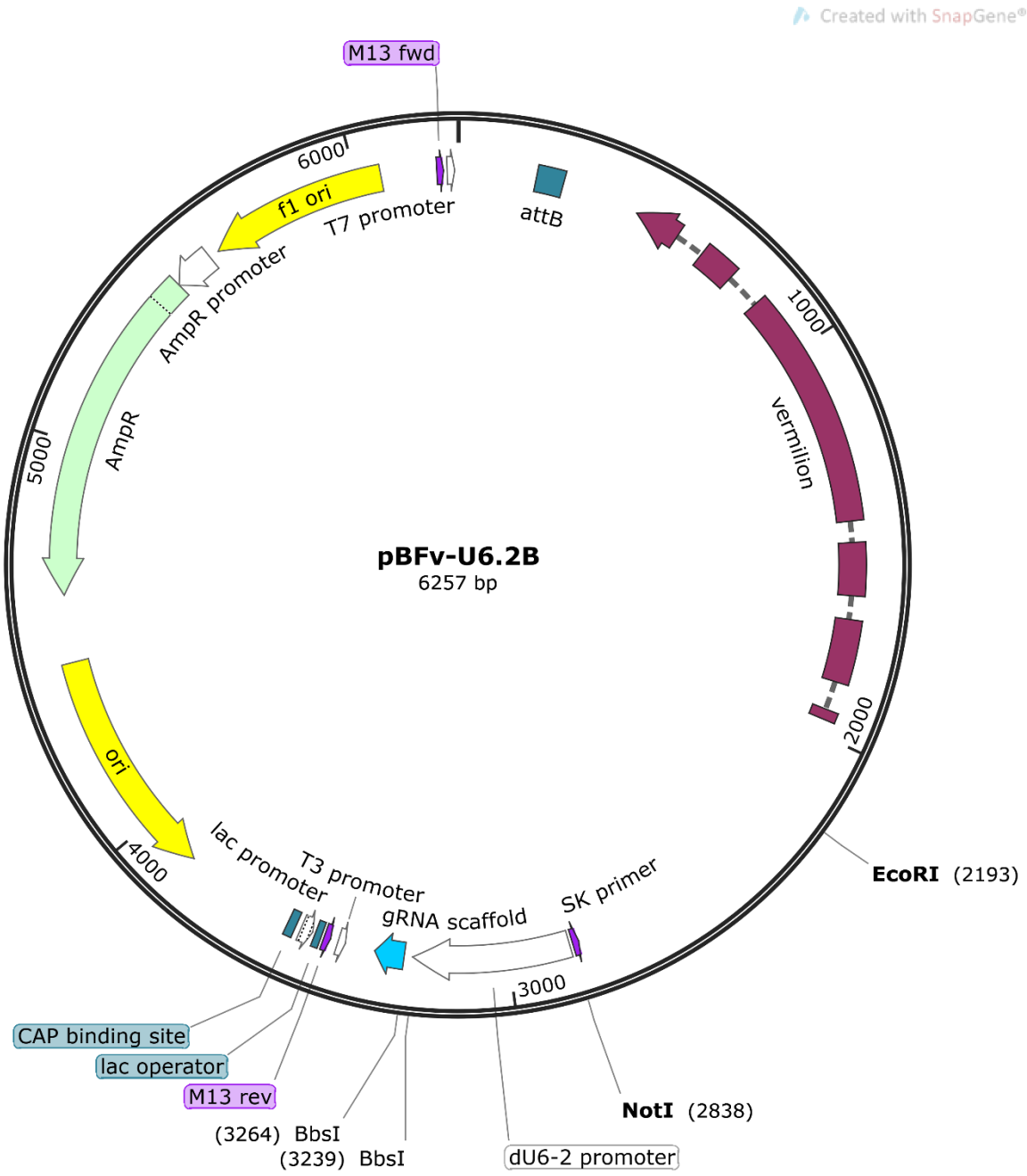

Figure 36: Map of unaltered pBFv-U6.2B and sequence below

GGTACCTCGACATGCCCGCCGTGACCGTCGAGAACCCGCTGACGCTGCCCCGCGTATCCGCACCCGCCGACGCCGTCGCA
CGTCCCGTGCTCACCGTGACCACCGCGCCCAGCGGTTTCGAGGGCGAGGGCTTCCCGGTGCGCCGCGCGTTCGCCGGGAT
CAACTACCGCCACCTCGACCCGTTCATCATGATGGACCAGATGGGTGAGGTGGAGTACGCGCCCGGGGAGCCCAAGGGC
ACGCCCTGGCACCCGCACCGCGGCTTCGAGACCGTGACCTACATCGTCGACAAGCTTGGATTTATTTTGTTATGTTATATGT
ATTATATGTCAGACATAAAGAAAAGGAACACATCAAATGTGATAACAAAGACTAAACAAGTAATTTTATTACACCAAAACG
ACAAAACAGTAGGCAGAACAAACAACGCATAGCCAAACATTGACGAATTGGATACCCTGCCGATTGTCAGACACTTTTGTT
GATCAGTTTCTTGCGAATGGTCTCGTCCAGCGGTGGAATCGCCTCGCGGGGAATCAGAAAAGTGGACAGATTGAACAGAT
CCAGAAACACCTTGTACCGATCACTGAAACCAAAAAAAAACAAAGGGAGAACAGTTTGAGTTCATTGATCCCCGATATAAT
CACATCTGCGATGATCACCTGAGAGTGGAGCGCAGATATTGATATCCAGACGAGCCACCAGTGCCCAACTGTTGGGATCC

AATCATGCGTTGCACCATGATCACGTGATTGTCTGCGGCGGGAATAGAAAGTATTTGGTTAGGAAAACCAGTCTTAAACAT
AAGATATATTTATAAAAGAGTATCAAAGAATGCAATACTTACATCTCCACTTGGTTATTAACGAGTCGATGTCCATGAGCA
GGGTGAGCAACTGGTGTGGTTGGCTGAACCTGGGTTCATCCCTATAGAAGGTGATCATGATGGCTCCCTGAAGGGCACGA
TGGCTAAACCGGCGATCCCCACGACGCACCAGTGCATCGTGCACTGCCGGATCAAAGATGGAGCGATACACCTCGCGTCG
CTTCTCAATGTCCATGAGGCGGTAGTTTTTCGCCTTCTCCACGGGCTCCTCCATGGCGCTCTGTACCTGCGCCTCCAGGAAT
CGATCGACGCTCTCCTGAAACTTGGCCCAGAAGTTGAAGCCACTCTCCTCCAGTCCGGGCGTCCTCTCCAGCCATCGCTGC
ACTAGCTCCAGTAGCGAGGGATCTTTCTCCGAGTTGCGAATCGAGTTCCGCGCCTCCTCGTCGCTAAAGACATCCGAGTAC
TTCTGGTTGTATCTCACCCGCTGCTCTGTCAGAACTCCCAGCTTGTTCTCGATCAAACGGAACTGCAGCGACTGAAAACCAG
ATGCGGGTGCCAGGTACTTGCGGAAGTCCATGAAGTCTAGCGGGGTCATGGTCTCCAGAATGGGCACTTGGTCCACCAGG
AGCTGTACAAAGGAAGTTATAAACGGATTTTGGTAAGAGATTCAGAAAGCACTCACTTTTAGAATCAGAACCACTCGGTTC
AGTCGCTTGACAATCTCCAGCGTCTTGGTTTCATCGATGACCTCTGCATCCAACATGTCTCGTATGGAGTCGAACTCAAAGA
TGATCTGCTTGAACCAAAGCTCGTAGGCTGTGGCGAAGGTACTTAAATGCCATTGAGTGTTGTCATCAAAGTTGTAAACCT
ACTCACCCTGGTGCGTGATGATGAACAGATGCTCATCGTGCACGGGTCGCTTGTCCTCCTCGGACAGCATACACTGGGCAT
CCAGCAGTTTGTCCAGCATCAGATACTCTCCATAGATTTTGCCCACTTCCGTGGTTAATGGCACCGCCGAATCATCGTGATC
GTTTCTGTATGGGTTTGAATTGAATCGCAGAACTGAAGATCGATTGGCATTCCTGGACAGCACGTGCTGGTGCTCACCCGT
TTCCTGCATAGGGACAGCTCATGGTGCACAGCTCAGATCAGATCGTGACTCCTCGAGCGGCGGATGCTGGCGAACTGATC
TCCGCCAGCGGACCGGAGATGAGACCCCAGCGAACCGATAACAGAGCGAGAGAGCTCCAGTTCCGACTGATTGCACAGT
CGGTGATCTGGGCGATGGGCACTGCCAGATAGGCTGGGAATTATCAATCACTTGAGGTGAAAGTGCGGCGCACACAAAT
CCAAGCTTGATATCGAATTCCCTGCAGGGCAGTTTGTTTGGCATCATCTCGGCCATCGTCTTATTCTTCTTCGTGGCCTTTGT
TACCGGAGCGGCTATGTTGGGCGCGGTGGAGCCCGGAAGCTGAAAGGTTAATCGAATGCGTTAACTTTTCTGCAACTCGA
AAGTTTGCCGCCTTTGTTCGACTGCCAATAACTGTTGATTCGAAAATTCGAATCGAAGCGGTTGAATTTCGTAGGGTGGCC
AACTACACCAAAGTTCGCCGGCGGTGTACATGCCTGTTTTTTTTTTTTTGTTCGCAATGAGGAATGGCTCTTAAAATCTACTA
GATAAAAAAAATATTCATTATTTCTATGCTGCTGGAACGCTTCATTAATCTTAAAAATTCTAAATTCGGTTACCATGATACTT
CGACGCATAACTGTAGATTTTGGATAGAATTAAAGAGAAAATGGCGAGAGAGTAAAATTCCGGCGTCGGCAAAGTAGAG
CAAAAAAATCAGTATACCATTTAGCTACCTCTCTCACTCGCACGCAGTGCCGGCTCAAGTTGGGCGCGGCTCTGCAATTATC
GATTTTCTTGGGGTGTGTAACTAATCATCCGTTTTCCCTTCCTCCTCATCCACAGCGTGAAGGCGCGCCGGATCCACTAGTT
CTAGAGCGGCCGCTTCGACTTGCAGCCTGAAATACGGCACGAGTAGGAAAAGCCGAGTCAAATGCCGAATGCAGAGTCTC
ATTACAGCACAATCAACTCAAGAAAAACTCGACACTTTTTTACCATTTGCACTTAAATCCTTTTTTATTCGTTATGTATACTTT
TTTTGGTCCCTAACCAAAACAAAACCAAACTCTCTTAGTCGTGCCTCTATATTTAAAACTATCAATTTATTATAGTCAATAAA
TCGAACTGTGTTTTCAACAAACGAACAATAGGACACTTTGATTCTAAAGGAAATTTTGAAAATCTTAAGCAGAGGGTTCTT
AAGACCATTTGCCAATTCTTATAATTCTCAACTGCTCTTTCCTGATGTTGATCATTTATATAGGTATGTTTTCCTCAATACTTC
GGGTCTTCGAGTTGAAGACCTGTTTTAGAGCTAGAAATAGCAAGTTAAAATAAGGCTAGTCCGTTATCAACTTGAAAAAGT
GGCACCGAGTCGGTGCTTTTTTTGCATGCACTTGGCTTTCCACCGTTGGTATCGATTCTCTGGGACGATGAGTCGAGCTCCA
GCTTTTGTTCCCTTTAGTGAGGGTTAATTGCGCGCTTGGCGTAATCATGGTCATAGCTGTTTCCTGTGTGAAATTGTTATCC
GCTCACAATTCCACACAACATACGAGCCGGAAGCATAAAGTGTAAAGCCTGGGGTGCCTAATGAGTGAGCTAACTCACAT
TAATTGCGTTGCGCTCACTGCCCGCTTTCCAGTCGGGAAACCTGTCGTGCCAGCTGCATTAATGAATCGGCCAACGCGCGG
GGAGAGGCGGTTTGCGTATTGGGCGCTCTTCCGCTTCCTCGCTCACTGACTCGCTGCGCTCGGTCGTTCGGCTGCGGCGAG
CGGTATCAGCTCACTCAAAGGCGGTAATACGGTTATCCACAGAATCAGGGGATAACGCAGGAAAGAACATGTGAGCAAA

AGGCCAGCAAAAGGCCAGGAACCGTAAAAAGGCCGCGTTGCTGGCGTTTTTCCATAGGCTCCGCCCCCCTGACGAGCATC
ACAAAAATCGACGCTCAAGTCAGAGGTGGCGAAACCCGACAGGACTATAAAGATACCAGGCGTTTCCCCCTGGAAGCTCC
CTCGTGCGCTCTCCTGTTCCGACCCTGCCGCTTACCGGATACCTGTCCGCCTTTCTCCCTTCGGGAAGCGTGGCGCTTTCTCA
TAGCTCACGCTGTAGGTATCTCAGTTCGGTGTAGGTCGTTCGCTCCAAGCTGGGCTGTGTGCACGAACCCCCCGTTCAGCC
CGACCGCTGCGCCTTATCCGGTAACTATCGTCTTGAGTCCAACCCGGTAAGACACGACTTATCGCCACTGGCAGCAGCCAC
TGGTAACAGGATTAGCAGAGCGAGGTATGTAGGCGGTGCTACAGAGTTCTTGAAGTGGTGGCCTAACTACGGCTACACTA
GAAGGACAGTATTTGGTATCTGCGCTCTGCTGAAGCCAGTTACCTTCGGAAAAAGAGTTGGTAGCTCTTGATCCGGCAAAC
AAACCACCGCTGGTAGCGGTGGTTTTTTTGTTTGCAAGCAGCAGATTACGCGCAGAAAAAAAGGATCTCAAGAAGATCCTT
TGATCTTTTCTACGGGGTCTGACGCTCAGTGGAACGAAAACTCACGTTAAGGGATTTTGGTCATGAGATTATCAAAAAGGA
TCTTCACCTAGATCCTTTTAAATTAAAAATGAAGTTTTAAATCAATCTAAAGTATATATGAGTAAACTTGGTCTGACAGTTAC
CAATGCTTAATCAGTGAGGCACCTATCTCAGCGATCTGTCTATTTCGTTCATCCATAGTTGCCTGACTCCCCGTCGTGTAGAT
AACTACGATACGGGAGGGCTTACCATCTGGCCCCAGTGCTGCAATGATACCGCGAGACCCACGCTCACCGGCTCCAGATTT
ATCAGCAATAAACCAGCCAGCCGGAAGGGCCGAGCGCAGAAGTGGTCCTGCAACTTTATCCGCCTCCATCCAGTCTATTAA
TTGTTGCCGGGAAGCTAGAGTAAGTAGTTCGCCAGTTAATAGTTTGCGCAACGTTGTTGCCATTGCTACAGGCATCGTGGT
GTCACGCTCGTCGTTTGGTATGGCTTCATTCAGCTCCGGTTCCCAACGATCAAGGCGAGTTACATGATCCCCCATGTTGTGC
AAAAAAGCGGTTAGCTCCTTCGGTCCTCCGATCGTTGTCAGAAGTAAGTTGGCCGCAGTGTTATCACTCATGGTTATGGCA
GCACTGCATAATTCTCTTACTGTCATGCCATCCGTAAGATGCTTTTCTGTGACTGGTGAGTACTCAACCAAGTCATTCTGAG
AATAGTGTATGCGGCGACCGAGTTGCTCTTGCCCGGCGTCAATACGGGATAATACCGCGCCACATAGCAGAACTTTAAAA
GTGCTCATCATTGGAAAACGTTCTTCGGGGCGAAAACTCTCAAGGATCTTACCGCTGTTGAGATCCAGTTCGATGTAACCC
ACTCGTGCACCCAACTGATCTTCAGCATCTTTTACTTTCACCAGCGTTTCTGGGTGAGCAAAAACAGGAAGGCAAAATGCC
GCAAAAAAGGGAATAAGGGCGACACGGAAATGTTGAATACTCATACTCTTCCTTTTTCAATATTATTGAAGCATTTATCAG
GGTTATTGTCTCATGAGCGGATACATATTTGAATGTATTTAGAAAAATAAACAAATAGGGGTTCCGCGCACATTTCCCCGA
AAAGTGCCACCTAAATTGTAAGCGTTAATATTTTGTTAAAATTCGCGTTAAATTTTTGTTAAATCAGCTCATTTTTTAACCAA
TAGGCCGAAATCGGCAAAATCCCTTATAAATCAAAAGAATAGACCGAGATAGGGTTGAGTGTTGTTCCAGTTTGGAACAA
GAGTCCACTATTAAAGAACGTGGACTCCAACGTCAAAGGGCGAAAAACCGTCTATCAGGGCGATGGCCCACTACGTGAAC
CATCACCCTAATCAAGTTTTTTGGGGTCGAGGTGCCGTAAAGCACTAAATCGGAACCCTAAAGGGAGCCCCCGATTTAGA
GCTTGACGGGGAAAGCCGGCGAACGTGGCGAGAAAGGAAGGGAAGAAAGCGAAAGGAGCGGGCGCTAGGGCGCTGGC
AAGTGTAGCGGTCACGCTGCGCGTAACCACCACACCCGCCGCGCTTAATGCGCCGCTACAGGGCGCGTCCCATTCGCCATT
CAGGCTGCGCAACTGTTGGGAAGGGCGATCGGTGCGGGCCTCTTCGCTATTACGCCAGCTGGCGAAAGGGGGATGTGCT
GCAAGGCGATTAAGTTGGGTAACGCCAGGGTTTTCCCAGTCACGACGTTGTAAAACGACGGCCAGTGAGCGCGCGTAATA
CGACTCACTATAGGGCGAATTG

Acknowledgements:

Removed in online version

Eidesstaatliche Erklärung

Hiermit versichere ich, dass ich die vorliegende Promotionsschrift selbstständig verfasst und keine anderen als die angegebenen Quellen und Hilfsmittel benutzt habe, alle Ausführungen, die anderen Schriften wörtlich oder sinngemäß entnommen wurden, kenntlich gemacht sind. Des Weiteren versichere ich das diese Arbeit noch an keiner anderen deutschen oder ausländischen Hochschule zur Erlangung eines akademischen Grades eingereiht wurde. Diese Arbeit wurde somit in Übereinstimmung mit §12, (2) der Promotionsordnung vom 01.04.2018 des Fachbereiches Biologie der Johannes Gutenberg-Universität Mainz angefertigt.

…….

Removed Cv

Removed Cv